



저작자표시-비영리-변경금지 2.0 대한민국

이용자는 아래의 조건을 따르는 경우에 한하여 자유롭게

- 이 저작물을 복제, 배포, 전송, 전시, 공연 및 방송할 수 있습니다.

다음과 같은 조건을 따라야 합니다:



저작자표시. 귀하는 원저작자를 표시하여야 합니다.



비영리. 귀하는 이 저작물을 영리 목적으로 이용할 수 없습니다.



변경금지. 귀하는 이 저작물을 개작, 변형 또는 가공할 수 없습니다.

- 귀하는, 이 저작물의 재이용이나 배포의 경우, 이 저작물에 적용된 이용허락조건을 명확하게 나타내어야 합니다.
- 저작권자로부터 별도의 허가를 받으면 이러한 조건들은 적용되지 않습니다.

저작권법에 따른 이용자의 권리는 위의 내용에 의하여 영향을 받지 않습니다.

이것은 [이용허락규약\(Legal Code\)](#)을 이해하기 쉽게 요약한 것입니다.

[Disclaimer](#)

理學博士學位論文

분열성 효모에서 Aconitase-2
단백질의 다중기능 연구

**Multiple Functions of Aconitase-2 in
*Schizosaccharomyces pombe***

2016年 8月

서울대학교 大學院

生命科學部

鄭 秀 珍

분열성 효모에서 Aconitase-2 단백질의 다중기능 연구

지도교수 노정혜

이 論文을 理學博士學位論文으로 提出함

2016年 6月

서울대학교 大學院

生命科學部

鄭秀珍

鄭秀珍의 理學博士學位論文을 認准함

2016年 6月

委員長 허원기

副委員長 노정혜

委員 김현아

委員 이대엽

委員 조은정

ABSTRACT

Aconitase functions as an enzyme in TCA cycle (Krebs cycle), converting citrate to isocitrate in bacteria and mitochondria of eukaryotes. In many organisms, aconitase serves additional roles, being a nucleic acids binding protein. In mammals and prokaryotes, aconitases are known to bind RNA as well. DNA binding has been demonstrated in *Saccharomyces cerevisiae*.

In fission yeast *Schizosaccharomyces pombe*, the *aco2⁺* gene encodes a fusion protein between aconitase and a putative mitochondrial ribosomal protein bL21 (Mrpl49). In this study, the expression of the *aco2⁺* gene to transcripts and protein products was analyzed. Two types of *aco2⁺* transcripts were generated via alternative poly (A) site selection, producing both a single aconitase domain protein and the fusion form. The bL21-fused aconitase-2 Aco2 protein resides in mitochondria as well as in cytosol and the nucleus. In mitochondria, Aco2 is needed for mitochondrial translation. The viability defect of *aco2* mutation was complemented not by the aconitase domain but by the bL21 domain, which enables mitochondrial translation. This suggests that essentiality of Aco2 protein is due to its role in mitochondrial translation.

Based on the localization of Aco2 in the nucleus, novel nuclear functions of Aco2 were investigated. There has been a report from genome-wide genetic screenings that aconitase could be involved in RNAi pathway. Intrigued by this observation, involvement of Aco2 in heterochromatin formation in *S. pombe* was examined. Genetic and physical interaction of Aco2 with heterochromatin assembly factors and its effect on modulating

transcription from the centromeric and subtelomeric regions were investigated. Loss of nuclear Aco2 (*aco2ΔN*) restored the defects of RNAi mutants, such as *Δago1* and *Δdcr1*, in forming heterochromatin in the centromeric region. However, the *aco2ΔN* mutation did not restore the defect of *Δchp1*. Chp1, a component of RITS (RNA induced transcriptional silencing) complex, directly interacted with Aco2, especially through the chromodomain as monitored by GST pull-down assay. ChIP analysis demonstrated that Chp1 can recruit Aco2 to the centromeric region. RNA-IP assay showed that Aco2 can bind to the centromeric noncoding RNA from the repeat (*dg/dh*) region in a Chp1-dependent manner. These results support a model that Aco2 binds Chp1 through the chromodomain and deters Chp1 from being recruited to chromosome in an RITS complex-independent manner, and hence inhibits heterochromatin formation. Actually in the *aco2ΔN* mutant, the H3K9me2 level in the centromere core region that does not form heterochromatin is elevated compared to the wild-type cell. Therefore, it can be postulated that Aco2 inhibits Chp1 recruitment where RITS complex does not exist, so that heterochromatin may form in the right place. To modulate centromeric heterochromatin formation, the full-length Aco2 protein with both aconitase and bL21 domains are required as well as the three cysteine residues for [FeS] ligation.

Aco2 (*aco2ΔN*) also restored the phenotype of elevated RNA level in *Δswi6* mutant, one of the HP1 protein which can bind to H3K9me2. But unlike RNAi mutants, functional heterochromatin was not restored. Even though interaction between Aco2 and Swi6 was not detected by co-IP. It

was monitored that Aco2 directly interacted with Swi6 hinge domain by GST pull-down assay. It is known that the hinge domain of Swi6 has RNA binding activity, so there is a possibility that RNA may interfere interaction between Aco2 and Swi6. Actually when RNase was treated in pull-down assay, interaction between two proteins was enhanced, as expected.

Aco2 also interacted with Rrp6, a key component of a RNA exosome, that plays a role in supporting transcription of the *dg/dh*-like repeat-containing *tlh1+* gene in the subtelomeric region. Involvement of Aco2 in the heterochromatin formation in the mating type locus has also been examined by monitoring mating type switch. Iodine staining of the homothallic h90 *aco2ΔN* cells resulted in pale color, suggesting that Aco2 may also function in mating type switching, possibly via the heterochromatin formation. Taken together, this study revealed novel functions of Aco2 in the nucleus, related with heterochromatin formation and transcriptional modulation.

Key Words; Aconitase, nuclear localization sequence, mitochondrial targeting sequence, dual localized protein, mitochondrial translation, heterochromatin gene silencing

Student number; 2009-20354

CONTENTS

ABSTRACT	I
CONTENTS	IV
LIST OF TABLES	VIII
LIST OF FIGURES.....	IX
LIST OF ABBREVIATIONS	XIV
CHAPTER I. INTRODUCTION.....	1
I.1. Biology of <i>Schizosaccharomyces pombe</i>	2
I.1.1. The early research and phylogeny of <i>S. pombe</i>	2
I.1.2. Life cycle of <i>S. pombe</i>	3
I.1.3. Cell cycle of <i>S. pombe</i>	5
I.1.3. Genomic information of <i>S. pombe</i>	5
I.2. The citric acid cycle.....	9
I.3. Dual localization (dual targeting) proteins	13
I.4. Mitochondrial DNA translation	17
I.5. Heterochromatin silencing	20

I.6. Multiple functions of aconitase.....	24
I.6.1. General function of aconitase.....	24
I.6.2. Aconitase in mammalian cells.....	24
I.6.3. Aconitase in budding yeast.....	28
I.6.4. Aconitase in bacteria	29
CHAPTER II. MATERIALS AND METHODS.....	33
II.1. Strains and plasmids.....	34
II.2. Transformation of <i>Escherichia coli</i> and Yeast.....	34
II.3. Yeast genomic DNA extraction.....	34
II.4. Analysis of RNA.....	34
II.4.1. RNA isolation	34
II.4.2. Northern analysis.....	35
II.4.3. 5' and 3' RACE	35
II.4.4. Quantitative RT-PCR.....	35
II.4.5. Small RNA extraction	36
II.5. Analysis of Proteins and their interaction.....	36
II.5.1. Western blot analysis	36
II.5.2. Co-immunoprecipitation analysis	37
II.5.3. GST-Pull down assay	37
II.6. Fluorescence microscopy	38
II.7. FACS analysis.....	38
II.8. Cell survival spotting assay.....	38

II.9. Mitochondrial translation	39
II.10. Chromatin immunoprecipitation.....	39
II.11. RNA immunoprecipitation	40
CHAPTER III. RESULTS & DISCUSSION	47
III.1. Characteristics of <i>S. pombe</i> aconitases	48
III.1.1. Two kinds of aconitases in <i>S. pombe</i>	48
III.1.2. Localization of Aco2 in mitochondria as well as in the cytosol and the nucleus.	48
III.1.3. RNAs and Proteins produced from <i>aco2+</i> gene.....	52
III.1.3.1. The <i>aco2+</i> gene produces two kinds of transcripts by alternative selection of poly (A) site.	52
III.1.3.2. Two kinds of proteins produced from <i>aco2+</i> transcripts.....	52
III.2. Roles of Aco2 in mitochondria.....	57
III.2.1. Aco2 is essential for cell viability due to the ribosomal protein domain.	57
III.2.2. Aco2 is needed for mitochondrial translation.	59
III.2.3. Mitochondrial membrane potential is decreased in <i>nmt42 aco2</i> mutant.	63
III.2.4. Aco2 interacts with Aco1 in mitochondria.	63
III.3. Roles of Aco2 in the nucleus.....	67
III.3.1. Aco2 nuclear function is not essential for cell viability.	67
III.3.2. Functions of Aco2 in centromeric heterochromatin maintenance.....	71
III.3.2.1. Aco2 nuclear mutant restores elevated RNA levels in RNAi mutants at centromere.....	71
III.3.2.2. Aco2 nuclear mutant restores functional heterochromatic defects in RNAi	

mutants at centromere.....	72
III.3.2.3. Aco2 nuclear mutant restores heterochromatic function as small RNA independent pathway.....	73
III.3.2.4. Aco2 is recruited to centromeric locus by Chp1.....	78
III.3.2.5. Aco2 directly binds to centromeric RNA and it is dependent on Chp1.....	78
III.3.2.6. Chp1 interacts with Aco2 via Chromo-domain.....	81
III.3.2.7. Aco2 nuclear mutant restores elevated RNA levels but not functional heterochromatin defects in Swi6 mutant at centromere.....	83
III.3.2.8. Aco2 interacts with Swi6 hinge region via RNA dependent manner.....	83
III.3.2.9. Aco2 affects RNA binding ability of Chp1 and Swi6 but not their recruitment.....	88
III.3.2.10. Aco2 affects heterochromatin assembly independent to Mlo3 and Tfs1.....	91
III.3.2.11. Both aconitase domain and bL21 domain are needed for nuclear function of Aco2.....	95
III.3.2.12. Iron-sulfur cluster is required for Aco2 nuclear function.....	98
III.3.3. Functions of Aco2 in sub-telomeric heterochromatin maintenance.....	100
III.3.3.1. Aco2 directly interacts with Rrp6 and they may work together in sub-telomeric loci.....	100
III.3.4. Functions of Aco2 in mating type heterochromatin maintenance.....	107
III.4. Prospects for future studies	109
III.4.1. Roles of Aco2 in mitochondria.....	109
III.4.2. Roles of Aco2 in the nucleus.....	109
REFERENCES.....	111
국문초록	123

LIST OF TABLES

TABLE II-1. YEAST STRAINS USED IN THIS STUDY.....	41
TABLE II-2. PLASMIDS USED IN THIS STUDY	43
TABLE II-3. PRIMERS USED IN THIS STUDY	45

LIST OF FIGURES

FIG. I-1. LIFE CYCLE OF FISSION YEAST <i>S. POMBE</i>	8
FIG. I-2. OVERVIEWS OF THE TCA CYCLE.....	12
FIG. I-3. NUCLEO-MITOCHONDRIAL DUAL TARGETING OF PROTEINS IS CONTROLLED BY DIFFERENT MECHANISMS.....	16
FIG. I-4. MAP OF THE <i>S. POMBE</i> MTDNA.....	19
FIG. I-5. HETEROCHROMATIC SILENCING PATHWAY IN FISSION YEAST	23
FIG. I-6. REACTION OF ACONITASE.....	26
FIG. I-7. REGULATION OF CELLULAR IRON METABOLISM.....	27
FIG. I-8. A MODEL FOR THE METABOLIC REMODELING OF MITOCHONDRIAL NUCLEOIDS IN YEAST.....	32
FIG. III-1. DISTRIBUTION OF ACO1 AND ACO2 PROTEINS AMONG CELL COMPARTMENTS	50
FIG. III-2. CONTRIBUTION OF NLS ON THE DISTRIBUTION OF ACO2	51

FIG. III-3. GROWTH CHARACTERISTICS OF <i>NMT42-ACO2</i> CONDITIONAL MUTANT	54
FIG. III-4. TWO KINDS OF TRANSCRIPTS PRODUCED FROM THE <i>ACO2</i> ⁺ GENE.....	55
FIG. III-5. PRODUCTION OF TWO KINDS OF <i>ACO2</i> PROTEINS	56
FIG. III-6. RESTORATION OF VIABILITY OF <i>ACO2</i> -DEPLETED CELLS BY BL21	58
FIG. III-7. CONTRIBUTION OF <i>ACO2</i> TO MITOCHONDRIAL TRANSLATION.....	61
FIG. III-8. CONTRIBUTION OF <i>IMG2</i> TO MITOCHONDRIAL TRANSLATION.....	62
FIG. III-9. MITOCHONDRIAL MEMBRANE POTENTIAL IN <i>ACO2</i> CONDITIONAL MUTANT	65
FIG. III-10. BIFC ANALYSIS OF <i>ACO2</i> WITH <i>ACO1</i>	66
FIG. III-11. DIAGRAM OF <i>ACO2</i> NUCLEAR MUTANTS.....	69
FIG. III-12. SPOTTING ASSAYS OF <i>ACO2</i> NUCLEAR MUTANTS....	70
FIG. III-13. EFFECT OF NLS-DELETION OF <i>ACO2</i> GENE (<i>ACO2</i> Δ N)	

ON RNA EXPRESSION IN THE CENTROMERIC REGION	74
FIG. III-14. EFFECT OF <i>ACO2ΔN</i> MUTATION ON THE HETEROCHROMATIN FORMATION IN THE CENTROMERIC REGION	76
FIG. III-15. H3K9ME2 LEVEL IN VARIOUS MUTANTS	77
FIG. III-16. CHIP AND RIP ANALYSIS OF <i>ACO2</i>	80
FIG. III-17. RELATIONSHIP BETWEEN <i>ACO2</i> AND <i>CHP1</i>	82
FIG. III-18. EFFECT OF <i>ACO2ΔN</i> MUTATION IN <i>ΔSWI6</i> MUTANT ON THE HETEROCHROMATIN FORMATION IN THE CENTROMERIC REGION	85
FIG. III-19. RELATIONSHIP BETWEEN <i>ACO2</i> AND <i>SWI6</i>	86
FIG. III-20. INTERACTION BETWEEN <i>ACO2</i> AND <i>SWI6</i>	87
FIG. III-21. INTERACTION OF <i>CHP1</i> AND <i>SWI6</i> WITH CENTROMERIC (DH) RNA	89
FIG. III-22. CHROMATIN IMMUNOPRECIPITATION (CHIP) OF <i>CHP1</i> AND <i>SWI6</i>	90
FIG. III-23. <i>ACO2</i> AFFECTS HETEROCHROMATIN ASSEMBLY	

INDEPENDENT OF MLO3 AND TFS1.....	92
FIG. III-24. MODEL-I OF ACO2 IN HETEROCHROMATIN FORMATION	93
FIG. III-25. MODEL-II OF ACO2 IN HETEROCHROMATIN FORMATION	94
FIG. III-26. FUNCTIONAL DOMAINS OF ACO2 IN MAINTAINING RNAI MUTANT PHENOTYPE OF CENTROMERIC HETEROCHROMATIN FAILURE.....	97
FIG. III-27. COMPLEMENTATION TEST WITH ACO2 CYSTEINE MUTANTS (C388S, C451S, C454S).....	99
FIG. III-28. EFFECT OF ACO2 NUCLEAR MUTANT ON RNA EXPRESSION IN THE SUB-TELOMERIC REGION (<i>TLH1</i>)	102
FIG. III--29. CHROMATIN IMMUNOPRECIPITATION (CHIP) IN ACO2 Δ N MUTANT IN THE SUB-TELOMERIC REGION (<i>TLH1</i>)	103
FIG. III-30. EFFECT OF Δ RRP6 MUTANT ON THE HETEROCHROMATIN FORMATION IN THE SUB- TELOMERIC REGION (<i>TLH1</i>)	104
FIG. III-31. INTERACTION BETWEEN ACO2 AND RRP6.....	105

FIG. III-32. MODEL OF ACO2 IN SUB-TELOMERIC LOCI.....106

**FIG. III-33. EFFECT OF ACO2 Δ N MUTANT ON THE
HETEROCHROMATIN FORMATION IN MATING TYPE
LOCUS.....108**

LIST OF ABBREVIATIONS

BiFC	Bimolecular fluorescence complementation
DTT	dithiothreitol
dsRNA	double stranded RNA
DNA	deoxyribonucleic acid
EDTA	ethylenediamine tetraacetate
EMM	Edinburgh minimal medium
EtBr	Ethidium bromide
GFP	green fluorescence protein
IP	Immunoprecipitation
IPTG	isopropyl- β -D-thiogalactopyranoside
Kb	kilo base pair
kDa	kilo Dalton
MTS	Mitochondrial Targeting Sequence
nmt	no message in thiamine
NLS	Nuclear localization sequence
OD	optical density
ORF	open reading frame
PAGE	polyacrylamide gel electrophoresis
PCR	polymerase chain reaction
PTGS	post transcriptional gene silencing
qPCR	Quantitative PCR

RISC	RNA-induced silencing complex
RNA	ribonucleic acid
RNAi	RNA interference
SDS	sodium dodecyl sulfate
siRNA	small interfering RNA
TCA	tricarboxylic acid
TGS	transcriptional gene silencing
WT	wild-type

CHAPTER I.

INTRODUCTION

I.1. Biology of *Schizosaccharomyces pombe*

I.1.1. The early research and phylogeny of *S. pombe*

In 1893, Lindner discovered *Schizosaccharomyces pombe* in East African millet beer, locally called 'pombe'. The strain currently used for genetic research was isolated by Urs Leupold (University of Berne, Switzerland) in 1950 from a grape-derived yeast culture of the 'Centraalbureau voor Schimmelcultures' (Central depository for fungi cultures) in the Netherlands.

The fission yeast *S. pombe* is proving increasingly attractive as an experimental system for investigating problems of eukaryotic cells and molecular biology. Many of the powerful molecular genetic procedures developed for *Saccharomyces cerevisiae* can now be applied to *S. pombe* (Moreno, Klar et al., 1991). The single genus *Schizosaccharomyces* embraces a small group of possibly quite divergent ascomycete yeasts that share the common feature of division by medial fission. With the exception of *S. pombe*, the fission yeasts are studied relatively little. However, the relationships between the various members of the group have been clarified (Sipiczki, 1989). *S. pombe* and *S. malidevorans* produce four spore asci. Since these strains are cross-fertile, they are, strictly speaking, varieties of a single species, i.e., *S. pombe* var. *pombe* and *S. pombe* var. *malidevorans*. *S. octosporus* and *S. japonicus* produce eight spore asci, and the latter species is also subdivided into two varieties, *S. japonicus* var. *japonicus* and *S. japonicus* var. *versatilis*, on the basis of their growth form.

S. pombe is classified as a fungus, namely an ascomycete fungus characterized by the formation of an ascus. Over the past century, ascomycete fungi have been reclassified frequently, based on various phenotypic characteristics, such as the shape of the ascospore, type of cell division (budding vs. fission), presence of hyphae, ability to ferment certain sugars or grow on various carbon and nitrogen sources. Recently, DNA and RNA sequence analyses have been used to

determine sequence divergence among ascomycete fungi and, thus, to quantitate genetic differences between species. These molecular techniques demonstrate that fission yeast *S. pombe* is phylogenetically as distant from budding yeasts as it is from humans. The *Schizosaccharomyces* lineage separated about 1 billion years ago to form an ancestral branch of the ascomycetes, denoted archaeascomycetes. However, the view that *S. pombe* maps to a different part of the tree than expected is supported by phylogenetic analyses using mitochondrial sequence data. The universal translation code is used for all ubiquitous mitochondrial genes of *S. pombe*, which clearly distinguishes it from other ascomycetes that have one or more codon reassignments. The universal translation code is also used in mitochondria of several lower fungi, such as the zygomycetes (e.g., *Rhizopus stolonifer*) and certain lineages of the chytridiomycetes (e.g., *Allo-myces*, belonging to the Blastocladales; as well as *Monoblepharella* and *Harpo-chytrium*, belonging to the Monoblepharidales). The universal translation code in *S. pombe* can be explained as a primitive character inherited from its lower fungal ancestors. In view of this special position of *S. pombe* within the ascomycetes, the common name "fission yeast" is misleading, because it has not more in common with budding yeasts (e.g., *Saccharomyces*, or *Pichia*) as have non-yeast ascomycetes (e.g., *Neurospora* or *Penicillium*). Despite its use of a mitochondrial universal translation code, however, the tiny *S. pombe* mitochondrial genome rather reflects a very derived fungus.

I.1.2. Life cycle of *S. pombe*

During its normal life cycle, fission yeast cells are haploid, meaning that they have only one copy of each chromosome. Haploid yeast cells are used for research because both recessive and dominant mutations will result in mutant phenotype. Haploid cells multiply asexually through mitosis. Newly born

daughter cells grow at the tips of their cylindrical rod shape. When they have grown to a mature length, cells stop growing and produce septa in the middle of the cells. The septum divides the mother cell into two equal-size daughter cells. In rich medium, the daughter cells will separate to start over the haploid cell cycle; each haploid cell cycle takes about 3 hours (In contrast, the mammalian cell cycle takes about 24 h). In the wild, yeast cells often live under nutrient-deprived conditions. Because *S. pombe* is a dimorphic yeast, it can switch from a yeast-form morphology to a pseudo-hyphal morphology, in which the daughter cells remain attached. Pseudo-hyphal growth allows the cells to spread out more efficiently and forage for fresh nutrients.

S. pombe has two opposite mating types, namely '+' and '-' mating types. When rich conditions are followed by starvation conditions, haploid yeast-form cells of the opposite mating type will conjugate pair-wise and fuse at their tips. Subsequently, the nuclei will fuse to form diploid cells, called zygotes. Usually, zygotes undergo meiosis immediately, followed by sporulation and formation of four-spore zygotic asci. The ascus wall will auto-lyse, liberating the haploid ascospores, which are able to survive long periods of stress. When environmental conditions become favorable for growth, the spores will germinate and the haploid cell cycle will begin again. If zygotes encounter rich conditions, they infrequently can undergo mitosis instead of meiosis and enter the diploid cell cycle.

Diploid cells divide by medial fission, like haploid cells, but are longer and wider than haploid cells. Haploid cells measure 7-8 (newly born) to 12-15 μm (at division) in length and 3-4 μm in width, while diploid cells measure 11-14 (newly born) to 20-25 μm (at division) in length and 4-5 μm in width. Diploid cells will continue mitotic growth until nutrients run out. Then, they undergo meiosis and form azygotic asci, containing four haploid ascospores. After environmental condition become favorable for growth, the spores will germinate and the normal

haploid cell cycle will begin.

I.1.3. Cell cycle of *S. pombe*

S. pombe has been used for cell cycle investigations since 1950s. A major reason for choosing *S. pombe* in initial studies was its mode of growth by length extension, which continues until the onset of mitosis. The cell cycle of *S. pombe* is typically eukaryotic, consisting of distinct G₁, S, G₂, and mitotic (M) phases. The G₂ phase occupied three quarters of the cycle of a cell growing under normal conditions, with the remainder being divided roughly equally among the M, G₁, and S phases. At mitosis, chromosome condensation can be visualized, and a long mitotic spindle forms that separated the chromosomes into daughter nuclei. The nuclear envelope remains intact throughout, however, as in most fungi. Mitosis is followed by formation of the septum centrally across the cell, which brings about physiological division of the cytoplasm. Subsequently the septum is cleaved, resulting in separation of the two daughter cells. In general S and M phases are interdependent, so that arresting S phase prevents spindle formation and chromosome condensation and blocking cells in mitosis prevents DNA synthesis in the following cycle. A similar dependency relationship of “checkpoint” ensures that, in general, septum formation only takes place once mitosis is completed.

I.1.3. Genomic information of *S. pombe*

The fully annotated genome sequence of *S. pombe* has been completed (WoodGwilliam et al., 2002). It becomes the sixth eukaryotic genome to be sequenced, following *Saccharomyces cerevisiae*, *Caenorhabditis elegans*, *Drosophila melanogaster*, *Arabidopsis thaliana*, and *Homo sapiens*. The 13.8 Mb genome of *S.*

pombe is distributed between chromosomes I (5.7 Mb), II (4.6 Mb) and III (3.5 Mb), together with a 20 kb mitochondrial genome. It contains the smallest number of protein-coding genes yet recorded for a eukaryote: 4,824 genes (including 11 mitochondrial genes), substantially less than the 5,570 ~ 5,651 genes predicted for *S. cerevisiae*, the 6,752 genes predicted for *Mesorhizobium loti*, the largest published prokaryote genome sequence to date, and the 7,825 genes estimated in the 8.67 Mb genome of the prokaryote *Streptomyces coelicolor* (Wood et al., 2002).

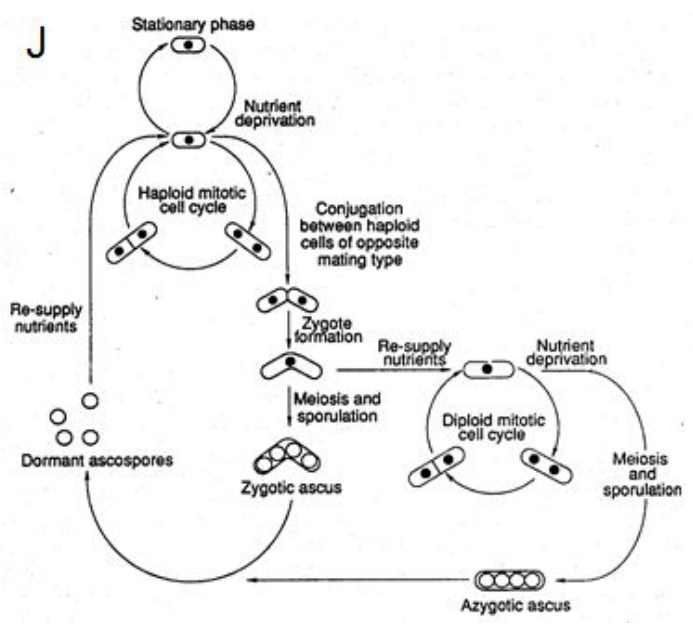
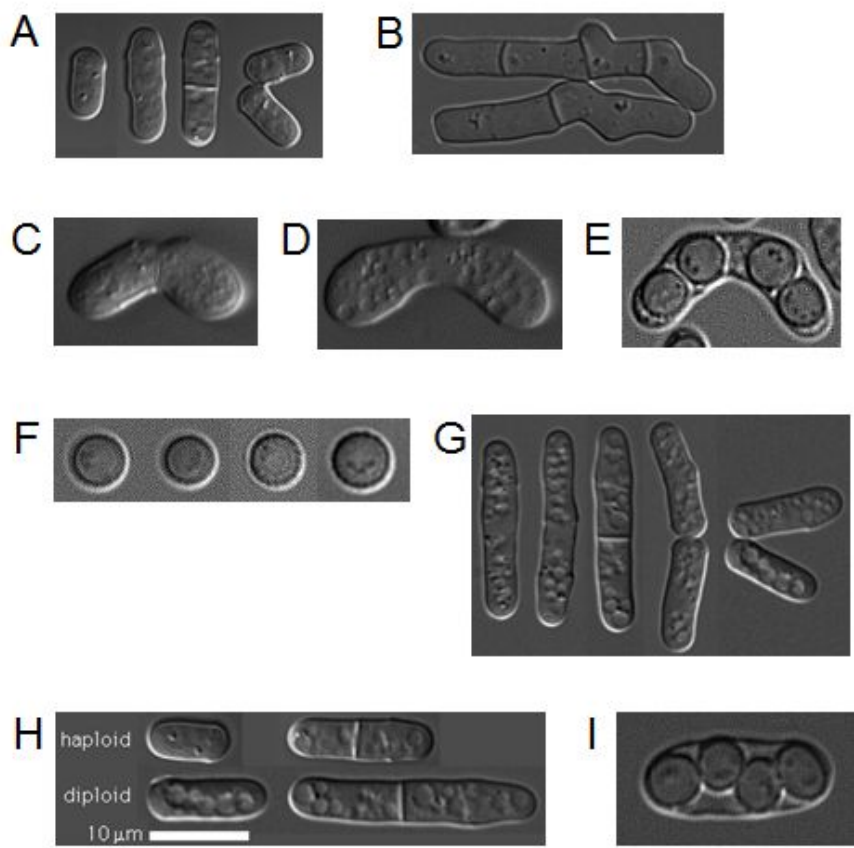


Fig. I-1. Life cycle of fission yeast *S. pombe*

(‘www information on *Schizosaccharomyces pombe* by Frans Hochstenbach at the University of Amsterdam’ (<http://www.bio.uva.nl/pombe/cycle/lifetext.html>))

- A. Haploid cells multiply asexually through mitosis.
- B. Pseudo-hyphal morphology cells.
- C. Conjugation of two different mating type cells.
- D. Formation of zygotes, the diploid cells.
- E. Formation of four-spore zygotic asci.
- F. Spore germination.
- G. Diploid cells divided by medial fission.
- H. Diploid cells are longer and wider than haploid cells.
- I. Formation of azygotic asci.
- J. Life cycle of fission yeast. (top left) Haploid mitotic cell cycle; (center and lower left) haploid cells mating to form a diploid zygote, followed by meiosis and sporulation leading to zygotic ascus formation; (lower right) re-entry of diploid zygotes into mitotic cycle (copied from MacNeill and Nurse, 1997).

I.2. The citric acid cycle

The TCA (tricarboxylic acid) cycle – also known as the citric acid cycle or Krebs cycle – is one of the major chemical reactions of all aerobic organisms. It has two main functions; generation of energy and synthesis of precursors (Vuoristo, Mars et al., 2016). The name of this metabolic pathway is derived from citric acid that is consumed and then regenerated by this sequence of reactions to complete the cycle. In eukaryotic cells, the citric acid cycle occurs in the matrix of the mitochondrion and in prokaryotic cells, which lack mitochondria, the TCA reaction occurs in the cytosol.

The TCA cycle generates energy through the oxidation of acetyl-CoA derived from carbohydrates, fats and proteins. Pyruvate dehydrogenase complex provides a link between glycolysis and the TCA. The reducing equivalents in the form of NADH and FADH₂ produced in the TCA, comprise the first step of oxygen-dependent ATP synthesis. Intermediates of the TCA cycle are used as precursors for anabolism (Velot & Srere, 2000).

Products of the first turn of the TCA cycle are one GTP (or ATP), three NADH, one QH₂ and two Co₂. Because two acetyl-CoA molecules are produced from each glucose molecule, two cycles are required per one glucose molecule. Therefore, at the end of two cycles, the products are two GTP, six NADH, two QH₂ and four CO₂.

Many enzymes are involved in the TCA cycle reaction; Aconitase, isocitrate dehydrogenase, α-ketoglutarate dehydrogenase, succinyl-CoA synthetase, succinic dehydrogenase, fumarase, malate dehydrogenase, citrate synthase. Many of the TCA cycle enzymes have additional functions in addition to their roles in the TCA cycle (Sriram, Martinez et al., 2005). For example, aconitase and isocitrate dehydrogenase are components of the mitochondrial DNA nucleoid (Chen, Wang et al., 2005) and role in mitochondrial DNA stability, while

fumarase serves in tumor suppression (Costa, Dettori et al., 2010) and succinate dehydrogenase serves in oxidative stress response (Slane, Aykin-Burns et al., 2006).

Several of the citric acid cycle intermediates are used for the synthesis of important compounds, which will have significant catabolic effects on the cycle. The cytosolic acetyl-CoA is used for fatty acid synthesis and the production of cholesterol. Cholesterol can be used to synthesize the steroid hormones, bile salts and vitamin D (Sreere, 1990). The carbon skeletons of many non-essential amino acids are made from citric acid cycle intermediates. Of these amino acids, aspartate and glutamine are used to form the purines that are used as the bases in DNA and RNA, as well as in ATP, AMP, GTP, NAD, FAD and CoA. The pyrimidines are partly assembled from aspartate. The pyrimidines, thymine and uracil from the complementary bases to the purine bases in DNA and RNA and are also components of CTP, UMP, UDP and UTP. The majority of the carbon atoms in the porphyrins, come from the citric acid cycle intermediate, succinyl-CoA. These molecules are an important component of the hemoproteins, such as hemoglobin, myoglobin and various cytochromes. During gluconeogenesis mitochondrial oxaloacetate is reduced to malate which is then transported out of the mitochondrion, to be oxidized back to oxaloacetate in the cytosol. Cytosolic oxaloacetate is then decarboxylated to phosphoenolpyruvate by phosphoenolpyruvate carboxykinase, which is the rate limiting step in the conversion of nearly all the gluconeogenic precursors (such as the glucogenic amino acids and lactate) into glucose by the liver and kidney. Because the citric acid cycle is involved in both catabolic and anabolic processes, it is known as an amphibole pathway.

The regulation of the TCA cycle is largely determined by product inhibition and substrate availability. If the cycle were permitted to run unchecked, large amounts of metabolic energy could be wasted in overproduction of reduced

coenzyme such as NADH and ATP. The major eventual substrate of the cycle is ADP which gets converted to ATP. A reduced amount of ADP causes accumulation of precursor NADH which in turn can inhibit a number of enzymes. Citrate is used for feedback inhibition, as it inhibits phosphofructokinase, an enzyme involved in glycolysis that catalyses formation of fructose 1,6-bisphosphate, a precursor of pyruvate (Denton, Randle et al., 1975).

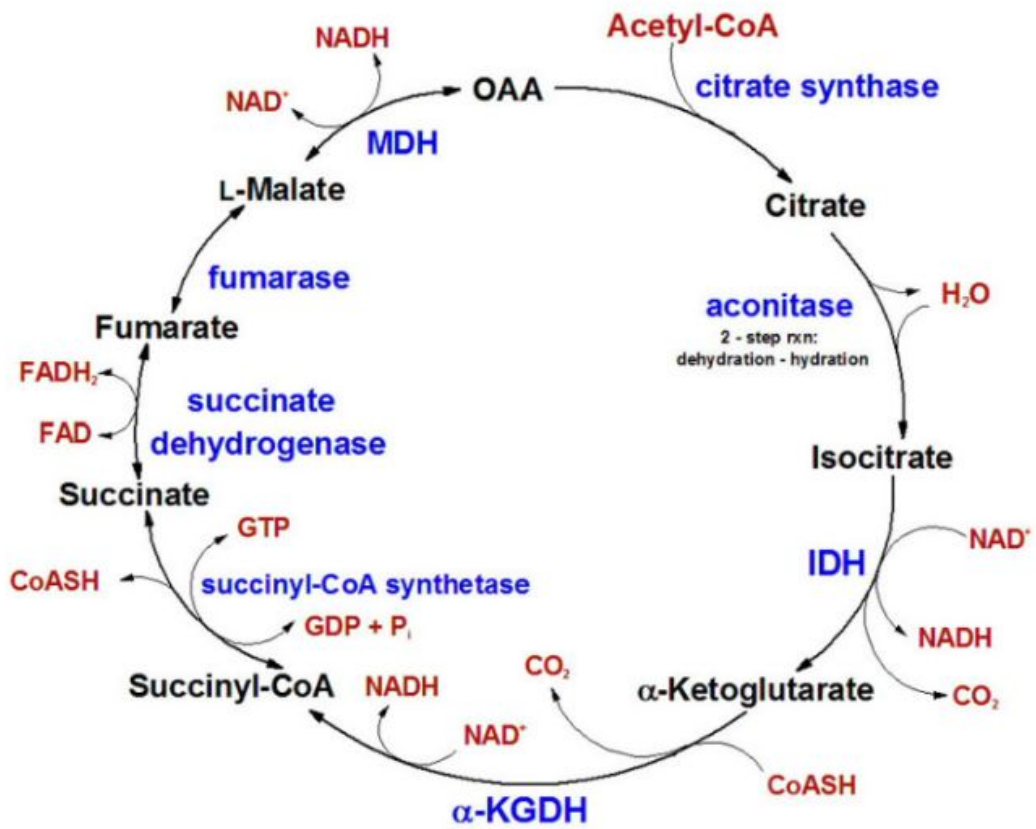


Fig. I-2. Overviews of the TCA cycle

(The picture is taken from the Medical Biochemistry page online, <http://themedicalbiochemistrypage.org/tca-cycle.php>)

I.3. Dual localization (dual targeting) proteins

Dual-targeted proteins are defined as proteins encoded by a single gene and localized in two cellular compartments. In consequence, the two isoforms have identical sequences in most of their length but can slightly differ in their extremities, due to the presence of targeting sequence (Duchene & Giege, 2012). Dual targeting of protein was first reported for *Pisum sativum* (pea) glutathione reductase (GR) in 1995 (Creissen, Reynolds et al., 1995). It is now becoming increasingly evident that organellar protein multi-localization is a much more widespread phenomenon than previously thought. Dual targeting of proteins can expand the functions of a protein, in that a protein located in more than one location, will presumably function with a distinct biochemical process in each location.

The mechanisms allowing dual localization are multiple. Sometimes post-translational modifications are shown to allow dual targeting, for example in *Arabidopsis*, farnesylation is proposed to control the localization of AtLPT3 to either plastids or the nucleus (Galichet, Hoyerova et al., 2008). Re-localization mechanisms have been also proposed (Buren, Ortega-Villasante et al., 2011). Most of the dual mitochondrial-plastidial proteins have ambiguous targeting signals in their N-terminal, for example MTS (mitochondrial targeting sequence) and are reorganized by mitochondrial and chloroplastic import apparatus. In contrast, distinct sorting sequences were identified in some mitochondria-peroxisome proteins, a N-terminal MTS and a C-terminal peroxisomal targeting signal, respectively (Carrie, Kuhn et al., 2009).

Among dual localization proteins, mitochondria and the nucleus dual localization is a common phenomenon and has been described in several instances. In particular, up to one third of the mitochondrial proteome of yeast is composed of dual localized proteins (Ben-Menachem, Tal et al., 2011). Besides, in

many eukaryotes, it has become obvious that many number of mitochondrial proteins have more than one localization. Among them, a significant proportion of proteins could be localized to both mitochondrial and the nucleus (Yogev & Pines, 2011).

Dual targeting process especially mitochondria and nucleus is achieved through several strategies. Fig. I-3 shows four different cases of dual targeting strategies.

The growing list of proteins dual localized to mitochondria and the nucleus shows that many of these proteins have a role in gene expression or genome maintenance or telomere shortening. It has been hypothesized that because some cases, proteins are even shown to be relocated from one compartment to another upon environmental or developmental cues, one rational of dual targeting is storage or sequestration of these proteins inside the organelles until specific conditions require their activity in the nucleus (Krause & Krupinska, 2009). Alternatively, proteins might be dual targeted to mitochondria and the nucleus to perform the same functions for the respective genomes expression in the two compartments and thus to act as direct effectors of gene expression coordination (Duchene & Giege, 2012). Overall the analysis of the identified instances of dual localized proteins suggests that these proteins have evolved different strategies to achieve dual localization, which enables them to act as regulators for the coordinated expression of the mitochondrial and nuclear genome.

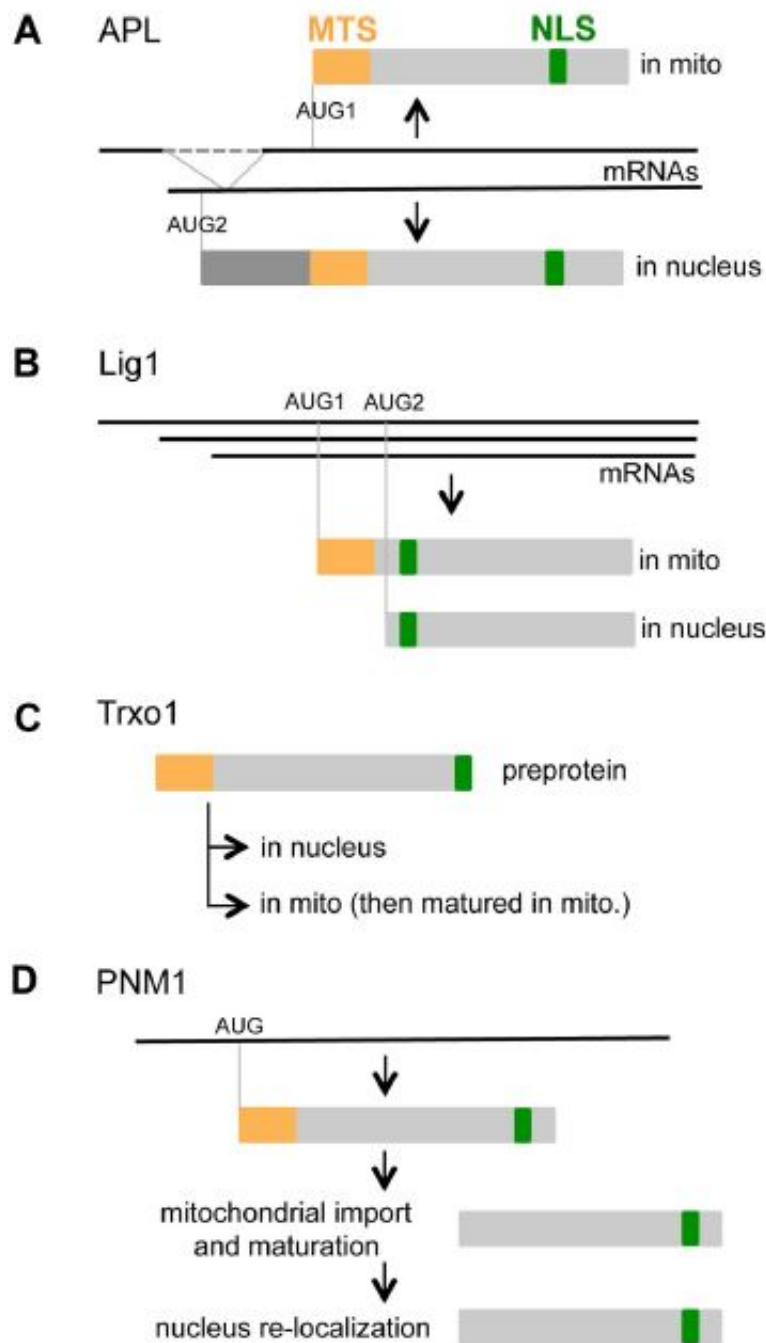


Fig. I-3. Nucleo-mitochondrial dual targeting of proteins is controlled by different mechanisms

(Duchene & Giege, 2012)

A Alternative splicing of APL (altered phloem development) generates two transcripts that code for different proteins.

B Alternative initiation of transcription and of translation controls the balance of mitochondrial and nuclear Lig1.

C The Trxo1 pre-protein is imported into both mitochondria and the nucleus, although the control of partition between the two organelles is not yet understood.

D The nuclear localization of PNM1 can be explained by re-localization of the mitochondrial mature proteins into the nucleus.

I.4. Mitochondrial DNA translation

Mitochondria are involved in numerous essential cellular processes: they produce adenosine triphosphate (ATP) by oxidative phosphorylation, participate in various metabolic pathways, contribute to calcium homeostasis and signaling, and play a key role in apoptosis. Mitochondria represent a single cellular compartment where DNA and proteins are exchanged through continuous fusion and fission reactions (Legros, Lombes et al., 2002). Mitochondria allow continuous communication with the rest of the cell.

Mitochondrial biogenesis requires the contribution of two genomes and of two compartmentalized protein synthesis system (nuclear and mitochondrial). The mitochondrial DNA encodes small portion of structural subunits (seven in the yeasts *Saccharomyces cerevisiae* and *Schizosaccharomyces pombe*). The mtDNA also encodes two rRNAs, 25 tRNAs and mitochondrial ribosomal proteins, Rps3 in the case of *S. pombe* (Bullerwell, Leigh et al., 2003). Seven polypeptides synthesized in mitochondria are components of the respiratory chain enzyme complex (Cox1, Cox2, Cox3, Atp6, ATP8/9, Cytb, Rps3). The remaining components of respiratory complexes, as well as proteins essential for expression of mitochondrial genes, are synthesized in the cytosol and subsequently imported into mitochondria. Thus, communication between mitochondria and the nucleus is very important in sustaining respiratory competence of the cell (Towpik, 2005).

Mitochondria are semiautonomous organelles containing their own independent translational machinery. *S. pombe* is a petite-negative yeast, similarly to mammalian cells, and cannot survive without mtDNA and mitochondrial protein synthesis (Schafer, 2003). So most of the proteins which is involved in mitochondrial translation process are essential for cell viability. In *S. pombe* mitochondrial protein translation is regulated by the guanine nucleotide

exchange factor EF-Ts, conserved in higher eukaryotes, which controls the translation elongation factor EF-Tu (Das, Wiley et al., 2007).

Mitochondria are not isolated organelles and mitochondrial movement and distribution are mediated by the microtubule cytoskeleton (Weir & Yaffe, 2004) and mitochondria are an integral part of several transduction cascades involved in metabolism, cell cycle control and differentiation (McBride, Neuspiel et al., 2006). In this respect, studies of mitochondrial ribosomal proteins which serves in mitochondrial DNA translation may have additional functions in the control of cell metabolism and growth (Gaisne & Bonnefoy, 2006).

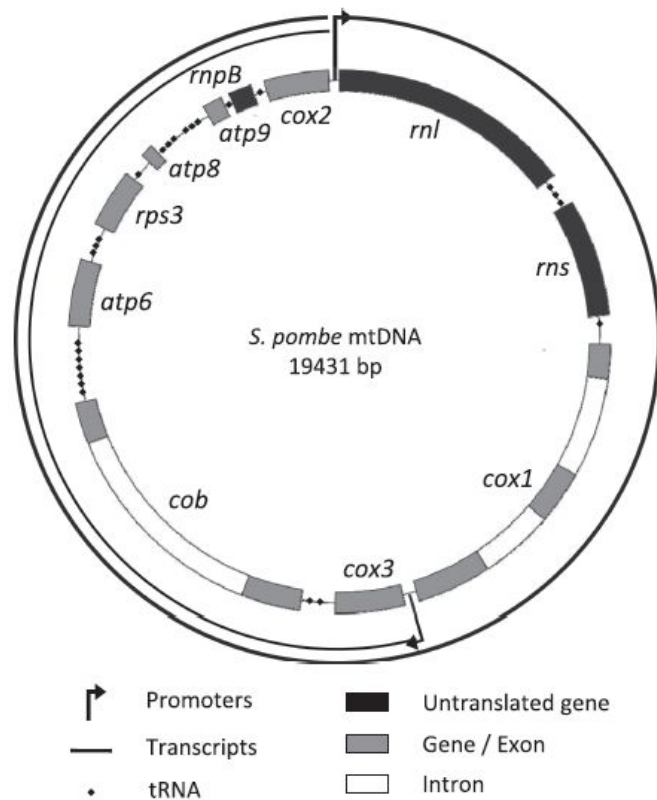


Fig. I-4. Map of the *S. pombe* mtDNA

(Kuhl, Dujancourt et al., 2011).

The promoter located in front of the large rRNA gene *rnl* is the major promoter that yields a 19.4 kb transcript corresponding to the full mtDNA. A second minor promoter is located between the *cox1* and *cox3* genes and drives the transcription of a 10.5 kb RNA containing the genes from *cox3* to *cox2*. The 5'-end of mature RNAs are processed through tRNA punctuation, except for *rnl* and *cox3* whose 5'-ends are determined by the start of the RNase P RNA (*rnpB*) is produced by tRNA processing and the processing signal of *rnl* is unknown (Schafer, 2005). Genes coding RNAs are depicted in black, protein encoding genes are in gray and introns in white

I.5. Heterochromatin silencing

In eukaryotic cells, genomic DNA is folded with histone and non-histone proteins to form chromatin. Each chromatin unit, or nucleosome, contains 146 bp of DNA, which is wrapped around an octamer of histones (Luger, Mader et al., 1997).

Emil Heitz first defined the concepts of euchromatin and heterochromatin in 1920s based on the differential compaction of chromatin during interphase. While euchromatin is less condensed, and more readily transcribed, heterochromatin is typically highly condensed and generally inhibitory to transcriptional machinery (Grewal & Jia, 2007).

Heterochromatic DNA domains are required for stable chromosome transmission and regulation of gene expression in variety of organisms ranging from yeast to human. In the fission yeast *Schizosaccharomyces pombe*, heterochromatin is associated with telomeres, the silent mating-type loci, and repetitive DNA elements surrounding centromeres, which contain *dg* and *dh* repeats served as heterochromatin nucleation centre (Grewal & Jia, 2007). The assembly of heterochromatin at these loci involves a series of steps that ultimately lead to the association of specific histone modifications and structural proteins with extended DNA domains. One of the key steps is the methylation of histone H3 lysine 9 (H3K9) by the Clr4 methyltransferase, which creates a binding site for the Swi6, Chp1 and Chp2 chromodomain proteins (Bjerling, Silverstein et al., 2002, Nakayama, Rice et al., 2001, Partridge, Borgstrom et al., 2000).

Heterochromatin assembly at fission yeast centromeres requires components of the RNA interference (RNAi) pathway. RNAi is a conserved silencing mechanism that is triggered by double-stranded RNA (dsRNA) (Bartel, 2004, Hammond, Boettcher et al., 2001). RNAi-dependent posttranscriptional gene

silencing (PTGS) involves the generation of small RNA molecules of ~22 nucleotides from longer dsRNAs by an RNase III-like enzyme called Dicer (Bernstein, Caudy et al., 2001). These small interfering RNAs (siRNAs) then load onto an effector complex called RISC (RNA-induced silencing complex). The RISC complex contains Argonaute, which is a member of the conserved Argonaute/PIWI family of proteins that are required for RNAi in a variety of systems (Caudy, Myers et al., 2002, Hammond et al., 2001, Hutvagner & Zamore, 2002, Mourelatos, Dostie et al., 2002). siRNA-programmed RISC acts in trans to target cognate mRNAs for degradation by an endonucleolytic cleavage event, also referred to as slicing, which is executed by Argonaute (Liu, Carmell et al., 2004, Song, Smith et al., 2004). *S. pombe* contains only a single gene for each of the main RNAi enzymes, Dicer, Argonaute and RNA-directed RNA polymerase, called *dcr1⁺*, *ago1⁺* and *rdp1⁺*, respectively, all of which are required for heterochromatin formation (Volpe, Kidner et al., 2002). Deletion of any of these genes results in defects in the spreading of H3K9 methylation and Swi6 localization (Jia, Noma et al., 2004a, Motamedi, Verdel et al., 2004, Verdel, Jia et al., 2004).

Heterochromatic silencing in *S. pombe* also occurs at transcriptional levels (Noma, Sugiyama et al., 2004). The SHEREC (Snf2/Hdac-containing Repressor Complex) is involved in TGS (transcriptional gene silencing) in *S. pombe* (Sugiyama, Cam et al., 2007). This complex containing histone deacetylase and remodeling factor affects to the heterochromatic TGS by leading to the formation of condensed heterochromatin. ClassI HDAC Clr6 and anti-silencing factor *epe1⁺* also involved in PTGS silencing (Fischer, Cui et al., 2009, Isaac, Walfridsson et al., 2007, Nicolas, Yamada et al., 2007).

More interestingly, heterochromatin is dynamically regulated by RNA polymerase II (RNAPII) during the cell cycle (Chen, Zhang et al., 2008). S phase is enforced by heterochromatin, which restricts RNAPII accessibility at centromeric

repeats for most of the cell cycle. RNAPII transcription during S phase is linked to loading of RNA interference and heterochromatin factors such as the Ago1 subunit of the RITS complex and the Clr4 methyltransferase complex subunit Rik1 (Jia, Kobayashi et al., 2005). Moreover, Set2, an RNAPII-associated methyltransferase that methylates histone H3 lysine 36 at repeat loci during S phase, acts in a pathway parallel to Clr4 to promote heterochromatin assembly. These cell cycle dependent processes probably facilitate heterochromatin maintenance through successive cell divisions.

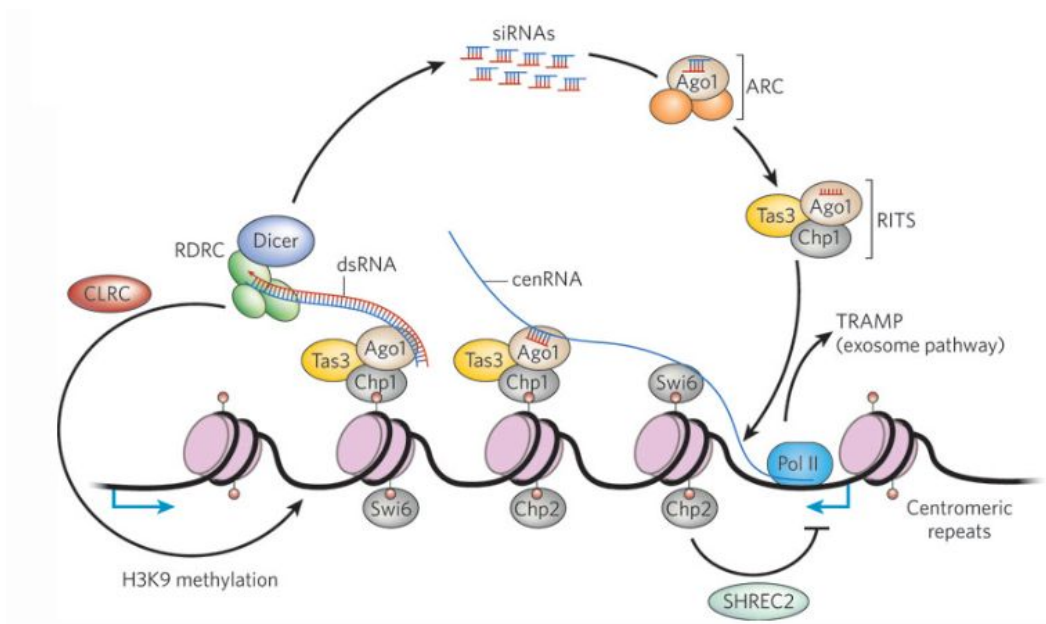


Fig. I-5. Heterochromatic silencing pathway in fission yeast

(Moazed, 2009)

siRNAs originated from pericentromeric repeat elements target histone-modifying enzymes such as Clr4 methyltransferase to target sequences to bring about their methylation. The methylated residues in turn recruit chromatin domain proteins such as Chp1, Chp2 and Swi6. Furthermore, low levels of H3K9me at centromere allow initial recruitment of the RNAi machinery to centromere through siRNA-independent mechanism. This triggers a positive feedback loop to enforce heterochromatin assembly and silencing.

I.6. Multiple functions of aconitase

I.6.1. General function of aconitase

Aconitases are expressed in bacteria to human. The aconitases convert citrate to isocitrate via *cis*-aconitate in the citric acid and glyoxylate cycles. They are monomeric enzymes containing single iron-sulfur clusters which are interconvertible between the catalytically active [4Fe-4S] forms and the inactive [3Fe-4S] and apo-enzyme forms (Beinert, Kennedy et al., 1996). The iron sulfur cluster is highly sensitive to oxidation by superoxide (Lauble, Kennedy et al., 1992).

Aconitases are monomeric proteins containing single, labile [4Fe-4S] clusters. Crystallographic studies with porcine heart mitochondrial aconitase have revealed the presence of three structural domains (1, 2 and 3) tightly-packed around the iron-sulfur cluster, and a fourth domain that is connected by a long linker peptide in such a way as to create a deep active-site cleft (Robbins & Stout, 1989). This arrangement provides the structural prototype for the aconitase family.

I.6.2. Aconitase in mammalian cells

Mammalian IRPs (Iron regulatory proteins) are members of the aconitase family (Gruer, Artymiuk et al., 1997). Active Aconitases require a 4Fe-4S cluster, where the first three irons are ligated by conserved cysteines, and the remaining most labile iron is available for participation in the isomerization reaction (Volz, 2008). The structural prototype of the family is mitochondrial aconitase, but most eukaryotes also possess a cytoplasmic version of the enzyme that has ~30% amino acid sequence identity. IRP1 with a complete Fe-S cluster is the cytoplasmic aconitase.

When IRP1 (c-aconitase) possesses Fe-S cluster, it is committed to its aconitase

state. In normal tissues with abundant iron, most IRP1 is in the c-aconitase form. c-Aconitase does not bind RNA with high affinity. But in iron depleted condition, IRPs bind, through the active-site clefts, to specific sequences termed iron-responsive elements (IRE), which form stem-loop structures at the 5'- or 3'-ends of relevant mRNA transcripts (Jaffrey, Haile et al., 1993, Klausner & Rouault, 1993). Binding at the 5'-end blocks translation, whereas binding at the 3' end promotes translation by enhancing transcript stability. Phosphorylation, reactive oxygen and nitrogen species also facilitate this process (Volz, 2008).

Fig. I-7 shows the regulatory mechanism of c-aconitase. The binding of IRPs to single IREs in the 5' UTRs of target mRNAs inhibits their translation, whereas IRP interaction with multiple 3' UTR IREs in transferrin receptor 1 (TfR1) transcript increases its stability. As a consequence, TfR1-mediated iron uptake increases whereas iron storage in ferritin and export via ferroportin decrease. In iron-replete cells (left), the FBXL5 iron-sensing F-box protein interacts with IRP1 and IRP2 and recruits the SKP1-CUL1 E3 ligase complex that promotes IRP ubiquitination and degradation by the proteasome. IRP1 is primarily subject to regulation via the assembly of a cubane Fe/S cluster that triggers a conformational switch precluding IRE-binding and conferring aconitase activity to the holoprotein. IRPs also modulate the translation of the mRNA encoding the erythroid-specific ALAS2 heme synthesis enzyme, the mitochondrial aconitase (ACO2), and the HIF2 α hypoxia-inducible transcription factor. Single 3' UTR motifs are present in the DMT1 and CDC14A mRNAs, but their role and mechanism of function are not fully defined (Hentze, Muckenthaler et al., 2010).

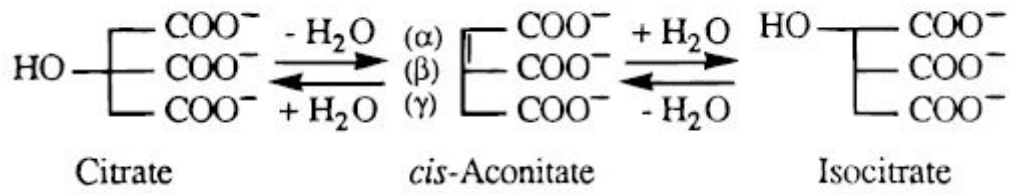


Fig. I-6. Reaction of aconitase

(Beinert et al., 1996).

Aconitase catalyses the stereo-specific isomerization of citrate to isocitrate via cis-aconitate in the tricarboxylic acid cycle, a non-redox-active proteiss.

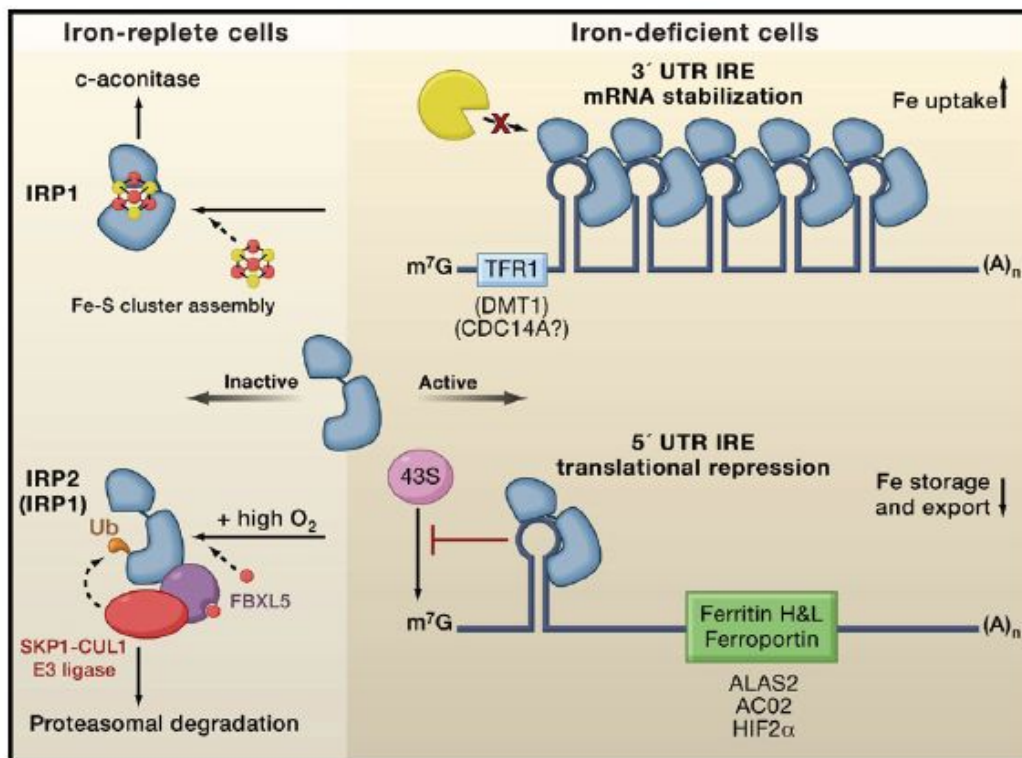


Fig. I-7. Regulation of cellular iron metabolism

(Hentze et al., 2010)

In iron-deficient cells (right), iron regulatory protein 1 (IRP1) or IRP2 bind to *cis*-regulatory hairpin structures called iron-responsive elements (IREs), present in the untranslated regions (UTRs) of mRNAs encoding proteins involved in iron transport and storage. In iron-replete cells (left), the FBXL5 iron-sensing F-box protein interacts with IRP1 and IRP2 and recruits the SKP1-CUL1 E3 ligase complex that promotes IRP ubiquitination and degradation by the proteasome; IRP1 is primarily subject to regulation via the assembly of a cubane Fe/S cluster that triggers a conformational switch precluding IRE-binding and conferring aconitase activity to the holoprotein.

I.6.3. Aconitase in budding yeast

Mitochondrial DNA (mtDNA) nucleoids have been purified from several organisms (Garrido, Griparic et al., 2003, Miyakawa, Sando et al., 1987). In *Saccharomyces cerevisiae*, Aco1 protein was screened out among proteins that are associated with mt DNA nucleoid (Kaufman, Newman et al., 2000), which are protein-DNA complexes associated with the inner mitochondrial membrane. These structures package mtDNA and otherwise assist in mtDNA transactions, including mtDNA inheritance.

Aco1 mutants lose mtDNA (Chen et al., 2005). Like other bifunctional nucleoid protein, the enzymatic and mtDNA maintenance functions of Aco1 are separable by mutation. For example, mutations in cysteine residues that coordinate to and thus attach the Iron-Sulfur cluster to the protein result in a complete loss of Aco1 enzymatic activity but have only minor effects on mtDNA maintenance (Chen et al., 2005). Aco1 has an intrinsic affinity for both ds- and ssDNA, and that it potently protects mtDNA from damage (Chen, Wang et al., 2007). Whether 'iron-sulfur switch' controls, similar to mammalian cell, the conversion between the enzymatic and mtDNA maintenance form of Aco1 is unknown. However the model, such a regulatory mode could allow Aco1 to function as a stress sensor for the protection of mtDNA, was proposed (Shadel, 2005). In this model, the disassembly of the Aco1 iron-sulfur cluster, induced by free radicals, could result in the reallocation of Aco1 from the Krebs cycle to mt-nucleoids, stabilizing mtDNA under oxidative stress conditions.

Fig. I-8 shows a model for the metabolic remodeling of mitochondrial nucleoids in yeast (Chen & Butow, 2005). In conditions in which respiration is repressed by the presence of glucose, mitochondrial DNA is tightly packaged by the protein Abf2, limiting mtDNA transactions. When cells are shifted to respiratory conditions, or when mitochondrial dysfunction activates the retrograde (RTG)

pathway, Aco1 expression is increased, resulting in more Aco1 in mitochondrial nucleoids. Similarly, in conditions of amino-acid starvation, the expression of Ilv5 is activated by the general amino-acid control pathway and Ilv5 accumulates in mt-nucleoids.

Another mitochondrial aconitase Aco2 was screened for proper telomere structure (Poschke, Dees et al., 2012) in *S. cerevisiae*. Individual study of Aco2 whether it directly affects to telomere structure is not yet progressed. But this data gives possibility of another function of aconitase not yet discovered.

I.6.4. Aconitase in bacteria

I.6.4.1. Aconitase in *E. coli*

Escherichia coli contains a stationary-phase aconitase (AcnA) that is induced by iron and oxidative stress, and major but less stable aconitase (AcnB) synthesized during exponential growth (Tang & Guest, 1999). Sequence comparisons show that AcnA is 53% identical to human IRP1 and 27-29% identical to mitochondrial aconitases, whereas AcnB is only 15-17% identical to AcnA, the IRPs and mitochondrial aconitases. The major IRE-binding site of IRP1 (DLVIDHSIQVD), identified by UV cross-linking (Basilion, Rouault et al., 1994), is likewise conserved at nine of the eleven positions in AcnA but only at two positions in AcnB.

Specific roles for AcnA and AcnB have been identified by physiological and enzymological studies with can mutants (Gruer & Guest, 1994), and it is discovered that AcnB is the major aconitase synthesized during the exponential phase, whereas AcnA is a stationary-phase enzyme which is also specifically induced by iron and oxidative stress.

Affinity chromatography and gel retardation analysis showed that the AcnA and AcnB apo-proteins each interact with the 3H untranslated regions (3HUTRs) of

acnA and *acnB* mRNA at physiologically significant protein concentrations (Tang & Guest, 1999). AcnA and AcnB synthesis was enhanced *in vitro* by the apo-aconitases and this enhancement was abolished by 3HUTR deletion from the DNA templates, presumably by loss of *acn*-mRNA stabilization by bound apo-aconitase. *In vivo* studies showed that although total aconitase activity is lowered during oxidative stress, synthesis of the AcnA and AcnB proteins and the stabilities of *acnA* and *acnB* mRNAs both increase, suggesting that inactive aconitase mediates a post-transcriptional positive autoregulatory switch (Tang & Guest, 1999). Evidence for an iron-sulfur-cluster-dependent switch was inferred from the more than three fold higher mRNA-binding affinities of the apo-aconitases relative to the holo-enzymes. Thus by modulating translation via site-specific interactions between apo-enzyme and relevant transcripts, the aconitases provide a new and rapidly reacting component of the bacterial oxidative stress response (Tang & Guest, 1999).

I.6.4.2. Aconitase in *B. subtilis*

The aconitase protein of *Bacillus subtilis* was able to bind specifically to sequences resembling the iron response elements (IREs) found in eukaryotic mRNA. The sequences bound include the rabbit ferritin IRE and IRE-like sequences in the *B. subtilis* operons that encode the major cytochrome oxidase and an iron uptake system. IRE binding activity was affected by the availability of iron both *in vivo* and *in vitro*. In eukaryotic cells, aconitase-like proteins regulate translation and stability of iron metabolism mRNAs in response to iron availability. A mutant strain of *B. subtilis* that produces an enzymatically inactive aconitase that was still able to bind RNA sporulated 403 more efficiently than did an aconitase null mutant, suggesting that a non-enzymatic activity of aconitase is important for sporulation. The results support the idea that bacterial aconitases, like their eukaryotic homologs, are bifunctional proteins, showing aconitase activity in the

presence of iron and RNA binding activity when cells are iron-deprived (Alen & Sonenshein, 1999a).

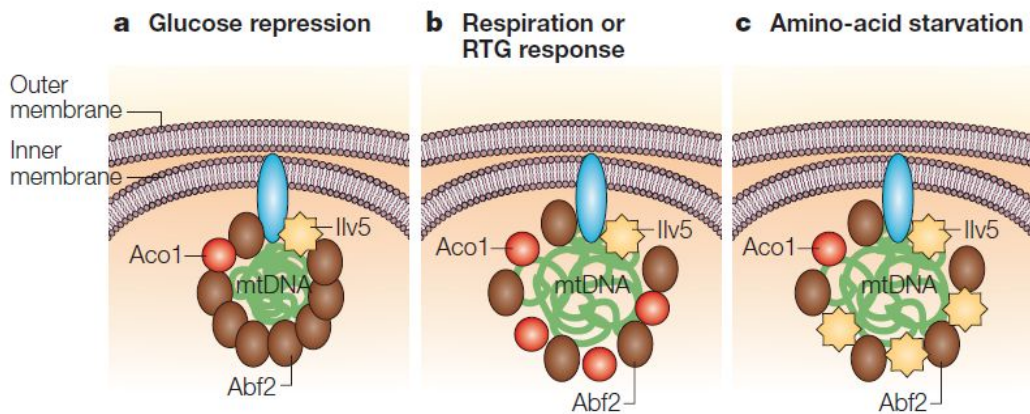


Fig. I-8. A model for the metabolic remodeling of mitochondrial nucleoids in yeast

(Chen & Butow, 2005)

In conditions in which respiration is repressed by the presence of glucose, mitochondrial DNA (mtDNA) is tightly packaged by the protein Abf2, limiting mtDNA transactions. **b** | When cells are shifted to respiratory conditions, or when mitochondrial dysfunction activates the retrograde (RTG) pathway, *ACO1* (aconitase 1) expression is increased, resulting in more Aco1 in mitochondrial nucleoids (mt-nucleoids). **c** | Similarly, in conditions of amino-acid starvation, the expression of *ILV5* is activated by the general amino-acid control pathway and Ilv5 accumulates in mt-nucleoids. The increased levels of Aco1 and Ilv5 that are shown in **b** and **c** substitute for Abf2 in packaging mtDNA into a metabolically favourable conformation and/or protect mtDNA in the remodelled conformation. The blue oval represents a putative protein, or complex of proteins, that connects mt-nucleoids to the inner mitochondrial membrane.

CHAPTER II.
MATERIALS AND METHODS

II.1. Strains and plasmids

All strains and plasmids used in this study were listed in Table1 and Table2. All the deletions and taggings were done through PCR-based methods (Krawchuk & Wahls, 1999).

II.2. Transformation of *Escherichia coli* and Yeast

For the purpose of general cloning, *E. coli* DH5 α competent cells were used for transformation by heat shock method (42°C for 1 min 30 sec.). High efficiency electroporation method of *E. coli* (XL1-Blue) was used to amplify *S. pombe* genomic library plasmid of interesting target gene from the purified yeast total genomic DNA.

The *S. pombe* transformation was routinely done using lithium acetate (LiAc) / Polyethylene glycol (PEG) method according to Moreno *et al.* (1991).

II.3. Yeast genomic DNA extraction

The chromosomal DNA of *S. pombe* was prepared as described by Alfa *et al.* (1993) with some modifications. Cells were resuspended in 200ul gDNA extraction buffer (2% triton X-100, 1% SDS, 100mM NaCl, 10mM Tris-HCl pH8.0, 1mM EDTA) and 200ul PCI and then disrupted with vortex for 5mins. After centrifugation, the aqueous phase was recovered for precipitation with 2 vol. of absolute ethanol. Ethanol-precipitated DNAs were dissolved in water.

II.4. Analysis of RNA

II.4.1. RNA isolation

Cells were grown upto A₅₉₅ of 1.0 (exponential), and total RNAs were prepared

with acidic hot phenol method as described (Schmitt, Brown et al., 1990). Cells were harvested and washed with RNase-free water. After resuspending the pellet in AE buffer (50 mM sodium acetate, pH 5.3, 10 mM EDTA, pH 8.0), 1/10 vol. of 10% SDS and equal vol. of AE-saturated phenol/chloroform were added. Cells were lysed by agitating vigorously with vortex mixer for 30 seconds, incubated at 65°C for 5 min for 3 times. After centrifugation at 4°C, the aqueous phase was recovered for precipitation with 2 vol. of absolute ethanol. Ethanol-precipitated RNAs were dissolved in RNase-free water.

II.4.2. Northern analysis

For Northern analysis, RNA samples were electrophoresed on 1.1% agarose gel, followed by transfer to a Hybond-N+ membrane (Amersham). The *aco2*⁺ gene-specific probes were generated by PCR and labeled with [α -³²P] dATP (10 μ Ci; IZOTOPE/ Institute of Isotopes Co., Ltd) with T4 Kinase (Koschem). Hybridization was done in Rapid-hyb buffer (Amersham) according to standard procedures. Signals were detected by PhosphorImager (BAS-5000) and analyzed with Multi Gauge (Fuji) program.

II.4.3. 5' and 3' RACE

To determine the 5' and 3' end region of mRNA, RACE (rapid amplification of cDNA ends) was carried out by adding RACE adaptor and reverse transcriptase (the FirstChoice® RLM-RACE kit; Ambion) to 1 μ g RNA sample, following the manufacturer's instructions. PCR was performed with the adaptor primer (RACE outer control primer) and the *aco2*⁺ gene-specific primer. Final PCR products were separated on an agarose gel, eluted, and then sequenced.

II.4.4. Quantitative RT-PCR

RNA was purified as described 'hot phenol' method (Schmitt et al., 1990).

Purified RNA was treated with DNase (rDNase I, Ambion) and subjected to RT-PCR. RNA samples were incubated with primers complementary to poly-A tails (oligo-dT) in cDNA synthesis reactions. Reverse transcribed cDNAs were amplified by real-time PCR using gene-specific check primers. A full list of primer is provided in Table3.

II.4.5. Small RNA extraction

For siRNA detection, 50ug of small RNA were resolved on 12.5% denaturing acrylamide gel and electrotransferred onto Hybond-N+ membranes (Amersham) and UV-crosslinked. siRNAs (21nt) were probed with 32P-labelled oligos homologous to the *dg/dh* repeats and loading control used an oligonucleotide homologous to a snoRNAs

II.5. Analysis of Proteins and their interaction

II.5.1. Western blot analysis

TCA-precipitated protein samples were dissolved in SDS gel running buffer with 3 min boiling, and electrophoresed on 10 % SDS PAGE gel. Gel was transferred onto PROTRAN (nitrocellulose transfer membrane; Schleicher & Schuell) using TransBlot system (BioRad) at 160 ~ 180 mA for 50 min.

Filters with bound protein were washed 3 times and blocked in 10 ml of Tris-buffered saline containing 0.1% Triton-X 100 (TBS-T) with 0.5% BSA. Filters were incubated for 1 hr with proper antibodies in TBS-T containing 0.5% BSA. Excess antibodies were removed by repeated washing in TBS-T. After 1 hr incubation in TBS-T containing the secondary antibody conjugated with horseradish peroxidase, the signal was visualized with LAS3000 (Fuji) and quantified with Multi Gauge (Fuji) program.

II.5.2. Co-immunoprecipitation analysis

Cells were harvested from overnight 2L cultures grown to OD₅₉₅ 1.5 and washed. Cells were lysed by bead-beating in buffer containing complete protease inhibitors (Sigma) and 1mM PMSF. Lysate was cleared by centrifugation at 55,000 rpm for 1h, and the supernatant was incubated with anti-FLAG M2 affinity gel (Sigma) or anti-c-MYC agarose affinity gel (Sigma) for 2h. Beads were washed extensively, and precipitated proteins were eluted with 200µl 1mg/ml FLAG or MYC peptides (Sigma). Proteins were precipitated with 10% TCA and resuspended in sample buffer. Samples were separated in 10 % SDS/PAGE gel for Western blot analysis.

II.5.3. GST-Pull down assay

For GST-pull down experiments, cells expressing FLAG-tagged Aco2 fusion proteins were lysed using NP-40% buffer containing 6 mM Na₂HPO₄, 4 mM NaH₂PO₄, 1% Nonidet P-40, 150 mM NaCl, 2 mM EDTA, 1 mM PMSF, 4 mg/ml leupeptin, 2 mM benzamidine. The whole cell lysates were incubated with GST alone and GST-Swi6 and Chp1 proteins in NP-40% buffer at 4°C for 2hr. GST fusion proteins and associated proteins were pulled down by adding 15 ul of glutathione-Sepharose (GE healthcare). After proteins were washed with the NP-40% buffer, the bound proteins were eluted by boiling 2XSDS/PAGE sample buffer for 3 min. The eluted proteins were resolved by 10% SDS-PAGE, and the pulled-down FLAG-tagged Aco2 proteins were detected by Western blotting using an anti-FLAG antibody (Sogma).

II.6. Fluorescence microscopy

The chromosomally integrated *aco1*-GFP and *aco2*-GFP fusion strains were grown to OD₅₉₅ of ~1.0 in YES media with supplements. Cells that express GFP-fused *aco2* genes on pREP42-based plasmids and VN, VC-fused *aco2* and *aco1* genes on pREP42-based plasmids were grown similarly in EMM media with supplements. Mitochondria and DNA were visualized by adding MitoTracker® Red CMXRos (Molecular Probes) and DAPI, respectively. Fluorescence and DIC (differential interference contrast) images were captured by Axiovert 200M microscope and analyzed by AxioVision 4.3 software (Carl Zeiss, Inc.).

II.7. FACS analysis

Perturbations in mitochondrial membrane potential were monitored by flow cytometry using a modification of the method described by Rajpurohit et al (Rajpurohit, Mansfield et al., 1999). Growing cells were harvested and resuspended in 50 mM potassium phosphate (pH 6.5), 0.1 M glucose at 10⁶ cells/ml. Cells were treated with 175 nM 3,3'-dihexyloxacarbocyanine (DiOC6(3); Molecular probes) for 15-30 min at 30 °C. Probes were excited with a laser at 488 nm and emission was measured through a 530/30 nm. Flow cytometry was performed with a Becton Dickson FACScan flow cytometer using LYSIS II software.

II.8. Cell survival spotting assay

Cells were grown in liquid EMM or YES media with supplements until OD₅₉₅ of 1.0. About 3 × 10⁷ cells and their ten-fold serial dilutions were spotted on proper solid media. Plates were incubated at 30°C for four days.

II.9. Mitochondrial translation

Labeling of mitochondrially synthesized proteins *in vivo* was done as described previously (Wiley, Catanuto et al., 2008) with some modifications. Cells were grown in 50 ml EMM with 0.1% glucose and 2% galactose with or without 10 μ M thiamine until OD₅₉₅ of ~1.0. Cells (3×10^7) were harvested, washed in 500 μ l reaction buffer (40 mM potassium phosphate, pH 6.0, 0.1% glucose, 2% galactose). After being pelleted, cells were re-suspended in 500 μ l reaction buffer with cycloheximide (10 mg/ml) to inhibit cytosolic protein synthesis for 15 min, prior to adding [³⁵S] methionine (50 μ Ci; IZOTOPE/ Institute of Isotopes Co., Ltd) for 1 hr at 30°C. After cell lysis by adding 75 μ l solubilization buffer (1.8 M NaOH, 1 M β -mercaptoethanol, 0.01 M PMSF), TCA-precipitated proteins were electrophoresed on 17.5% SDS PAGE gel, followed by autoradiography.

II.10. Chromatin immunoprecipitation

ChIP was performed as described (Takahashi, Chen et al., 2000) with modifications. Briefly, 200mL of YES cultures were fixed with 1 % formaldehyde, harvested, and frozen. Cells were lysed by bead-beating in 0.2mL of immunoprecipitation buffer (50 mM HEPES/KOH pH7.5, 150 mM NaCl, 1 mM EDTA, 1 % Triton X-100, 0.1 % sodium deoxycholate, 0.2 % SDS, 1 mM PMSF, 1 mM benzamide, 1 μ g/ml leupeptin). Extracts were diluted to 2 mL with immunoprecipitation buffer and sonicated for eight times (20 sec on, 180 sec off). Supernatant obtained by centrifugation was used for immunoprecipitation and immune complexes were recovered with 20 μ l of protein A/G agarose beads (Sigma). Precipitates were successively washed for 10 min each with 1 ml of immunoprecipitation buffer, immunoprecipitation buffer/500 mM NaCl, LiCl buffer (10 mM Tris-Cl pH8.0, 250 mM LiCl, 1 mM EDTA, 0.5 % NP-40, 0.5 %

sodium deoxycholate) and 1 ml of TE. Finally, the samples were eluted by adding elution buffer (1 % SDS, 1XTE, 250 mM NaCl) to the protein A/G beads and re-extracted with phenol/chloroform, ethanol precipitated, and resuspended in TDW.

II.11. RNA immunoprecipitation

RNA-IP experiments were performed as described previously (Motamedi et al., 2004). Cells were grown to an OD600 of 1.5–2, crosslinked with formaldehyde for 30 min, and frozen. Whole-cell extracts were prepared from frozen pellets as described previously (Gilbert, Kristjuhan et al., 2004, Hurt, Luo et al., 2004) and treated with DNase I (invitrogen) for 1 hr at 30°C in the buffer supplemented with 25 mM MgCl₂ and 5 mM CaCl₂. RNA was precipitated and used to perform semiquantitative RT-PCR reactions.

Table II-1. Yeast strains used in this study

strain	Description	Source
ED665	<i>h⁻ ade6-210 leu1-32 ura4-D18</i>	Fantes, P., lab stock
JH43	<i>h⁻ ade6-M210 leu1-32</i> , pRIP42 integrated	Jeong, JH., lab stock
JH42	<i>h⁻ ade6-M210 leu1-32</i> , pJK148 integrated	
SJ01	<i>h⁻ ade6-M210 leu1-32 Δaco2/nmt42-aco2::ura4+</i>	
SJ02	<i>h⁻ ade6-210 leu1-32 ura4-D18 aco1 GFP::kanMX</i>	
SJ03	<i>h⁻ ade6-210 leu1-32 ura4-D18 aco2 GFP::kanMX</i>	
H90	<i>H90 ade6-210 leu1-32 ura4-D18</i>	
FY511	<i>H90 ade6-210 leu1-32 ura4-D18 mat3-M::ura4+</i>	From Dr. Allshire
<i>aco2ΔN</i>	<i>h⁻ ade6-210 leu1-32 ura4-D18 aco2ΔN::Nat</i>	
<i>aco2ΔN nmt42</i>	<i>h⁻ ade6-210 leu1-32 ura4-D18 aco2ΔN::Nat/ nmt42-</i>	
<i>aco2</i>	<i>aco2::leu1+</i>	
FY511	<i>H90 ade6-210 leu1-32 ura4-D18 mat3-M::ura4+</i>	
<i>aco2ΔN</i>	<i>aco2ΔN::Nat</i>	
<i>H90 aco2ΔN</i>	<i>H90 ade6-210 leu1-32 ura4-D18 aco2ΔN::Nat</i>	
<i>Δago1</i>	<i>h⁻ ade6-210 leu1-32 ura4-D18 Δago1::KanMX</i>	
<i>aco2ΔNΔago1</i>	<i>h⁻ ade6-210 leu1-32 ura4-D18 aco2ΔN::Nat</i> <i>Δago1::KanMX</i>	
<i>Δdcr1</i>	<i>h⁻ ade6-210 leu1-32 ura4-D18 Δdcr1::Nat</i>	
<i>aco2ΔNΔdcr1</i>	<i>h⁻ ade6-210 leu1-32 ura4-D18 aco2ΔN::KanMX</i> <i>Δdcr1::Nat</i>	
<i>Δclr3</i>	<i>h⁺ ade6-210 leu1-32 ura4-D18 Δclr3::KanMX</i>	
<i>aco2ΔNΔclr3</i>	<i>h⁺ ade6-210 leu1-32 ura4-D18 aco2ΔN::Nat Δclr3::KanMX</i>	
<i>aco2ΔNΔago1</i>	<i>h⁻ ade6-210 leu1-32 ura4-D18 aco2ΔN::Nat Δclr3::KanMX</i> <i>Δago1::hphMX</i>	
<i>Δclr3</i>	<i>Δago1::hphMX</i>	
<i>Δrrp6</i>	<i>h⁺ ade6-210 leu1-32 ura4-D18 Δrrp6::hphMX</i>	
<i>aco2ΔNΔrrp6</i>	<i>h⁺ ade6-210 leu1-32 ura4-D18 aco2ΔN::Nat Δrrp6::hphMX</i>	
<i>Δclr4</i>	<i>h⁻ clr4Δ::LEU2 otr1R(SphI)::ura4+ ura4-D/SE arg3-D3</i> <i>leu1-32</i>	From Dr. Allshire
<i>aco2ΔNΔclr4</i>	<i>h⁻ ade6-210 leu1-32 ura4-D18 aco2ΔN::Nat clr4Δ::LEU2</i>	
<i>Δmlo3</i>	<i>h⁻ ade6-210 leu1-32 ura4-D18 Δmlo3::KanMX</i>	From Dr. Yoon
<i>aco2ΔNΔmlo3</i>	<i>h⁻ ade6-210 leu1-32 ura4-D18 aco2ΔN::Nat</i> <i>Δmlo3::KanMX</i>	

<i>Δtfs1</i>	<i>h⁺ ade6-216 leu1-32 ura4-D18 Δtfs1::KanMX</i>	Bioneer
<i>aco2ΔNΔtfs1</i>	<i>h⁻ ade6-210 leu1-32 ura4-D18 aco2ΔN::Nat Δtfs1::KanMX</i>	
<i>Δchp1</i>	<i>h⁻ ade6-210 leu1-32 ura4-D18 Δchp1::KanMX</i>	
<i>aco2ΔNΔchp1</i>	<i>h⁻ ade6-210 leu1-32 ura4-D18 aco2ΔN::Nat Δchp1::KanMX</i>	
<i>Δswi6</i>	<i>h⁻ ade6-210 leu1-32 ura4-D18 Δswi6::KanMX</i>	
<i>aco2ΔNΔswi6</i>	<i>h⁻ ade6-210 leu1-32 ura4-D18 aco2ΔN::Nat Δswi6::KanMX</i>	
Aco2 FLAG	<i>h⁻ ade6-210 leu1-32 ura4-D18 aco2-5FLAG::Nat</i>	
<i>Δswi6</i> Aco2 FLAG	<i>h⁻ ade6-210 leu1-32 ura4-D18 Δswi6::KanMX aco2-5FLAG::hphMX</i>	
<i>Δchp1</i> Aco2 FLAG	<i>h⁻ ade6-210 leu1-32 ura4-D18 Δchp1::KanMX aco2-5FLAG::hphMX</i>	
Chp1 MYC	<i>h⁻ ade6-210 leu1-32 ura4-D18 chp1-13MYC::Nat</i>	
Aco2 FLAG	<i>h⁻ ade6-210 leu1-32 ura4-D18 aco2-5FLAG::hphMX</i>	
Chp1 MYC	<i>h⁻ ade6-210 leu1-32 ura4-D18 chp1-13MYC::Nat</i>	
<i>aco2ΔN</i> Chp1 FLAG	<i>h⁻ ade6-210 leu1-32 ura4-D18 aco2ΔN::Nat chp1-5FLAG::hphMX</i>	
Swi6 MYC	<i>h⁻ ade6-210 leu1-32 ura4-D18 swi6-13MYC::KanMX</i>	
Aco2 FLAG	<i>h⁻ ade6-210 leu1-32 ura4-D18 aco2-5FLAG::hphMX</i>	
Swi6 MYC	<i>h⁻ ade6-210 leu1-32 ura4-D18 swi6-13MYC::KanMX</i>	
<i>aco2ΔN</i> Swi6 FLAG	<i>h⁻ ade6-210 leu1-32 ura4-D18 aco2ΔN::Nat swi6-5FLAG::hphMX</i>	
Rrp6 TAP	<i>h⁻ ade6-210 leu1-32 ura4-D18 rrp6-TAP::Kan</i>	
Aco2 FLAG	<i>h⁻ ade6-210 leu1-32 ura4-D18 aco2-5FLAG::hphMX</i>	
Rrp6 TAP	<i>h⁻ ade6-210 leu1-32 ura4-D18 rrp6-TAP::Kan</i>	
Mlo3 FLAG	<i>h⁻ ade6-210 leu1-32 ura4-D18 mlo3-5FLAG::hphMX</i>	
<i>aco2ΔN</i> Mlo3 FLAG	<i>h⁻ ade6-210 leu1-32 ura4-D18 aco2ΔN::Nat mlo3-5FLAG::hphMX</i>	
<i>Δckb1</i> Swi6 FLAG	<i>h⁻ ade6-210 leu1-32 ura4-D18 ckb1::KanMX swi6-5FLAG::hphMX</i>	
<i>Δckb1</i> Swi6 FLAG	<i>h⁻ ade6-210 leu1-32 ura4-D18 ckb1::KanMX swi6-5FLAG::hphMX</i>	
FLAG Aco2 MYC	<i>h⁻ ade6-210 leu1-32 ura4-D18 aco2-13MYC::Nat</i>	

Table II-2. Plasmids used in this study

Plasmid Name	Description	Source
pREP1	Cloning plasmid with Leu marker	Maundrell, K., lab stock
pREP42-EGFP	Cloning plasmid for GFP imaging (Ura marker)	Chung, WH., lab stock
pREP-aco2-GFP	<i>aco2</i> promoter(p)- <i>aco2</i> -EGFP fusion on pREP42	
pREP-aco2AD-GFP	<i>aco2p-aco2</i> aconitase domain (AD;1-785 aa)-EGFP	
pREP-aco2RD-GFP	<i>aco2p-aco2</i> ribosomal domain (RD; 807-912 aa)-EGFP	
pREP-aco2ΔNLS-GFP	<i>aco2p-aco2</i> with NLS (884-891aa) deletion-EGFP fusion	
pREP1-aco2	<i>aco2p-aco2</i> fusion on pREP1	
pREP1aco2AD	<i>aco2p-aco2</i> AD(1-785 aa) fusion on pREP1	
pREP1-NL	<i>aco2p-aco2</i> with sv40 NLS (GCT CCT AAG AAG AAG CGT AAG GTT)-aconitase domain (AD;1-785 aa) on pREP1	
pREP1-aco2RD S-aco2AD	<i>aco2p-aco2</i> -ribosomal domain (RD;807-912 aa) on pREP1	
pREP1-aco2RD	<i>aco2p-aco2</i> -ribosomal domain (RD;807-912 aa) on pREP1	
pREP-MTS-aco2RDΔNLS	<i>aco2p-MTS-aco2</i> RD with NLS deletion on pREP1	
pCM42	Template for PCR to generate <i>nmt42p-aco2</i> construct	Lee, KC., lab stock
pREP1-aco2-polyAmut	<i>aco2p-aco2</i> with polyA site (AATAAA) mutation on pREP1	
pREP1-aco2C388,451,454S	<i>aco2p-aco2</i> with cysteine (388, 451, 454) mutation on pREP1	
pREP1-aco2C388S	<i>aco2p-aco2</i> with cysteine (388) mutation on pREP1	
pREP1-aco2C451S	<i>aco2p-aco2</i> with cysteine (451) mutation on pREP1	
pREP1-aco2C454S	<i>aco2p-aco2</i> with cysteine (454) mutation on pREP1	
pREP1-aco2ΔNLS	<i>aco2p-aco2</i> with NLS (AAA CAC AAG CGT CGT CAT CGT C) deletion on pREP1	
pET15b-Aco2Short	Overproduction of His-tagged Aco2 fragment (39-285 aa)	
pET15b-chp1-1/4	<i>chp1</i> -1/4 (1-235 aa) on pET15b	
pET15b-chp1-2/4	<i>chp1</i> -2/4 (228-461 aa) on pET15b	
pET15b-chp1-3/4	<i>chp1</i> -3/4 (456-803 aa) on pET15b	
pET15b-chp1-4/4	<i>chp1</i> -4/4 (804-960 aa) on pET15b	

pET15b-swi6	<i>swi6</i> on pET15b	
pET15b-swi6-CD	<i>swi6</i> -chromo domain (1-140 aa) on pET15b	
pET15b-swi6-HG	<i>swi6</i> -hinge region (1-264 aa) on pET15b	
pET15b-swi6- Δ HG	<i>swi6</i> delta hinge region (1-140, 265-329 aa) on pET15b	

Table II-3. Primers used in this study

	Sequence (5' nt position from the start or stop codon) ^a	Used for	
aco2 L1 (F)	GAGATTTACCGACATCGTTATTAC (-359, start)	Mutant generation	
aco2 L2 (R)	AAGTTTCGTCAATATCACAAAGCGGTGGAGTGCAAAGGAGGAACGAG (-59, start)		
aco2 L3 (F)	GGCGTGGTAAATCAAAAGGTTATA (-415, stop)		
aco2 L4 (R)	<u>AATTAACCCGGGGATCCGTCGGTTCAGTTTGAGTTCGGTAACCCT</u> (-27, stop)		
aco2 L5 (F)	<u>TCGATACTAACGCCGCCATCCCCCATGTATGCTGCTGACAACCTAA</u> (+36, stop)		
aco2 L6 (R)	GACTGCAGCGGTTTAAGTACAGG (+349, stop)		
aco2 L7 (F)	TCGCTTTGTAAATCATATGAAGCTTTCGCTTTCGGGCTCTTCG (+3, start)		
aco2 L8 (R)	AGACCACACGTCATAAACTGAAGC (+320, start)		
aco1 L3 (F)	GCTGCTCTCGAACCTCGTTATTTG (-333, stop)		
aco1 L4 (R)	<u>AATTAACCCGGGGATCCGTCGGTTCAGTTTGATGTCATGTTGCCAT</u> (-27, stop)		
aco1 L5 (F)	<u>TCGATACTAACGCCGCCATCCGGTTCCTTTTTTGTATGACAGGTC</u> (+43, stop)		
aco1 L6 (R)	ATTGTAGCACTACGACTTTACTGC (+353, stop)		
ura4-nmt-F	GCTTGTGATATTGACGAACTT		
ura4-nmt-/R	CATATGATTTAACAAAGCGA		
KanMX-F	CGACGGATCCCCGGGTTA ATT		
KanMX-R	GGATGGCGGCGTTAGTATCGA		
AMP-F	TCTTACTGTCATGCCATCCG		
AMP-R	GAATTATGCAGTGCTGCCAT		
aco2ΔNLS-F	GATCGTGTAATGAAACATAAACAACG		
aco2ΔNLS-R	TACTCGAACACTTAATGCGCTTTTAG		
aco2-F(P)	GAATT <u>CTGCAGT</u> ACCACCATCAGC, PstI site underlined		Plasmid construction
aco2-AD-EGFP- R(B)	GATTTAC <u>GGATCC</u> AGAATGGGCC, BamHI site underlined		
aco2-EGFP-R(B)	GAAAGGGGATCCGTTTCAGTTTGAG, BamHI site underlined		
aco2RD-F(S)	CCTGAGT <u>CGACT</u> GCTGATGCGTAT, Sall site underlined		
aco2-R(B)	GCTTAAATTGGATCCGTTACTCCTC, BamHI site underlined		
aco2AD-R(B)	ATATATAC <u>GGATCC</u> GCTTAGTGGTC, BamHI site underlined		
aco2 NLS-RD-F(N)	GAGGAGCATATGCGCTCCTAAGAAGAAGCGTAAGGTTCCGCGAAAAGGC CCAT TCTGGCGTG, NdeI site underlined		
aco2-gibson-F	GCCGTCGATGCTATGACCAATACA		

aco2-gibson-R	GGGAGACATTCTTTTACCCGG	
aco2-polyAmut-F	GTTATAGATAGCATCAAGCAACAACCT	
aco2-polyAmut-R	AGGTTGTTGCTTGATGCTATCTATAAC	
AMP-F	TCTTACTGTCATGCCATCCG	
AMP-R	GAATTATGCAGTGCTGCCAT	
aco2ΔNLS-F	GATCGTGTAAATGAAACATAAACAACG	
aco2ΔNLS-R	TACTCGAACACTTAATGCGCTTTTATG	
Oligo dT	TTTTTTTTTTTTTTTTTTTT	RT PCR
<i>act1</i> ⁺ Forward	TGAGGAGCACCTTGCTTGT	q-RT PCR and CHIP
<i>act1</i> ⁺ Reverse	TCTTCTCACGGTTGGATTTGG	
<i>ura4</i> ⁺ Forward	TCGCAGACATTGGAATACC	
<i>ura4</i> ⁺ Reverse	ATGGCAATTTGTGATATGAGC	
GPO987 (<i>dg</i> Forward)	GCGATGCCAAACAACAATATTG	
GPO986 (<i>dg</i> Reverse)	GATACTGATAATATTGAGATCCACAGCAC	
GTO223 (<i>dh</i> Forward)	GAAAACACATCGTTGTCTTCAGAG	
GTO226 (<i>dh</i> Reverse)	CGTCTGTAGCTGCATGTGAA	
JPO816 (<i>tlh1</i> ⁺ Forward)	CGTTTTTGATACCGGCGC	
JPO819 (<i>tlh1</i> ⁺ Reverse)	TTGCCGTAACGACATCATGG	
<i>IK8</i>	ATTCCTTTCTGAACCTCTCTGTTAT	siRNA northern
<i>IK9</i>	TTTGATGCCCATGTTCACTCCACTTG	
<i>IK10</i>	GGGAGTACATCATTCTACTTCGATA	
<i>SnR58</i>	GATGAAATTCAGAAGTCTAGCATC	
aco2-RACE-F	CGTGCCATGAATGGTCGTATTATT	RACE probe
aco2-NP-F	CGGTTTCTACCAATTCTTCTTAC	Northern probe
aco2-NP-R	GTGTTTGCAATGTATCATGCG	

CHAPTER III.
RESULTS & DISCUSSION

III.1. Characteristics of *S. pombe* aconitases

III.1.1. Two kinds of aconitases in *S. pombe*.

As an initial step to understand aconitase functions in *S. pombe*, I examined cellular localization of Aco1 and Aco2 by fusing GFP to their C-termini. Both Aco1 and Aco2 have mitochondrial targeting sequence (MTS) at N-termini, whereas Aco2 has a nuclear localization signal (NLS) near the C-terminus (Fig. III-1. A). Both Aconitase has conserved three cysteine residues. As predicted, Aco1-GFP was detected almost exclusively in mitochondria (Fig. III-1. B). On the other hand, Aco2-GFP signal is more diffuse, raising the possibility that Aco2-GFP is residing not only in mitochondria but also in the cytosol and in the nucleus (Fig. III-1. C). This contrasts with the report by genome-wide localization study (Matsuyama, Arai et al., 2006), but coincides with the presence of NLS in Aco2 (Jung, Seo et al., 2015).

III.1.2. Localization of Aco2 in mitochondria as well as in the cytosol and the nucleus.

To gain further insight of Aco2 localization, I made various Aco2 constructs with or without NLS in pREP42-based EGFP-fusion plasmids. Fluorescence signals from transformed WT cell were observed. Fig. III-2 demonstrated that in contrast to the wild type Aco2 that are distributed in mitochondria, cytosol, and possibly in the nucleus (Fig. III-2. A), deletion of NLS (KHKRRHR; residue 884-890) caused Aco2 to be localized almost exclusively in mitochondria (Fig. III-2. D). The variant that contains MTS and aconitase domain (AD) without ribosomal protein domain (RD), similarly to Aco1, was also confined almost exclusively to mitochondria (Fig. III-2. B). The ribosomal bL21 domain (RD) with NLS and

without MTS was localized almost exclusively to the nucleus (Fig. III-2. C). These observations demonstrate that the NLS in the bL21 domain is functional, and supports the possibility that the full-length Aco2 protein reside in the nucleus (Jung et al., 2015).

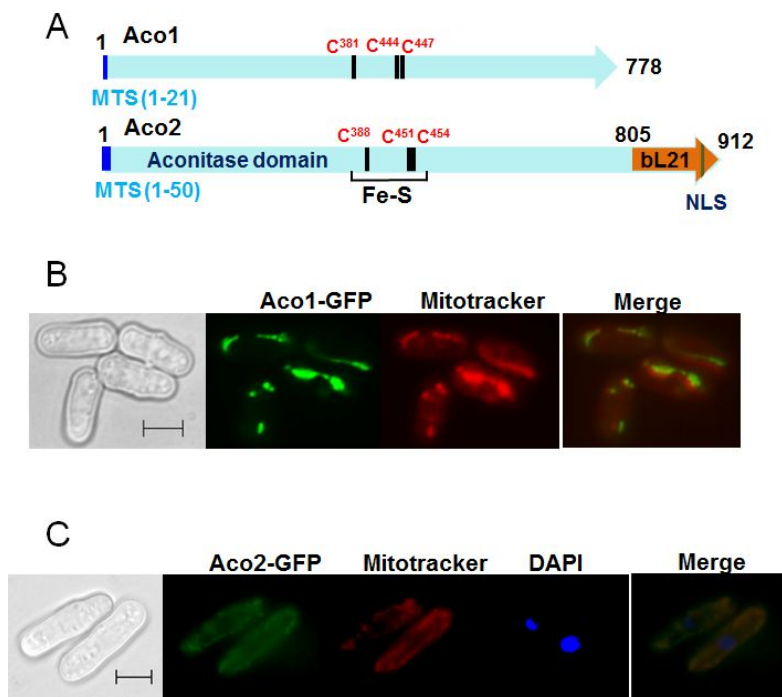


Fig. III-1. Distribution of Aco1 and Aco2 proteins among cell compartments

(Jung et al., 2015)

A. Diagram of domains and localization signals in Aco1 and Aco2. Predicted mitochondrial targeting sequences (MTS) at N-termini of Aco1 (1MGSRIFTQST LRSFSCAPVAA21) and Aco2 (1MKLCLSGSSQAIPSKGISLVAARFQSTASRASY VTPPYEKLGMGKLQQVRK50), nuclear localization signal (NLS) in the bL21 domain of Aco2 (KHKRRHR) were shown. Conserved cysteine residues predicted to bind [4Fe-4S] cluster were also indicated.

B. Fluorescence signals from Aco1-GFP expressed from a chromosomal fusion gene were shown along with Mitotracker signals. **(C)** Fluorescence signals from Aco2-GFP expressed from a chromosomal fusion gene were shown along with Mitotracker and DAPI signals. Scale bar, 5 μ m.

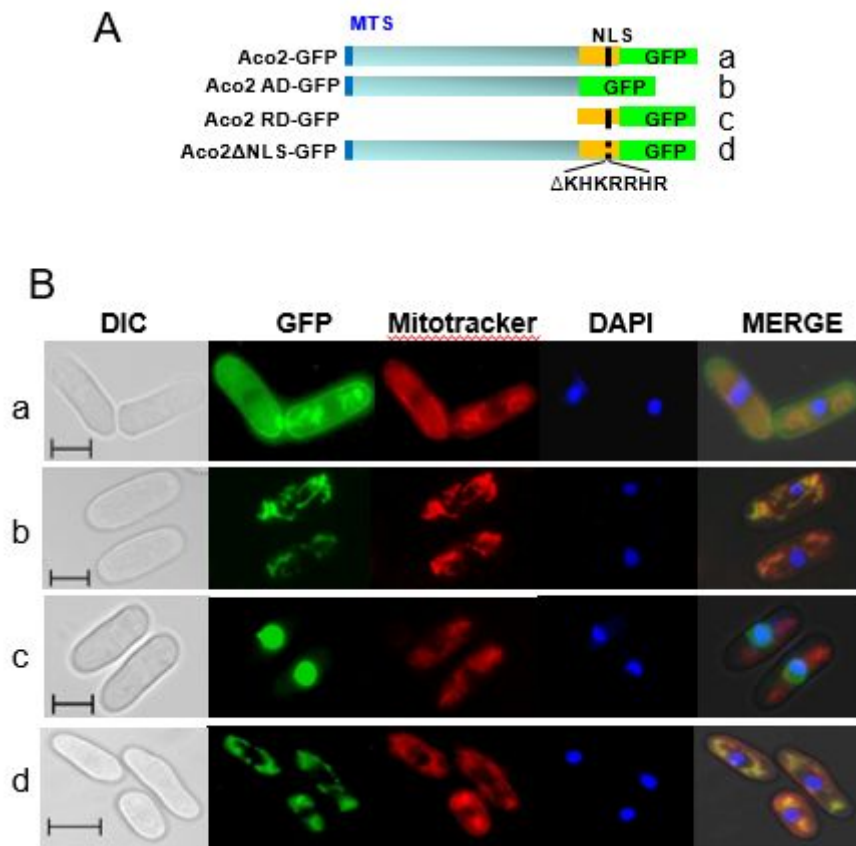


Fig. III-2. Contribution of NLS on the distribution of Aco2

(Jung et al., 2015)

A. Various Aco2 variants were cloned in pREP42-based EGFP-fusion plasmid.

B. Full-length Aco2 coding sequence (a), Aco2 aconitase domain (AD; 1-788 aa; b), ribosomal protein domain (RD; 807-912 aa; c), and NLS-deleted Aco2 (Δ NLS; d). Fluorescence from GFP, mitotracker, and DAPI in cells that express each of pREP42-based Aco2-GFP fusion constructs. Scale bar, 5 μ m.

III.1.3. RNAs and Proteins produced from *aco2*⁺ gene.

III.1.3.1. The *aco2*⁺ gene produces two kinds of transcripts by alternative selection of poly (A) site.

Since the null mutant of *aco2* is non-viable as reported (Kim, Hayles et al., 2010), I constructed a conditional mutant by placing the *aco2*⁺ gene under the control of *nmt42* promoter (no message in thiamine) which is repressible by thiamine. *Aco2*⁺ conditional mutant showed growth defects on EMM containing thiamine (Fig. III-3).

When the transcripts of the *aco2*⁺ gene were analysed by Northern blot, two *aco2*⁺-specific transcripts were detected in WT cell (Fig. III-4. A). I determined the 5' and 3' ends of these transcripts by RACE analysis. The 5' RACE revealed that the two transcripts have 5' ends at the same position, 53 nucleotides upstream from the start codon (Fig. III-4. C). On the other hand, the 3' RACE revealed that the two transcripts differ by the site of poly (A) addition (Fig. III-4. B). Whereas the longer one encompassed all the coding sequences of aconitase and bL21, the shorter one had poly (A) tail added at the 2418 nt (relative to start codon), changing the 806th codon from TAT (for Tyr) to TAA stop codon. Hence, the short transcript encompassed only the aconitase domain. Fig. III-4. C summarizes the structure of two transcripts generated from the *aco2*⁺ gene (Jung et al., 2015).

III.1.3.2. Two kinds of proteins produced from *aco2*⁺ transcripts.

I then examined Aco2 proteins by Western blot using polyclonal antibodies against Aco2 protein. Results in Fig. III-5. A demonstrate two *aco2*-specific bands, whose mobility coincides with the full-sized fusion product (912 aa; 99 kDa) and the shorter one with aconitase domain only (805 aa; 87 kDa). This antibody cross-reacted with Aco1 protein (82 kDa), as judged by its mobility shift in *aco1*-GFP

strain by 26 kDa (data not shown). Whether the bL21 domain can be cleaved off from the fusion protein was examined by detecting GFP portion of the Aco2-GFP protein produced in the fusion strain. Results in Fig. III-5. B demonstrated that GFP-tagged full-sized protein was detectable, whereas the smaller GFP-linked ribosomal protein (44.3 kDa) was not. This supports the conclusion that bL21 may not exist as a single domain form, unless GFP inhibited processing. Therefore, the *aco2*⁺ gene produces two kinds of proteins; one with aconitase domain only that is targeted almost exclusively to mitochondria, and the other with both aconitase and bL21 domains, which are targeted to both mitochondria and the nucleus (Jung et al., 2015).

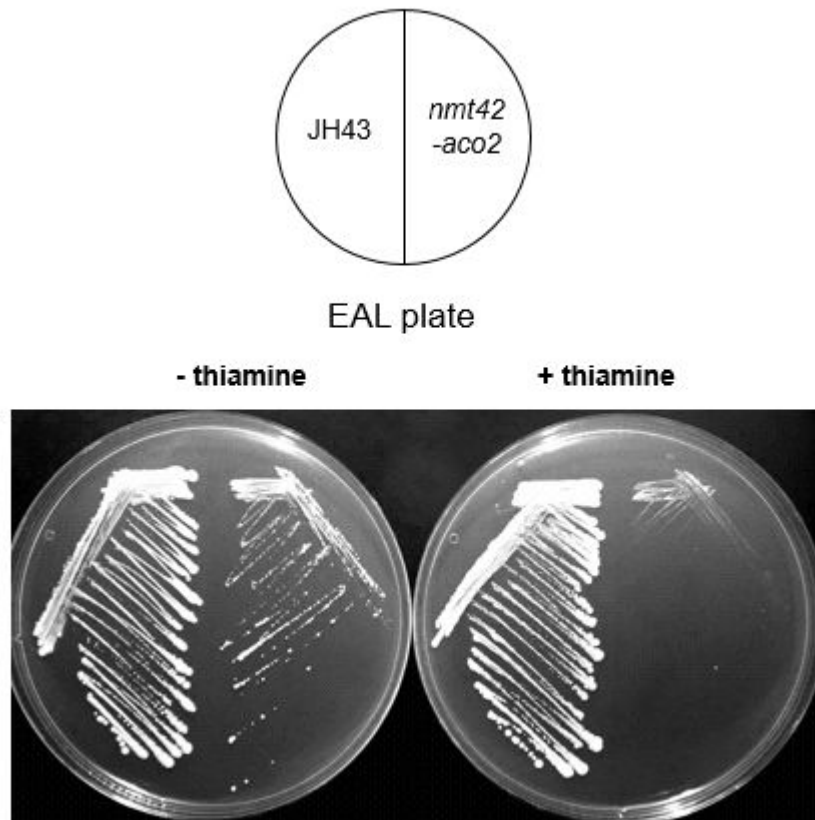


Fig. III-3. Growth characteristics of *nmt42-aco2* conditional mutant

Wild type (JH43) and *nmt42-aco2* conditional mutant strains were streaked on EMM plate w/ or w/o 10 μ M thiamine followed by incubation at 30 $^{\circ}$ C.

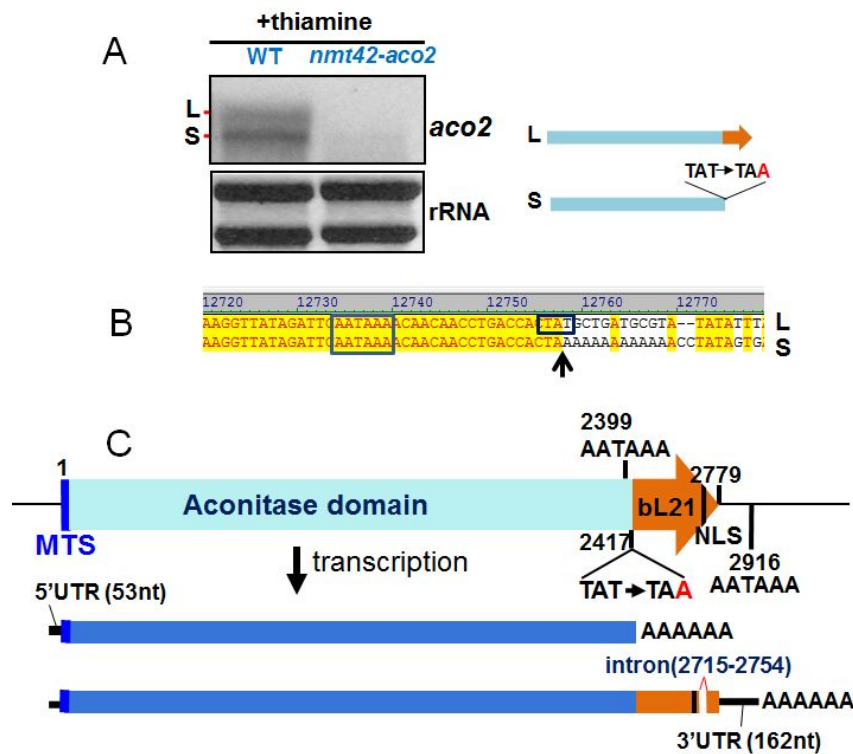


Fig. III-4. Two kinds of transcripts produced from the *aco2*⁺ gene

(Jung et al., 2015)

A. Northern blot analysis of *aco2*⁺ transcripts produced from the wild type (JH43) and *nmt42-aco2* cells grown in the presence of thiamine.

B. The long (L) and short (S) transcripts were analysed by 3' RACE to yield sequences near 3' ends. The position of poly (A) addition in short transcript, and the changes of codon from TAT (in long transcript) to TAA (in short transcript) were indicated.

C. Diagram of two *aco2*⁺ transcripts generated by alternative selection of poly (A) site. The position of NLS and the spliced intron in bL21 domain was also indicated.

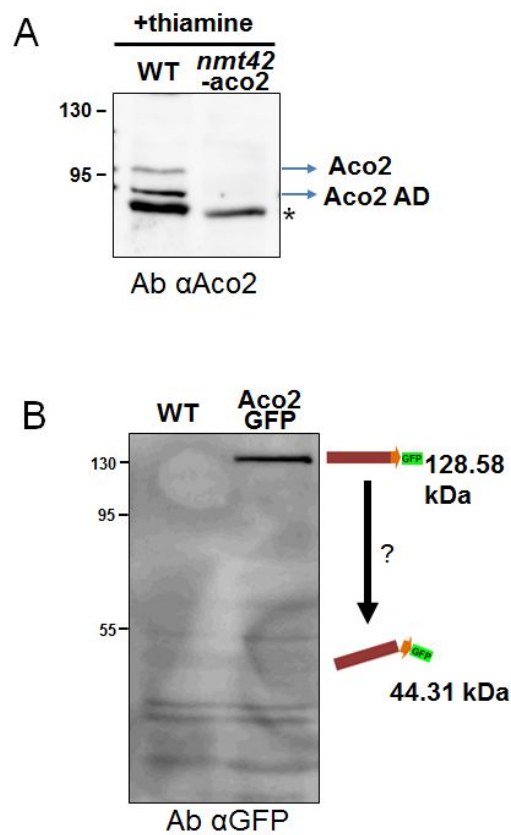


Fig. III-5. Production of two kinds of Aco2 proteins

(Jung et al., 2015)

A. Western blot analysis of proteins obtained from the wild type and *nmt42-aco2* mutant treated with thiamine (10 μ M). Polyclonal antibodies against Aco2 were used. Two protein bands with predicted sizes for full length Aco2 and Aco2-AD were indicated. Cross-reactivity with Aco1 was marked with an asterisk.

B. Western blot analysis with antibody against GFP. Protein samples from the wild type and *aco2*-GFP fusion strains were analyzed by antibody against GFP.

III.2. Roles of Aco2 in mitochondria.

III.2.1. Aco2 is essential for cell viability due to the ribosomal protein domain.

Whether both domains of Aco2 are needed for cell viability was examined by introducing variants of *aco2* gene on multi-copy plasmid to the conditional *nmt42-aco2* mutant strain. In addition to the *aco2*⁺ gene that produces two types of transcripts and proteins (L and S), I made four additional constructs of *aco2* on pREP-based plasmid, producing various single-domain or two-domain products expressed from its own (*aco2*) promoter (Table 2). Cell viability assay in Fig. III-6 demonstrates that the non-viable phenotype of *nmt42-aco2* strain on thiamine-containing plates was fully complemented by the wild type *aco2*⁺ expression (pAco2). Expression of the aconitase domain only (pMTS-Aco2AD; 1-785 aa) or the ribosomal protein domain only (pAco2RD; 807-912aa without MTS; RD1) did not rescue the viability defect. However, the ribosomal domain linked with MTS (1-50 aa) without NLS (pMTS-Aco2RDΔNLS; RD2) was able to restore cell viability dramatically. The Aco2 variant whose poly (A) signal (AATAAA at 2399 nt) was mutated from TCA ATA AAA to AGC ATC AAG (pAco2-polyAmut; AAT) and hence produces only the long two-domain product, restored the growth as well as the wild type *aco2*⁺. These results indicate that it is primarily due to the presence of the bL21 domain that conferred essentially required function for cell viability. The slight difference between the effects of wild type or poly (A) mutated *aco2* and the single domain bL21 (RD2) construct may reflect the contribution from the fusion of aconitase domain in conferring optimal viability (Jung et al., 2015).

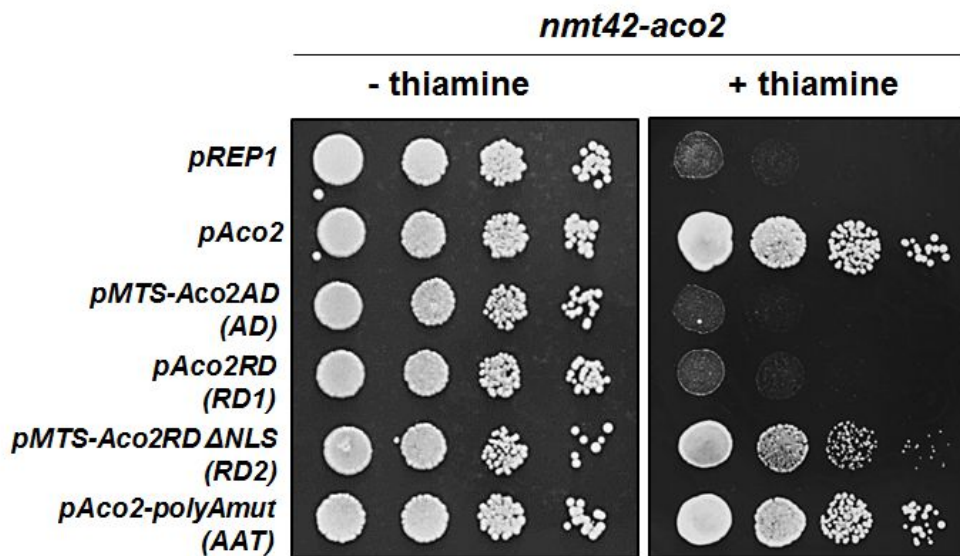


Fig. III-6. Restoration of viability of Aco2-depleted cells by bL21

(Jung et al., 2015)

Restoration of viability of Aco2-depleted cells by bL21. Spotting assays were done on EMM plates in the presence and absence of 10 μ M thiamine. The *nmt42-aco2* strain was transformed with pREP1-based plasmids expressing wild type and variant Aco2 proteins from its own promoter; pREP-aco2 (full-length and aconitase domain of Aco2), pREP-MTS-Aco2AD (aconitase domain, 1-805 aa), pREP-aco2RD (ribosomal protein domain, RD1, 808-912 aa), pREP-MTS-aco2RD Δ NLS (mitochondrially targeted ribosomal protein domain, RD2), and pREP-aco2-polyAmut (full length two-main product only, AAT). In *aco2-polyAmut*, poly (A) signal at 2399 nt was mutated without changing codons by changing TCA ATA AAA to AGC ATC AAG.

III.2.2. Aco2 is needed for mitochondrial translation.

Some mitochondrial functions including translation are essentially required for cell viability. Whether bL21 domain of Aco2 contributes to mitochondrial translation was examined, by monitoring ³⁵S-methionine-incorporated proteins in the presence of cycloheximide that inhibits cytosolic translation. Fig. III-7. A demonstrated that the depletion of Aco2 by thiamine in *nmt42-aco2* strain inhibited synthesis of mitochondrial proteins. The lower level of translation in the *nmt42-aco2* strain than in the WT in the absence of thiamine is thought to be due to lower Aco2 expression from the *nmt42* promoter (Basi, Schmid et al., 1993), compared with the native promoter. I then examined the contribution of different domains and mutations of Aco2 in mitochondrial translation. The *nmt42-aco2* conditional mutant was transformed with various *aco2* mutants used in the viability assay (Fig. III-6). The results in Fig. III-7. B demonstrate that the constructs that restored cell viability (Fig. III-6) also enabled mitochondrial translation. Therefore, the ribosomal protein domain of Aco2 contributes primarily to ensure mitochondrial translation. The aconitase domain by itself was not effective, whereas its presence as a fused form in the wild type (*aco2*⁺) and poly (A) mutated (AAT) construct contributed to achieve optimal translation. I estimated whether Aco2 depletion affected mitochondrial DNA stability or mitochondrial transcription. Mitochondrial DNA copy number as determined by qRT-PCR was similar in the wild type and *nmt42-aco2* cells grown in the presence of thiamine (data not shown). The amount of mitochondrially encoded RNAs (*cox1*, *cox2*, *cox3*) did not change either by depleting Aco2 (data not shown). These results indicate that the bL21 domain by itself, and more optimally in the fused form with aconitase domain, contributes to mitochondrial translation. In *S. pombe*, there is an additional gene (*img2*; SPAC3H8.03) that is annotated to encode bL21 (Mrpl49). I obtained the Δ *img2* mutant from the Bioneer deletion collection, and confirmed its mutated sequence. As reported from genome-wide

studies, the mutant was grown normally (Hayles, Wood et al., 2013, Kim et al., 2010). When examined for mitochondrial translation, I found that *Img2* is dispensable (Fig. III-8). Therefore, the *aco2⁺* is the only critical gene that encodes mitochondrial ribosomal subunit protein L21 (Jung et al., 2015).

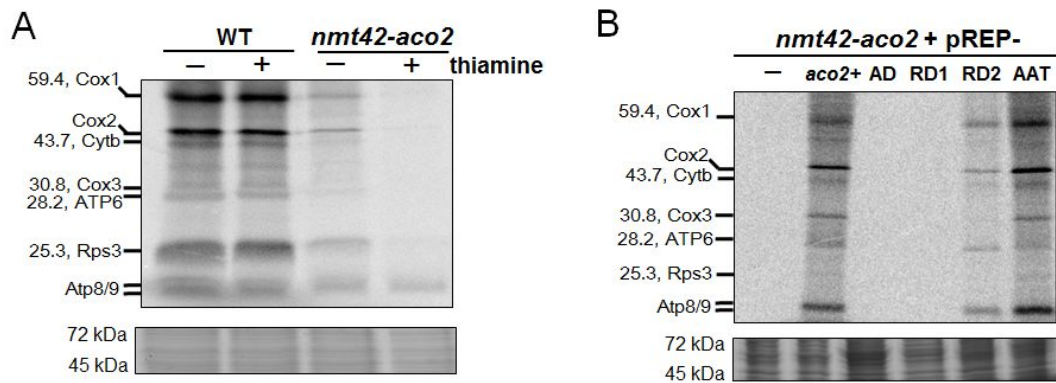


Fig. III-7. Contribution of Aco2 to mitochondrial translation

(Jung et al., 2015)

A. *In vivo* labeling of mitochondrial translation in the wild type and *nmt42-aco2* strains grown in EMM with 0.1% glucose and 2% galactose in the presence or absence of 10 μ M thiamine. TCA-precipitated proteins were analyzed on 17.5% SDS-PAGE, followed by autoradiography. A portion of Coomassie-stained gel of the same protein samples was presented as a loading control.

B. Complementation of *nmt42-aco2* strain with various Aco2 mutants for restoring mitochondrial translation. The *nmt42-aco2* strain was transformed with pREP1-based plasmids that express wild type Aco2 (*aco2+*), aconitase domain (AD; 1-804 aa), ribosomal protein domain (RD1, 808-912 aa), mitochondrially targeted ribosomal domain (RD2, MTS-RD Δ NLS), polyA-mutated *aco2* (AAT), in parallel with parental pREP1 plasmid (-).

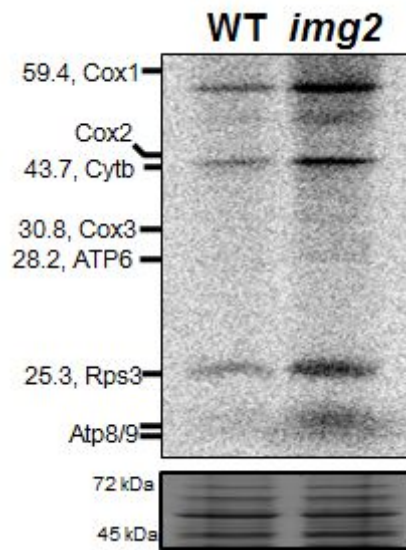


Fig. III-8. Contribution of *Img2* to mitochondrial translation

(Jung et al., 2015)

Contribution of *Img2* to mitochondrial translation. The wild type and *img2* mutant strains were grown in EMM with 0.1% glucose and 2% galactose. Proteins labeled with [³⁵S] methionine in the presence of cycloheximide were analyzed by 17.5% SDS PAGE and autoradiography as described in the text. A portion of Coomassie- stained gel of protein samples was presented as a loading control.

III.2.3. Mitochondrial membrane potential is decreased in *nmt42 aco2* mutant.

Because mitochondrial translation was decreased in *nmt42 aco2* mutant, it could be possible that mitochondrial membrane potential in *nmt42 aco2* mutant was decreased. To analysis the mitochondrial membrane potential of *aco2* conditional mutant, mitochondria were stained in live cells with Mitotracker Red, a fluorescent membrane-potential sensitive dye. The signal from mitochondria of *nmt42 aco2* mutant growing with thiamine was weaker than that of wild-type growing with thiamine (Fig. III-9. A). Next, mitochondrial membrane potential ($\Delta\psi$) monitored by flow cytometry using fluorescent probe, 3,3'-dihexyloxycarbocyanine (DiOC₆(3)) that has been recently used for analyzing $\Delta\psi$. Theoretically, due to the necessity of an adequate intracellular concentration of fluorescent dye, changes in membrane potential influence mitochondrial stainability, and it can mimic changes in $\Delta\psi$ (Rajpurohit et al., 1999). Expectedly, DiOC₆(3) fluorescence was decreased in *nmt42 aco2* conditional mutant growing with thiamine at stationary phase (Fig. III-9. B). Together, this result indicates that mitochondrial membrane potential were decreased in *aco2* conditional mutant.

III.2.4. Aco2 interacts with Aco1 in mitochondria.

To examine whether Aco2 interacts with Aco1 *in vivo*, each gene was cloned in pREP41-VC and pREP42-VN for BiFC analysis (Hu, Chinenov et al., 2002). Full size of Aco2 and aconitase domain-only proteins were fused with the N-terminal half of Venus (Aco2 VN and Aco2 AD VN) at C-terminus and Aco1 protein was fused with the C-terminal half of Venus (Aco1 VC) at C-terminus as previously described (Sung & Huh, 2007). Negative signal was detected in cells transformed with only pREP-VN and VC vectors. The fluorescence signals were detected in mitochondria in both Aco2 AD VN-Aco1 VC and Aco2 VN-Aco1 VC transformed

cells compared to negative control (Fig. III-10). Because Aco2 was localized not only in mitochondria but also in the nucleus while Aco2 AD protein was localized only in mitochondria, the fluorescence signal of Aco2 VN-Aco1 VC was weaker than Aco2 AD VN- Aco1 VC. So this data indicates that both Aco2 AD protein and Aco2 protein were interacted with Aco1 in mitochondria.

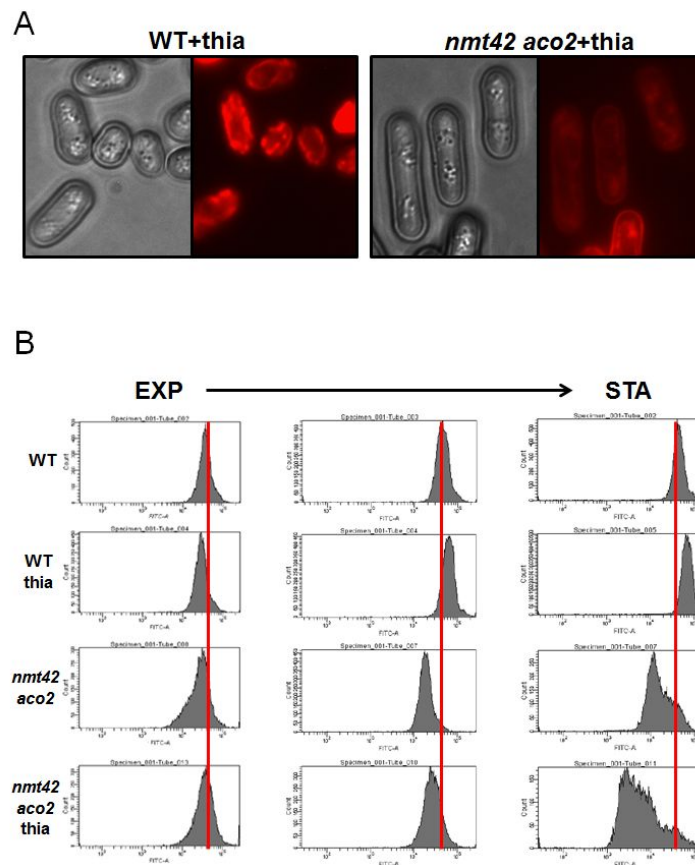


Fig. III-9. Mitochondrial membrane potential in Aco2 conditional mutant

A. JH43 and *nmt42 aco2* mutant were cultured in EMM medium with thiamine (10 μ M). At stationary phase, cells were stained with Mitotracker Red dye, which is mitochondrial membrane-potential sensitive dye. The Fluorescence signals were detected by Zeiss Axiovert 200M.

B. JH43 and *nmt42 aco2* mutant were cultured in EMM medium with and without thiamine (10 μ M). During growth phases, mitochondrial membrane potentials were monitored by flow cytometry.

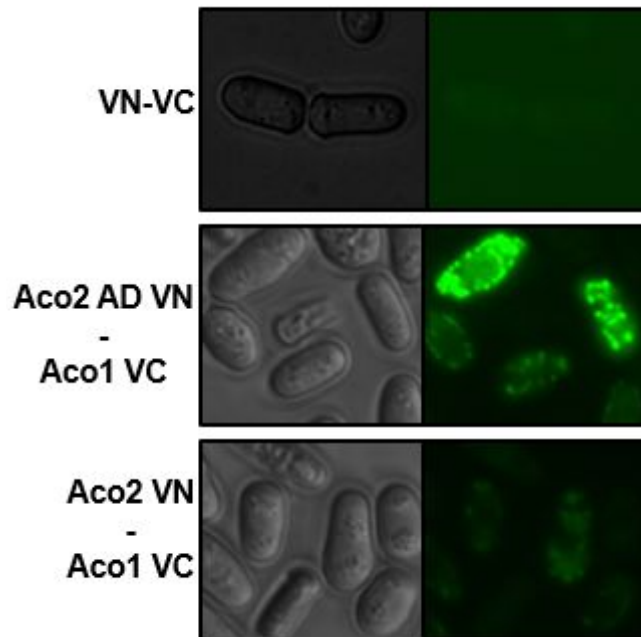


Fig. III-10. BiFC analysis of Aco2 with Aco1

Both VC tagged Aco2 AD protein and VC tagged Aco2 protein interact with Aco1 in mitochondria. Because Aco2 AD protein is localized only in mitochondria, whereas Aco2 protein is localized both mitochondria and the nucleus, fluorescence signal from mitochondria in VC tagged Aco2 AD protein is stronger than that of VC tagged Aco2 protein.

III.3. Roles of Aco2 in the nucleus

III.3.1. Aco2 nuclear function is not essential for cell viability.

In previous study, the possibility that Aco2 may localized not only in mitochondria but also in the cytosol and the nucleus was proposed (Jung et al., 2015). In many other organisms, aconitase serves additional roles in addition to enzymatic function (Alen & Sonenshein, 1999b, Chen et al., 2007, Chen et al., 2005, Hentze et al., 2010), so I continued to find out another function of Aco2 especially in the nucleus. To figure out nuclear function of Aco2, two types of *aco2* nuclear mutants which have defects only in the nucleus and normal function in mitochondria were constructed. Aco2 has an nuclear localization signal (NLS) near the C-terminus. In first type Aco2 nuclear mutant, an NLS sequence (aaacacaagcgtcgtcatcgtc) in the C-terminus of *aco2+* gene was deleted to make Aco2 localize only in mitochondria. This mutant was named as *aco2ΔNLS* mutant (Fig. III-11. A). It is confirmed that deletion of an NLS caused Aco2 to be localized almost exclusively in mitochondria before (Jung et al., 2015). Because eight amino acids (KHKRRHRH) were deleted in the bL21 domain of Aco2 in the *aco2ΔN* mutant, it may cause some defects in mitochondrial function. To avoid these kinds of side effects derived from deleting an NLS sequence, second type Aco2 nuclear mutant was constructed. With deleting NLS sequence in the bL21 domain in its own chromosomal location, whole *aco2* gene was integrated in *leu1* site under *nmt42* promoter. In normal condition (without thiamine), non-mutated Aco2 in *leu1* site was expressed along with *aco2ΔN* mutant. After thiamine was added, *leu1* site derived non-mutated Aco2 expression was repressed. After few divisions, only *aco2ΔN* mutant was existed in the cell and then Aco2 function in the nuclear could be monitored. This mutant was called *aco2ΔN nmt42 aco2* mutant (Fig. III-11. B). Because second type nuclear mutant has several benefits, some problems derived from first type *aco2ΔN* mutant could

be avoided. First, non-mutated normal Aco2 was expressed and resided in mitochondria before thiamine was added. Second, non-mutated Aco2 was resided in the nucleus before thiamine was added. At last, because majority of Aco2 was localized in mitochondria, after thiamine was added, for a while non-mutated Aco2 protein resided in mitochondria before degradation. Both mutants were used to identify nuclear function of Aco2 in the cell.

Aco2 is an essential protein. It is defined that the essentiality of Aco2 was because of the bL21 domain in C-terminus (Jung et al., 2015). With two types of Aco2 nuclear mutants, essentiality of Aco2 function in the nucleus was monitored with spotting assay (Fig. III-12. A and B). To test viability of these mutants, *aco2ΔN* mutant was spotted on YES plate. Because complex media YES has some thiamine, *aco2ΔN nmt42 aco2* mutant was spotted on EMM with or without thiamine (10uM). Both mutant had no growth defects on each media. From these results, it is clear that Aco2 nuclear function is not essential for cell viability. According to Pombase, almost all mitochondrial ribosomal proteins are essential, so Aco2 might have essentiality roles in mitochondrial translation not in the nuclear function.

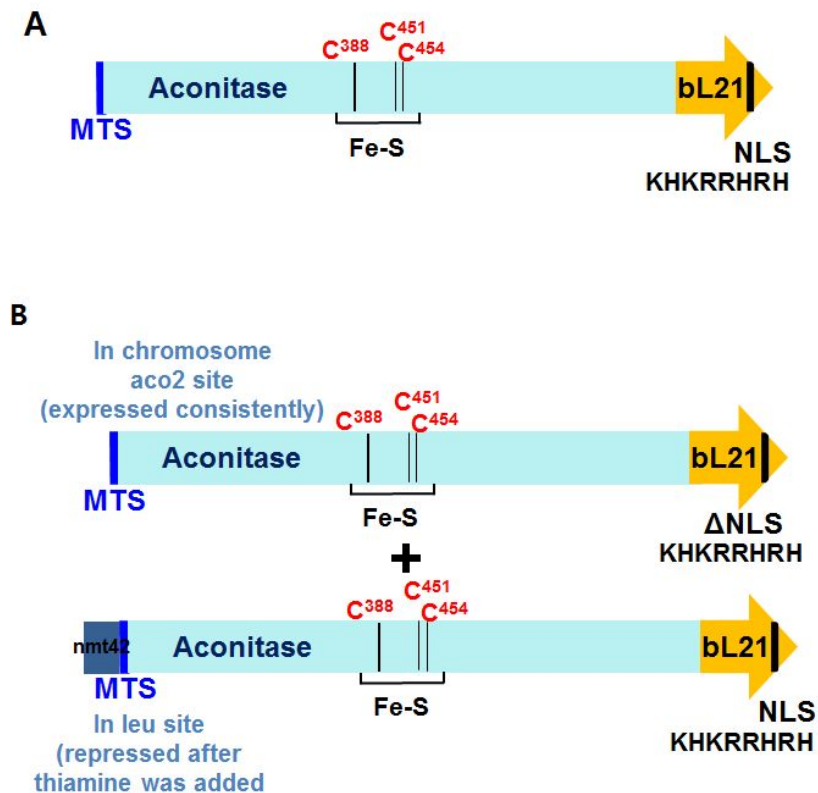


Fig. III-11. Diagram of Aco2 nuclear mutants

A. Diagram of Aco2 with major domains and localization signals. N-terminal mitochondrial targeting sequence (MTS) and nuclear localization signal imbedded in the mitochondrial ribosomal protein (bL21) domain were indicated. In the *aco2* Δ N mutant, where the NLS sequence (KHKRRHRH) was deleted, the mutant protein is absent in the nucleus, being exclusively localized in mitochondria (Jung et al., 2015).

B. Diagram of *aco2* Δ NLS *nmt42**aco2* mutant. In the *aco2* Δ NLS *nmt42* *aco2* mutant, NLS sequence (KHKRRHRH) deleted Aco2 is expressed along with Aco2 protein under *nmt42* promoter at *leu* site.

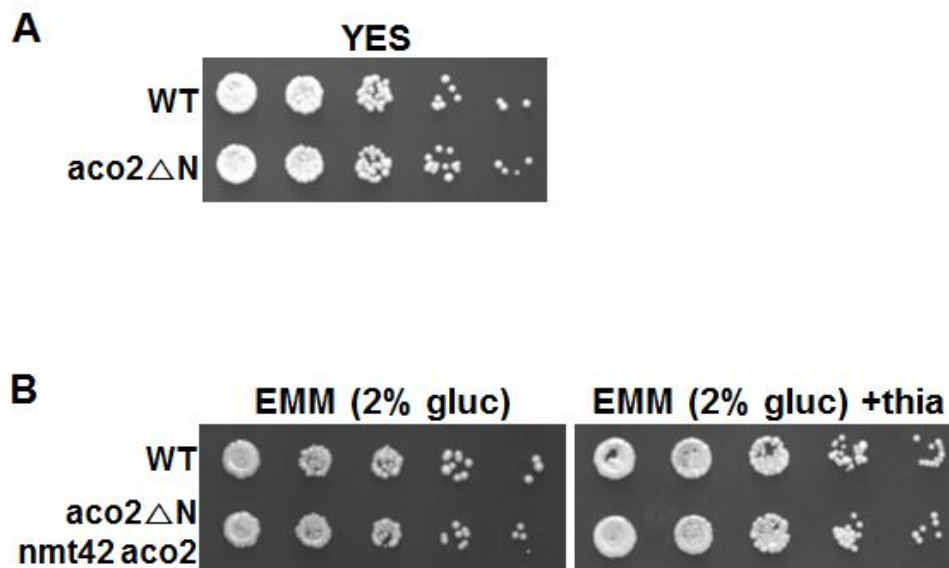


Fig. III-12. Spotting assays of Aco2 nuclear mutants

A. Spotting assays were done on YES plate. *Aco2ΔN* mutant has no growth defect on YES media.

B. Spotting assays were done on EMM plate with or without 10uM thiamine. *Aco2ΔN nmt42aco2* mutant has no growth defect on EMM media.

III.3.2. Functions of Aco2 in centromeric heterochromatin maintenance.

III.3.2.1. Aco2 nuclear mutant restores elevated RNA levels in RNAi mutants at centromere.

I continued to work on to figure out the function of Aco2 in the nucleus. In *C.elegans*, *aco2* (F54H12.1) was screened out among the genetic components required for the RNAi pathway and heterochromatin formation (Kim, Gabel et al., 2005). Aco2 protein in *S. pombe* is about 64% homologous to *C. elegans* Aco2. So I proposed the possibility that Aco2 may function in the RNAi related heterochromatin formation pathway. In fission yeast, the small RNA pathway acts in generating pericentromeric heterochromatin (Allshire & Karpen, 2008, Moazed, 2009). When RNA is transcribed at centromere, double-stranded RNA is generated by RNA-dependent RNA polymerase (RdRP, rdp1) (Volpe et al., 2002). These double-stranded RNA triggers RNAi pathway, which is processed by Dicer (Dcr1) into ~23nt siRNAs (Hannon, 2002). And then small RNAs (siRNAs) are loaded onto Argonaute (Ago1) which is a component of an effector complex called RITS (RNA-induced transcriptional silencing) (Verdel et al., 2004). So any of these genes are deleted, heterochromatin is disrupted (Hall, Shankaranarayana et al., 2002). To test whether Aco2 is involved in heterochromatin formation process, RNA levels of centromeric *dg/dh* regions in both type of *aco2* nuclear mutants were monitored. In both mutants, centromeric RNA levels were not changed (Fig. III-13. A and B). When thiamine was added in wild type cell, centromeric transcribed RNA levels were decreased (Fig. III-13. B). But compared to wild type cell with thiamine (10uM), in *aco2ΔN nmt42 aco2* mutant with thiamine, centromeric RNA levels were not changed though it has lower RNA levels compared to thiamine free *aco2ΔN nmt42 aco2* mutant. Because two types of *aco2* nuclear mutants have same effect at centromere, further experiments were performed with the *aco2ΔN* mutant.

Although in *aco2ΔN* single mutant, *dg/dh* RNA levels were not changed, it is clear that *aco2ΔN* restored elevated RNA levels in RNAi-deficient cells except *Δchp1 mutant* (Fig. III-13. A). From these results, it is proposed that Aco2 might related in centromeric heterochromatin formation in the nucleus.

III.3.2.2. Aco2 nuclear mutant restores functional heterochromatic defects in RNAi mutants at centromere.

To figure out *aco2ΔN* mutant also restores functional heterochromatin defects in RNAi mutants, heterochromatin indicator H3K9me2, RNA PolII and Swi6 enrichment was monitored with ChIP analysis. Loss of RNAi pathway results in decrease of H3K9me2 level at centromere (Hall et al., 2002). *Aco2ΔN* mutant restored H3K9me2 level in the *Δago1* mutant (Fig. III-14. A) and the *Δdcr1* mutant (Fig. III-14. B). In the absence of Clr3, which is known as histone deacetylase, H3K9me2 level at centromere is decreased (Buscaino, Lejeune et al., 2013). The H3K9me2 level at centromere was comparable in *Δclr3* and *aco2ΔN Δclr3* double mutants same as RNA level (Fig. III-14. A). In *Δago1 Δclr3* mutant, H3K9me2 level was lower than *Δago1* mutant and in *Δago1 Δclr3 aco2ΔN* triple mutant, H3K9me2 level was not restored at all (Fig. III-15. A). This observation suggested that *aco2ΔN* suppression pathway requires deacetylated H3K14 by Clr3. Because Clr4 is the sole H3K9 methyltransferase in fission yeast, in *Δclr4* mutant, H3K9methylation level is completely removed (Zhang, Mosch et al., 2008) which serves a role as a binding site of many heterochromatin proteins. *Aco2ΔN* mutant fail to suppress *Δclr4* mutant which means suppression required heterochromatin machinery (Fig. III-15. B). H3K9me recruited HP1 protein Swi6 is important for heterochromatin assembly and transcriptional silencing (Fischer et al., 2009, Yamada, Fischle et al., 2005). Similar to H3K9me2 level, *aco2ΔN* mutant restored Swi6 level at centromere (Fig. III-14. D).

Nascent transcript-bound RITS recruits the RNA-directed RNA polymerase

complex (RDRC; Rdp1, Cid12 and Hrr1) (Buhler & Moazed, 2007). Same as RNA levels, *aco2ΔN* mutant suppressed RNAPII level in the *Δago1* mutant (Fig. III-14. C).

Mitotic chromosome is impaired in the RNAi mutants and are sensitive to the microtubule destabilizing compound thiabendazole (TBZ) (Hall, Noma et al., 2003). *Aco2ΔN* mutant restored TBZ sensitivity in the *Δago1* mutant (Fig. III-14. E). Together, these results demonstrate that *aco2ΔN* mutant restores functional heterochromatin defects of RNAi mutants.

III.3.2.3. Aco2 nuclear mutant restores heterochromatic function as small RNA independent pathway.

Centromeric transcripts are processed in siRNAs by RNAi machinery, and these siRNAs promote heterochromatin assembly and the generation of additional siRNAs (Buker, Iida et al., 2007). So when RNAi machinery is impaired, siRNAs are undetectable (Halic & Moazed, 2010). To gain more information of how *aco2ΔN* mutant restores RNAi mutants, small RNA levels were monitored in double mutant. Unlike other factors, *aco2ΔN* mutant did not restore small RNA levels in RNAi mutants (Fig. III-14. F). From these results, it is clear that restoration pathway is not related to small RNA generation.

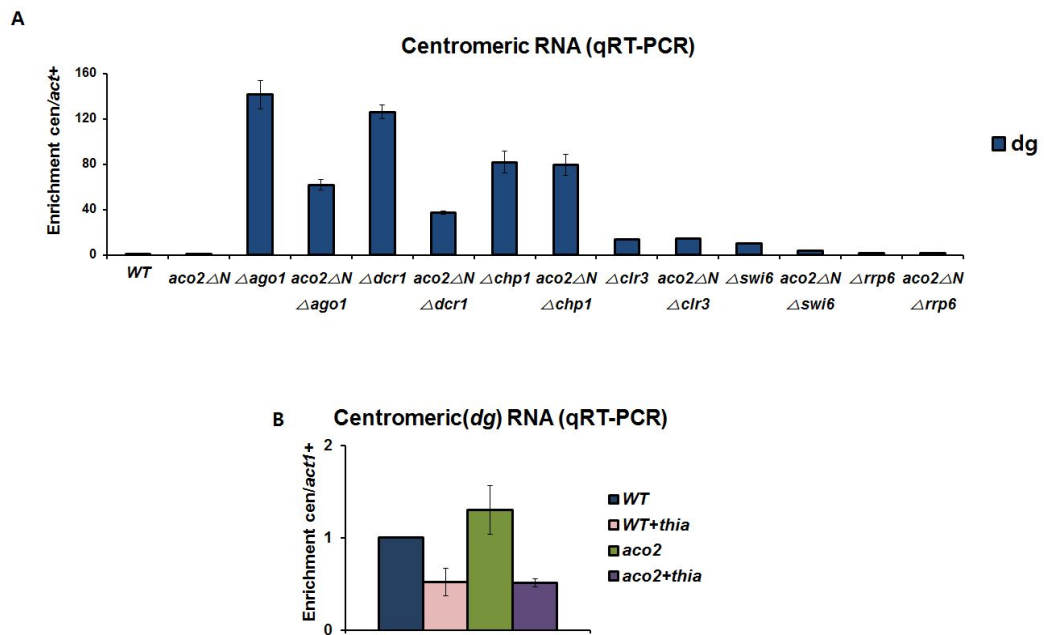


Fig. III-13. Effect of NLS-deletion of *aco2* gene (*aco2ΔN*) on RNA expression in the centromeric region

A. Production of centromeric *dg/dh* RNAs in *aco2ΔN* and other heterochromatin mutant strains. The *dg* and *dh* RNAs that reflect the extent of heterochromatin formation were monitored by qRT-PCR along with *act1+* RNA as a control. Relative enrichment (centromeric RNA/*act1+*) value was plotted for each sample. The *aco2ΔN* mutant restore elevated RNA level in $\Delta ago1$, $\Delta dcr1$ and $\Delta swi6$ mutant.

B. qRT PCR analysis of RNA level at centromeric-*dh* region relative to *act1+*. In *aco2ΔN nmt42* with thiamine, centromeric RNA level is same as WT with thiamine.

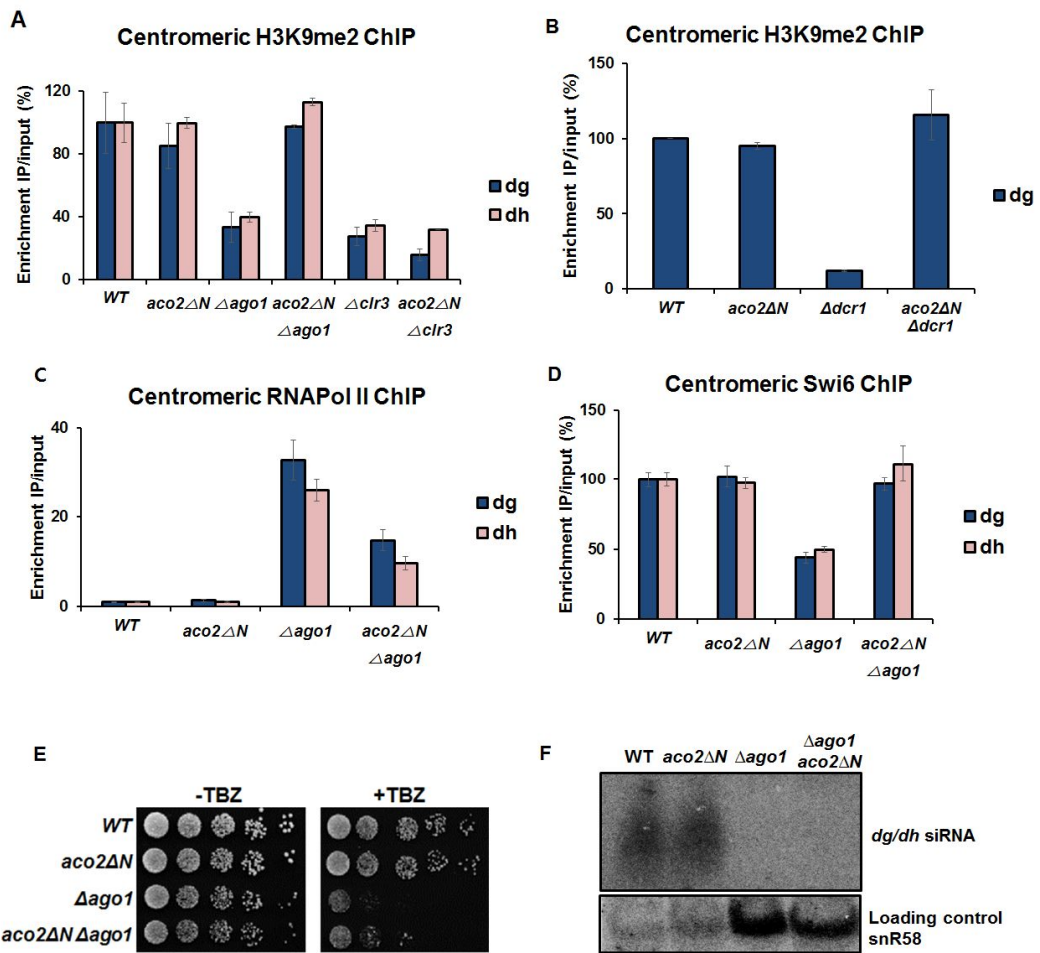


Fig. III-14. Effect of *aco2ΔN* mutation on the heterochromatin formation in the centromeric region

Levels of modified histone (H3K9me₂; **A** and **B**) and RNA polymerase II (**C**) and Swi6 level (**D**) bound in the centromeric region were monitored by chromatin immunoprecipitation (ChIP) in various strains. In addition to *Δago1* mutant, *Δclr3* lacking a histone deacetylase involved in SHREC complex was examined for the synthetic effect of *aco2ΔN*.

E. Sensitivity of *aco2ΔN* mutants to thiabendazole (TBZ), a microtubule destabilizing compound. Serially diluted *S. pombe* cells of wild type, *aco2ΔN*, *Δago1*, and the double mutant *aco2ΔN Δago1*, were spotted on YES plates containing 10μM TBZ.

F. Small RNA northern analysis of centromeric siRNAs. Small RNA levels are not changed in *aco2ΔN Δago1* double mutant against *Δago1* mutant. Loading control: snoRNA58 (snR58)

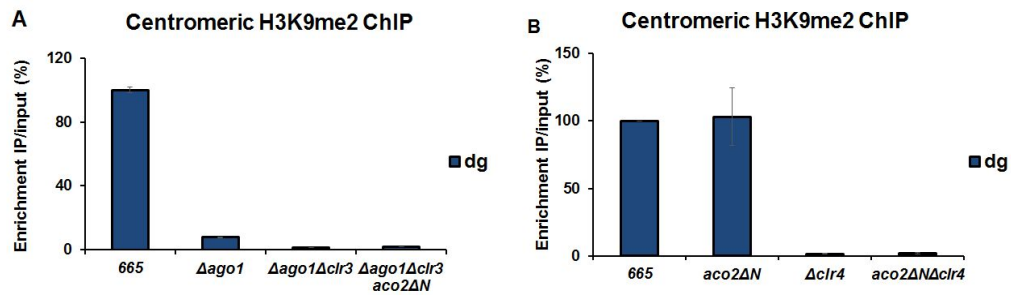


Fig. III-15. H3K9me2 level in various mutants

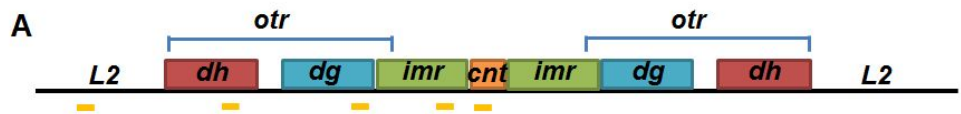
Level of modified histone (H3K9me2; **A** and **B**) bound in the centromeric region were monitored by chromatin immunoprecipitation (ChIP) in various strains.

III.3.2.4. Aco2 is recruited to centromeric locus by Chp1.

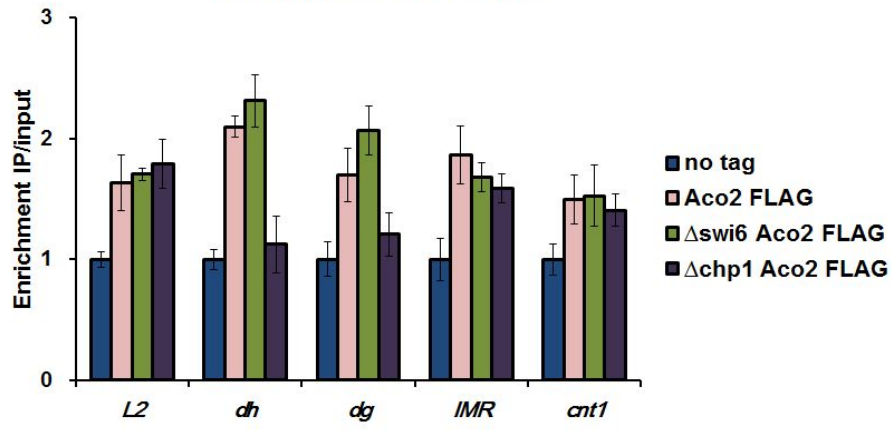
Because *aco2 Δ N* restores RNAi mutant phenotype except *Δ chp1* mutant, I focused on difference between *Δ chp1* mutant and other RNAi mutants. Because Chp1 is one of *S. pombe* HP1 homologue protein, it binds to methylated H3K9 and offers binding sites for other heterochromatin proteins (Fischer et al., 2009), so it was monitored that whether Aco2 recruitment at centromere is dependent on Chp1 or not by ChIP analysis. Because Swi6 binds to methylated H3K9 and serve as a platform for other heterochromatin proteins (Fischer et al., 2009, Schalch, Job et al., 2011), it is also tested. ChIP analysis show that Aco2-FLAG associates with centromeric loci and in *dg/dh* region which form heterochromatin, Aco2 recruitment was dependent on Chp1 not Swi6 (Fig. III-16. A). Except *dg/dh* region, Aco2 was recruited even though in *Δ chp1* mutant. Which proteins are involved in recruitment of Aco2 in centromere core, IMR and L2 regions is to be investigated.

III.3.2.5. Aco2 directly binds to centromeric RNA and it is dependent on Chp1.

In many organisms, aconitase is known as RNA binding protein (Alen & Sonenshein, 1999b, Hentze et al., 2010, Nanda & Leibowitz, 2001, Tang & Guest, 1999). So RNA binding ability of Aco2 was monitored by RNA-IP experiments with FLAG-tagged Aco2. As expected, it directly binds to centromeric *dh* RNA. And in *Δ chp1* mutant, RNA binding affinity of Aco2 was abolished but when Swi6 was deleted Aco2 RNA binding activity was not changed (Fig. III-16. B). These ChIP and RIP data indicate that Aco2 might bind to RNA after recruited by Chp1.



Centromeric Aco2 ChIP



B

Centromeric (dh) RNA-IP

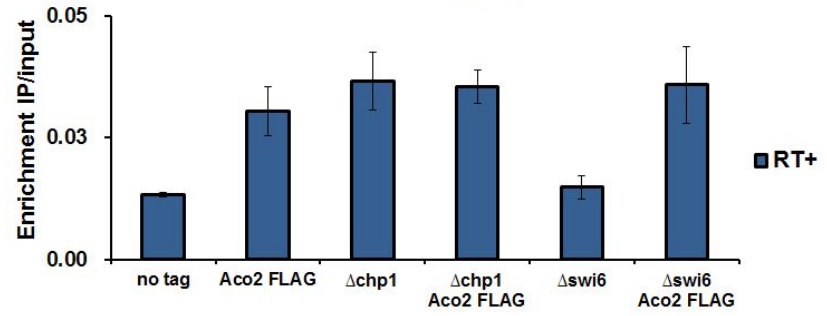


Fig. III-16. ChIP and RIP analysis of Aco2

A. Chromatin immunoprecipitation (ChIP) of Aco2 bound to the centromeric region. Binding of FLAG-tagged Aco2 to the *L2*, *dh*, *dg*, *imr*, *cnt* region was analyzed in the wild type, $\Delta swi6$, and $\Delta chp1$ mutants expressing Aco2-FLAG. The wild type strain with non-tagged Aco2 was examined as a negative control.

B. RNA-IP experiments were performed with anti-FLAG antibody to detect Aco2 binding to *dh* RNA in the wild type, $\Delta chp1$, or $\Delta swi6$ mutant expressing cells expressing Aco2-FLAG. As a negative control, cells with non-tagged protein were also examined in parallel.

III.3.2.6. Chp1 interacts with Aco2 via Chromo-domain

Because Aco2 recruitment in *dg/dh* region is dependent on Chp1, interaction between two proteins was monitored and confirmed by co-IP experiments (Fig. III-17. A). To find which domain of Chp1 is interacted with Aco2, GST pull down assay with *E. coli* overexpressed Chp1 proteins and FLAG-tagged Aco2 extract was performed. Chp1 has chromo-domain in N-terminus, RRM domain and PIN domain in C-terminus (Ishida, Shimojo et al., 2012, Petrie, Wuitschick et al., 2005, Schalch et al., 2011). Each domain was purified with GST tag and incubated with FLAG tagged Aco2 extract. Compared to background, Aco2 physically interacted with Chp1 via chromo-domain (1-235aa) (Fig. III-17. B).

It is known that Chp1 chromo-domain has RNA binding activity as well as H3K9me binding ability (Akhtar, Zink et al., 2000, Ishida et al., 2012), so pull-down assay with RNase and DNase treatment was performed. Although DNase treatment was not changed their interaction pattern, RNase treatment enhanced their interaction (Fig. III-17. C). So there is a chance that their interaction is dependent on RNA.

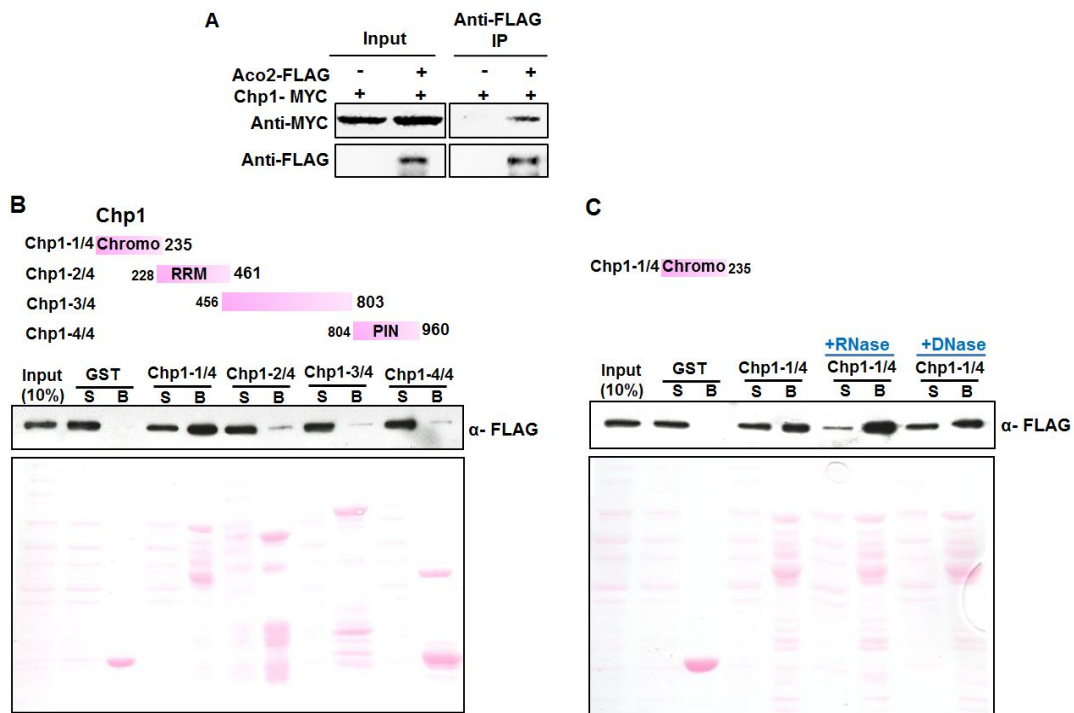


Fig. III-17. Relationship between Aco2 and Chp1

A. Co-immunoprecipitation assay between Aco2-FLAG and Chp1-MYC. Immunoprecipitation of Aco2 in cell extracts was done with anti-FLAG antibody, followed by immuno-blot analysis with anti-MYC antibody.

B-C. Interaction of Aco2 with Chp1 domains. Chp1 protein was divided into four fragments of 1-235 aa (Chp1-1/4; containing chromo domain), 228-461 (Chp1-2/4, containing RRM domain), 456-803 (Chp1-3/4), and 804-960 (Chp1-4/4, containing PIN domain), each of which was fused to GST. Purified proteins were incubated with *S. pombe* cell extracts expressing Aco2-FLAG, followed by GST-pulldown with glutathione resin. Presence of Aco2 in the supernatant (S) and bound (B) fractions was detected by immunoblot assay with anti-FLAG antibody.

III.3.2.7. Aco2 nuclear mutant restores elevated RNA levels but not functional heterochromatin defects in Swi6 mutant at centromere.

Besides RNAi mutants, *aco2ΔN* mutant restores elevated RNA levels in Δ *swi6* mutant (Fig. III-13. A and III-18. A). So whether *aco2ΔN* mutant restores functional heterochromatic defects in Δ *swi6* mutant was monitored with PolIII ChIP analysis and TBZ sensitivity test. Unlike RNAi mutants, *aco2ΔN* did not restore PolIII level (Fig. III-18. B) and TBZ sensitivity in Δ *swi6* mutant (Fig. III-18. C). So the restoration pathway occurs not heterochromatin formation but post-transcriptional gene silencing (RNA degradation) pathway.

III.3.2.8. Aco2 interacts with Swi6 hinge region via RNA dependent manner.

Though Aco2 recruitment in *dg/dh* region is independent on Swi6, their genetic interaction is evident. So physical interaction between two proteins was monitored by co-IP and GST pull-down assay. The interaction signal was not detected by co-IP (Fig. III-19. A) but detected by GST-pull down assay (Fig. III-19. B). The exact reason is not sure, but there are some possibilities. One is that Aco2 may interact with only soluble form of Swi6 which is not bound to chromatin. In this case, the signal is detected only in *E. coli* purified Swi6 since it's not bound to chromatin. So to confirm this possibility, co-IP analysis between Aco2 and Swi6 was monitored with DNase treatment (Fig. III-20. A). But the signal was not detected with DNase treatment. So it may not be the case. Other possibility is that Aco2 may interact with only un-phosphorylated form of Swi6 since Swi6 predominately exists as a phosphorylated form (Shimada, Dohke et al., 2009). In this case, the signal is detected only in with *E. coli* purified Swi6 also since it's not phosphorylated in *E. coli* cell. So next this possibility was tested. Interaction signal between Swi6 and Aco2 was not detected in Δ *ckb1* mutant, CK2 family regulatory subunit, which helps CK2 to phosphorylate Swi6 (Fig. III-20. B). So it

also might not be the case. At last, their interaction is not stronger enough to observe *in-vivo* co-IP experiment compared to interaction between Chp1 and Aco2. Because Aco2 recruitment at centromere is dependent only in Chp1 not Swi6, this possibility is plausible by now. Same as Chp1, Swi6 domain interaction with Aco2 was monitored. Swi6 has N-terminal chromodomain (CD), hinge region and C-terminal chromo shadow domain (CSD) (Keller, Adaixo et al., 2012). GST-tagged Swi6 proteins which had only chromodomain (1-140aa), chromodomain and hinge region (1-264aa) and full size of Swi6 with chromodomain, hinge region and chromo shadow domain (1-329aa) were cloned. *E.coli* purified Swi6 proteins were incubated with Flag-tagged Aco2 extract. The positive interaction signal was detected between hinge region of Swi6 and Aco2. And when hinge region was deleted, interaction between two proteins was disappeared (Fig. III-19. B). It is known that Swi6 hinge region has RNA binding activity (Keller et al., 2012). So pull-down assay with RNase and DNase treatment was monitored. When DNase was treated, binding affinity of Aco2 with swi6 hinge region was not changed, but when RNase was treated, binding affinity between two proteins was increased (Fig. III-19. C) and less Aco2 was existed in soup. So there is a chance that their interaction is dependent on RNA.

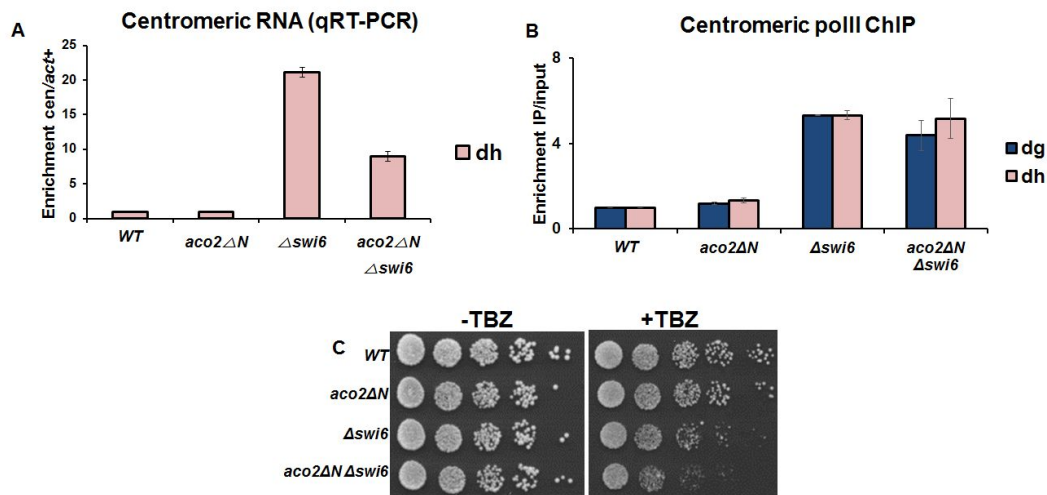


Fig. III-18. Effect of *Aco2ΔN* mutation in *Δswi6* mutant on the heterochromatin formation in the centromeric region

A. Production of centromeric dg RNAs in *aco2ΔN* and *Δswi6* mutant strains. The RNAs that reflect the extent of heterochromatin formation were monitored by qRT-PCR along with *act1+* RNA as a control. Relative enrichment (centromeric RNA/*act1+*) value was plotted for each sample.

B. Level of PolII was monitored by chromatin immunoprecipitation (ChIP) in *aco2ΔN* and *aco2ΔN Δswi6* double mutant strains.

C. Sensitivity of *aco2ΔN* mutants to thiabendazole (TBZ), a microtubule destabilizing compound. Serially diluted *S. pombe* cells of wild type, *aco2ΔN*, *Δswi6*, and the double mutant *aco2ΔN Δswi6*, were spotted on YES plates containing 10μM TBZ.

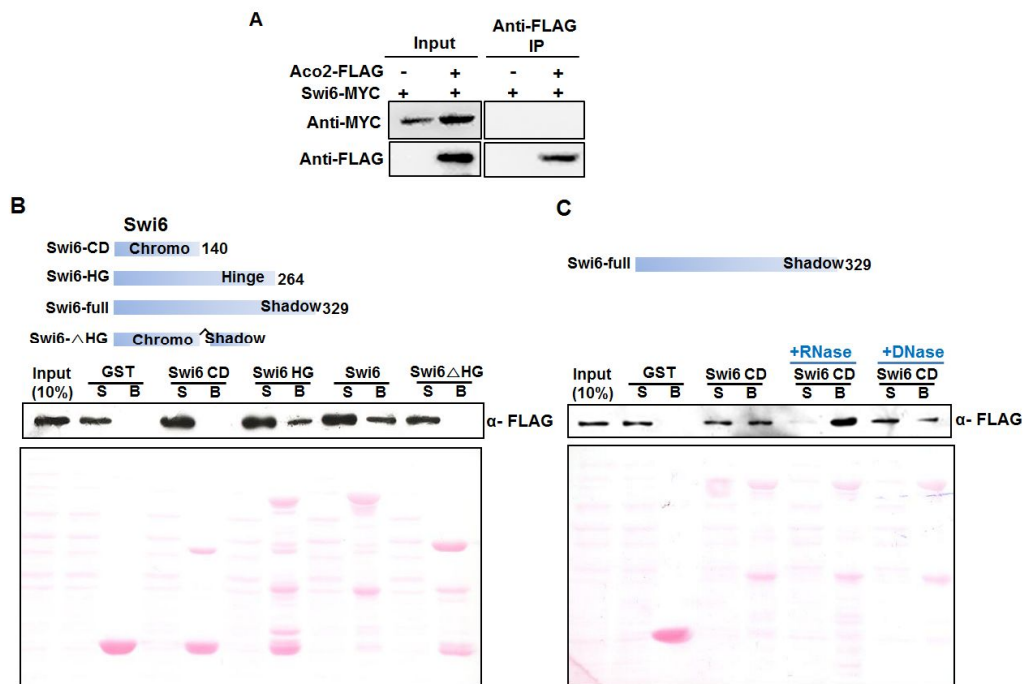


Fig. III-19. Relationship between Aco2 and Swi6

A. Co-immunoprecipitation assay between Aco2-FLAG and Swi6-MYC. Immunoprecipitation of Aco2 in cell extracts was done with anti-FLAG antibody, followed by immuno-blot analysis with anti-MYC antibody.

B-C. Interaction of Aco2 with Swi6 domains. Swi6 protein was prepared into four types of 1-140 (Swi6-CD; containing chromo domain), 1-264 (Swi6-HG; containing hinge region), 1-329 (Swi6-full; containing chromo shadow domain) and Swi6-ΔHG which has hinge deleted Swi6 protein, each of which was fused to GST. Purified proteins were incubated with *S. pombe* cell extracts expressing Aco2-FLAG, followed by GST-pulldown with glutathione resin. Presence of Aco2 in the supernatant (S) and bound (B) fractions was detected by immunoblot assay with anti-FLAG antibody.

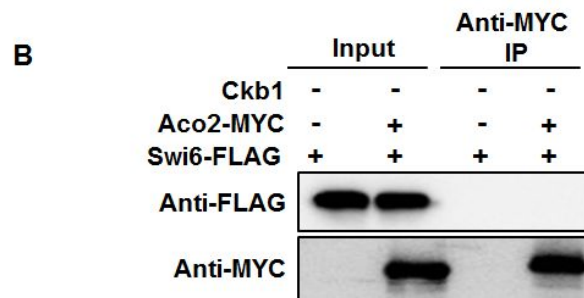
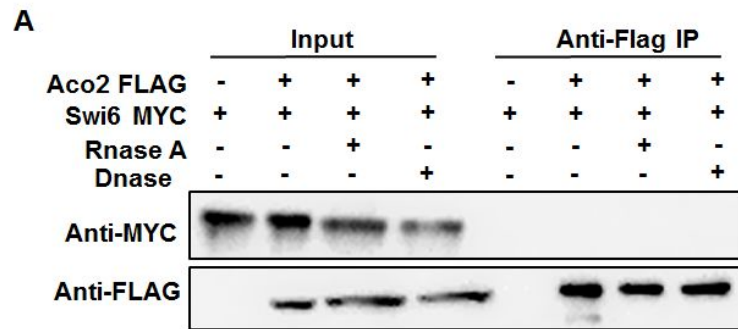


Fig. III-20. Interaction between Aco2 and Swi6

A. Co-immunoprecipitation assay between Aco2-FLAG and Swi6-MYC with RNase and DNase treatment. Immunoprecipitation of Aco2 in cell extracts was done with anti-FLAG antibody, followed by immuno-blot analysis with anti-MYC antibody.

B. Co-immunoprecipitation assay between Aco2-FLAG and Swi6-MYC in $\Delta ckb1$ mutant. Immunoprecipitation of Aco2 in cell extracts was done with anti-FLAG antibody, followed by immuno-blot analysis with anti-MYC antibody.

III.3.2.9. Aco2 affects RNA binding ability of Chp1 and Swi6 but not their recruitment.

To gain more information about relationship between Aco2, Chp1, Swi6 and RNA, RNA-IP experiment was performed. In *aco2ΔN* mutant, both Chp1 and Swi6 RNA binding activity was slightly decreased compared to wild type cell (Fig. III-21. A and B). It is not a large portion though their decrease was always observed.

Next I tested whether Aco2 affects Swi6 and Chp1 recruitment at centromere by ChIP experiments and Aco2 was not affected their enrichment at centromere (Fig. III-22. A and B). So Aco2 could help Chp1 and Swi6 RNA binding activity but their recruitment is independent on Aco2.

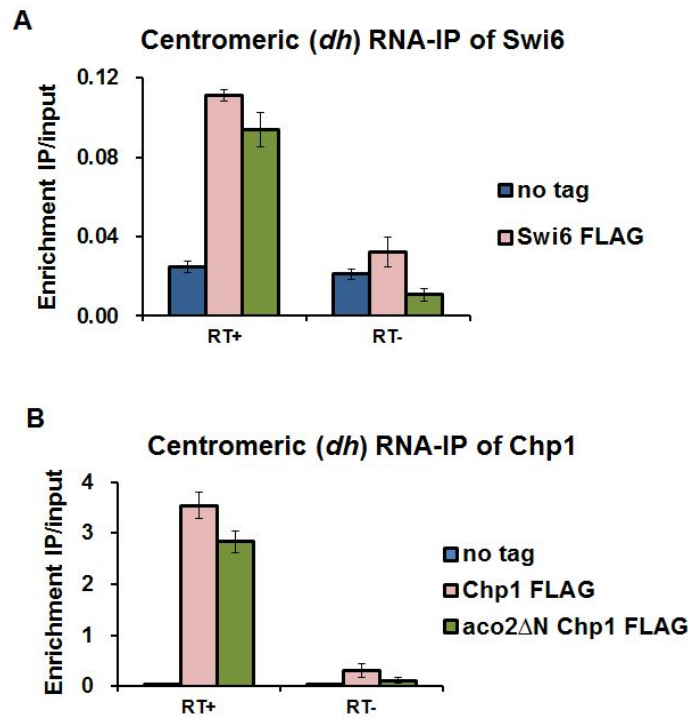


Fig. III-21. Interaction of Chp1 and Swi6 with centromeric (*dh*) RNA

RNA binding ability of Swi6 (**A**) or Chp1 (**B**) was examined in similar way in the wild type or *aco2*ΔN mutant expressing Swi6-FLAG or Chp1-FLAG proteins, respectively.

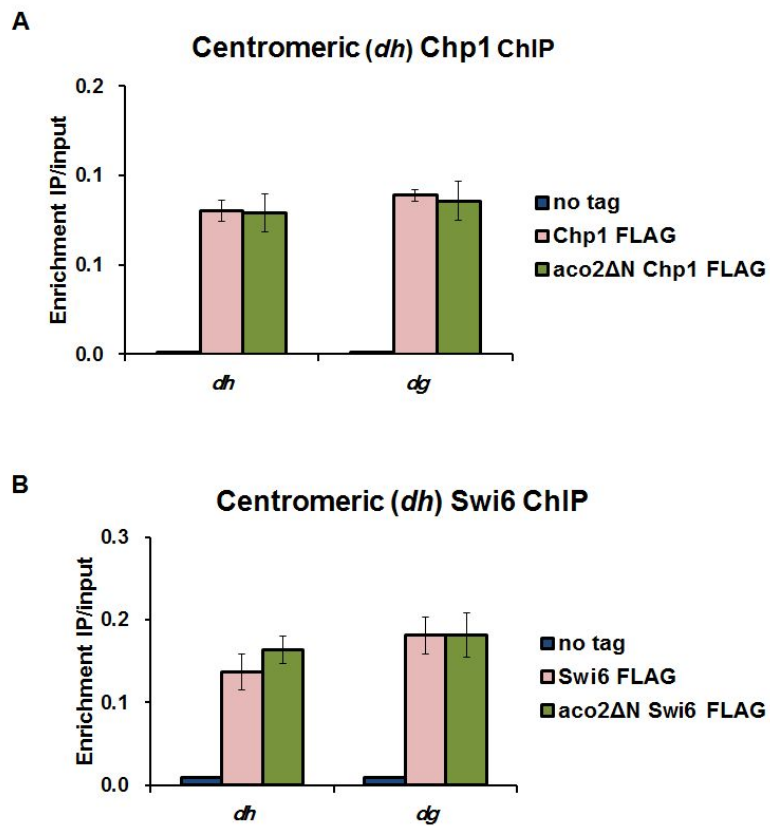


Fig. III-22. Chromatin immunoprecipitation (ChIP) of Chp1 and Swi6

Chromatin immunoprecipitation (ChIP) of Chp1 (A) and Swi6 (B) bound to the centromeric region. Binding of FLAG-tagged Chp1 and Swi6 to the *dh* region was analyzed in the wild type and *aco2ΔN* mutants expressing FLAG tag. The wild type strain with non-tag was examined as a negative control.

III.3.2.10. Aco2 affects heterochromatin assembly independent to Mlo3 and Tfs1.

It is known that loss of Mlo3, *Saccharomyces cerevisiae* Yra1 homolog which acts at the interface of RNAPII transcription and RNA metabolism (Strasser, Masuda et al., 2002, Thakurta, Gopal et al., 2005), and Tfs1, which is *S. pombe* homolog of TFIIS (Kulich & Struhl, 2001), rescue RNAi mutants (Reyes-Turcu, Zhang et al., 2011). To figure out correlation between Aco2 with Mlo3 and Tfs1, *aco2ΔN* was crossed with *Δmlo3* and *Δtfs1* to make double mutants. In order to find their relationship, centromeric-*dh* RNA level was checked compared to single mutants. In both double mutants, centromeric RNA level was same as single mutants (Fig. III-23. A and B), which means there is no synergetic effect between Aco2 with Mlo3 and Tfs1. This phenotype could be interpreted in two ways. One is the case Aco2 and these two mutants share same pathway. But it is already known that Mlo3 and Tfs1 works independently (Reyes-Turcu et al., 2011). So it might not be the case. The other is that each of them has independent pathway. Indeed, Aco2 did not interact with Mlo3 and Tfs1 (data not shown), and Mlo3 enrichment at centromere was not changed in *aco2ΔN* mutant (Fig. III-23. C). So together, this data indicates that Aco2, Mlo3 and Tfs1 rescue RNAi pathway at centromere independently.

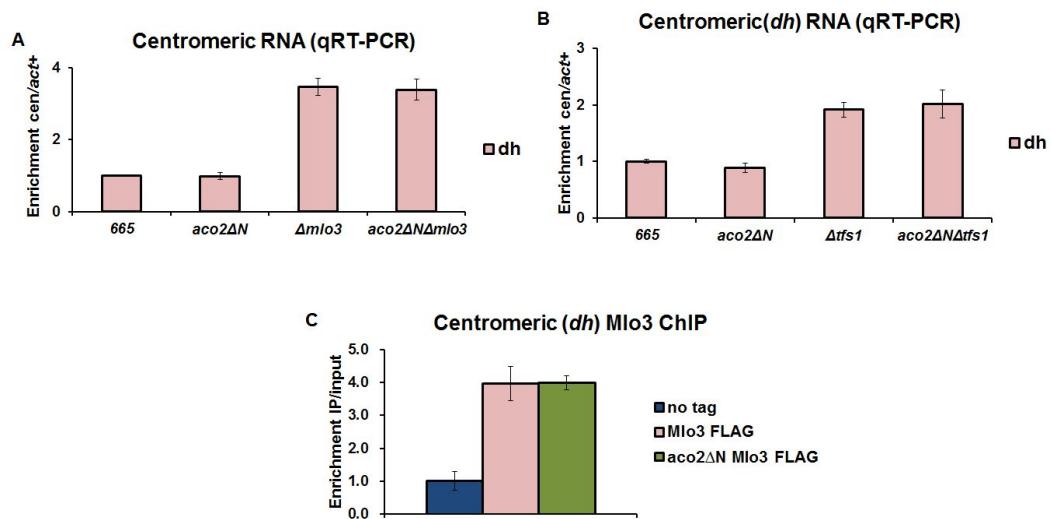


Fig. III-23. Aco2 affects heterochromatin assembly independent of Mlo3 and Tfs1

Production of centromeric *dg/dh* RNAs in *aco2ΔN*, *Δmlo3* and *Δtfs1* strains (A and B). RNAs were prepared from the wild type, *aco2ΔN*, *Δmlo3*, *Δtfs1*, double mutants of *aco2ΔN* with *Δmlo3* or *Δtfs1*. The *dh* RNA was monitored by qRT-PCR along with *act1+* RNA as a control. Relative enrichment (centromeric RNA/*act1+*) value was plotted for each sample.

C. Chromatin immunoprecipitation (ChIP) of Mlo3 bound to the centromeric region. Binding of FLAG-tagged Mlo3 to the *dh* region was analyzed in the wild type and *aco2ΔN* mutants expressing Mlo3-FLAG. The wild type strain with non-tagged Mlo3 was examined as a negative control.

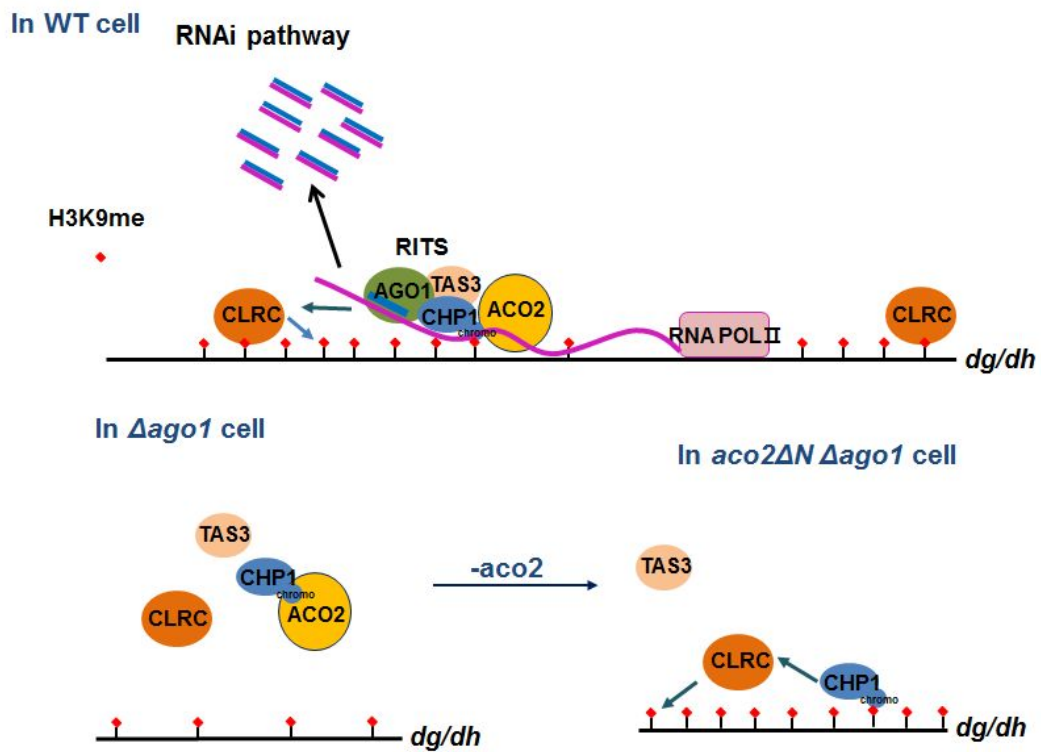


Fig. III-24. Model-I of Aco2 in heterochromatin formation

Aco2 interacts with Chp1 chromo-domain and Swi6 hinge-domain. Aco2 recruitment in *dg/dh* region and RNA binding activity is dependent on Chp1. Aco2 may inhibit Chp1 recruitment when RITS is absent. In *aco2 Δ N $\Delta ago1$* cell, Chp1 with free chromo-domain is easy to bind to H3K9me compared to *$\Delta ago1$* cell and may recruit CLRC complex. So H3K9me and heterochromatin formation is recovered sRNA independent manner.

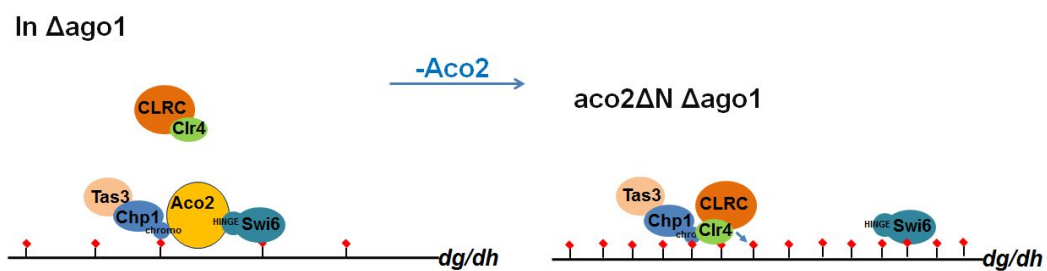


Fig. III-25. Model-II of Aco2 in heterochromatin formation

Aco2 interacts with Chp1 chromo-domain and Swi6 hinge-domain. Aco2 recruitment in *dg/dh* region and RNA binding activity is dependent on Chp1. In *aco2ΔNΔago1* cell, Chp1 with free chromo-domain is easy to interact with Clr4. So H3K9me level and heterochromatin formation could be recovered sRNA independent manner.

III.3.2.11. Both aconitase domain and bL21 domain are needed for nuclear function of Aco2.

Next which domains of Aco2 are needed for its nuclear function was monitored. Aco2 is a fusion protein which has an aconitase domain (44-805aa) in N-terminus and mitochondrial ribosomal domain (bL21, 806-912aa) in C-terminus. Because of an NLS sequence in the bL21 domain, Aco2 can localize in the nucleus (Jung et al., 2015). Various Aco2 mutant was cloned and transformed in WT, *aco2ΔN*, *Δago1* and *aco2ΔN Δago1* cell. RNA level in each strain was monitored by q-RT PCR. It is shown above that Aco2 restores RNAi mutant phenotype at centromere. Centromeric *dg*-RNA level relative to *act1+* in positive control which is *aco2+* transformed *aco2ΔNΔago1* cell put as 100% and in negative control which is vector transformed *aco2ΔNΔago1* cell put as 0% and then relative percentage of RNA level in Aco2 variant transformed *aco2ΔNΔago1* cell was calculated (Fig. III-26. A). From the *aco2+* gene, two kinds of RNAs are produced by alternative selection of poly (A) site. One has only aconitase domain and is localized almost in mitochondria, and the other has both aconitase and the bL21 domains which localized both mitochondria and the nucleus (Jung et al., 2015). AAT mutant has mutated poly (A) site at 2399 nt from AATAAA to CATCAA to produce and complement only fusion protein. In this case, nuclear localized Aco2 protein was produced same as positive control and only mitochondrial localized aconitase domain protein was not produced. As expected, in this case, *aco2ΔNΔago1* double mutant was complemented 96.4%, which means fusion protein is sufficient for nuclear function (Fig. III-26. B). Next, to figure out aconitase domain only effect in the nucleus, MTS-deleted aconitase domain with an additional SV40-NLS sequence in N-terminus was cloned to make aconitase domain localized in the nucleus artificially. In this case, NLS-acnitase domain complemented *aco2ΔNΔago1* double mutant restored *Δago1* mutant same as vector control, which means aconitase domain is not sufficient for Aco2 function in the nucleus

(Fig. III-26. B). Finally, the bL21 domain was tested. This domain has an NLS in C-terminus so additional NLS sequence is not needed. The bL21 domain complemented *aco2ΔNΔago1* double mutant restored nuclear phenotype 18.8% (Fig. III-26. B). Through complementation test, it is discovered that both aconitase and bL21 domain are important for nuclear function and each domain is not sufficient for nuclear function.

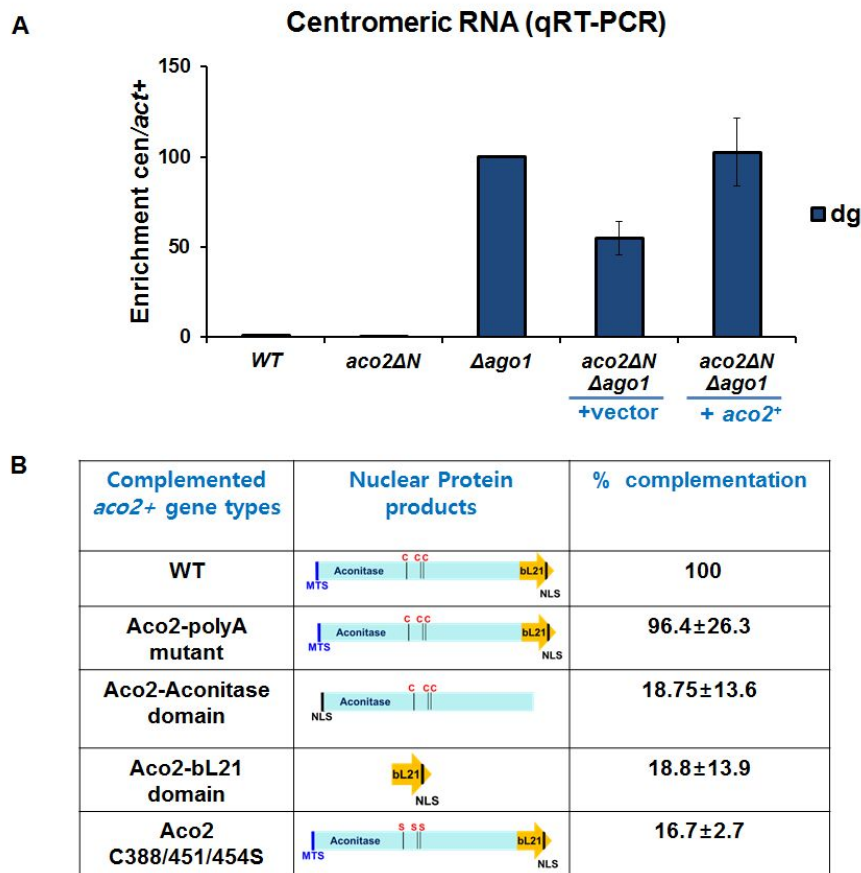


Fig. III-26. Functional domains of Aco2 in maintaining RNAi mutant phenotype of centromeric heterochromatin failure

The suppression of RNAi mutant phenotype by *aco2ΔN* mutation was restored by complementing with wild type *aco2+* gene. (panel A). The *aco2ΔN* Δ *ago1* mutant was complemented with various mutant forms of *aco2+* gene: polyA mutant that produces only the full-length Aco2, NLS-AD (NLS-linked aconitase domain), bL21 domain, and triple cysteine (C388/451/454S) mutant.

III.3.2.12. Iron-sulfur cluster is required for Aco2 nuclear function.

Aconitase has an iron-sulfur center (4Fe-4S) coordinated with three conserved cysteine (Cys388, Cys451 and Cys454) (Robbins & Stout, 1985). Iron-sulfur cluster integrity is essential for its enzymatic function (Hirling, Henderson et al., 1994). In mammalian cell, ACO1 (also known as IRP1) is interconverts between [4Fe-4S] cluster binding state which have enzymatic aconitase activity and [4Fe-4S] non-binding hair-pin RNA structure IRE-binding state (Eisenstein, 2000, Kennedy, Mende-Mueller et al., 1992, Wallander, Leibold et al., 2006). In budding yeast, Aco1 is a component of mitochondrial DNA nucleoid which needs for mtDNA stability (Chen et al., 2007, Chen et al., 2005). In this case, two cysteine residues among three conserved cysteine (Cys382, and Cys445) is required for its nucleoid function, which means iron-sulfur cluster is also important unlike mammalian ACO1. whether iron-sulfur cluster is important for Aco2 nuclear function was tested. If cysteine is replaced to serine, Aco2 cannot bind with iron-sulfur cluster. All of the cysteines in Aco2 were replaced to serine and transformed in *aco2ΔNΔago1* double mutant. This mutant transformed *aco2ΔNΔago1* cell was 16.7% complemented (Fig. III-26. B). Next to identify which cysteine is more important for nuclear function, each of cysteine was converted to serine and it seems that every cysteine is important for nuclear function (Fig. III-27). So it is clear that iron-sulfur cluster is required for Aco2 nuclear function.




Complemented <i>aco2</i> gene types	Nuclear Protein products	% complementation
Aco2 C388S		29.2±10.4
Aco2 C451S		23.1±8.9
Aco2 C454S		26±10

Fig. III-27. Complementation test with Aco2 cysteine mutants (C388S, C451S, C454S)

The suppression of RNAi mutant phenotype by *aco2ΔN* mutation was not restored by complementing with cysteine single mutants.

III.3.3. Functions of Aco2 in sub-telomeric heterochromatin maintenance.

III.3.3.1. Aco2 directly interacts with Rrp6 and they may work together in sub-telomeric loci.

Next, another heterochromatin loci sub-telomeric region was tested with two *aco2* nuclear mutants. Sub-telomeric region contains a high density of repetitive DNA elements (Grewal & Jia, 2007). At first, sub-telomeric *tlh1+* RNA level was monitored by q-RT PCR. As unexpected, in *aco2ΔN* mutant, sub-telomeric RNA level was decreased (Fig. III-28. A) and in *aco2ΔN nmt42 aco2* mutant, *tlh1+* RNA level was also decreased when thiamine was added (Fig. III-28. B). Compared with wild type cell, thiamine free *aco2ΔN nmt42 aco2* mutant had slightly lower *tlh1+* RNA level. It is thought to be due to lower Aco2 expression from the *nmt42* promoter (Basi et al., 1993), compared with the native promoter. For the same reason, *nmt42-aco2* mutant had lower level of mitochondrial translation in absence of thiamine (Jung et al., 2015). Because two types of *aco2* nuclear mutants had same phenotype at sub-telomeric region, *aco2ΔN* mutant was used for further experiments. Most of the case when sub-telomeric heterochromatin is disrupted, *tlh1+* level is increased (Hansen, Ibarra et al., 2006). But the *aco2ΔN* mutant has opposite phenotype. This phenotype is explained as two ways. One is that heterochromatin formation of sub-telomeric region in *aco2ΔN* is enhanced, which means Aco2 serves as anti-silencing factor in this loci. The other is that Aco2 serves in sub-telomeric transcribed mRNA stabilization in post-transcriptional level and when Aco2 is not existed, RNA degradation is activated. To determine which is the case, CHIP experiments was performed to check sub-telomeric chromosome status using antibodies against di-methylated H3K9 (H3K9me2), tri-methylated H3K9 (H3K9me3) and PolIII (Fig. III-29. A-C). H3K9me3, H3K9me2 levels and PolIII level were not changed in *aco2ΔN* mutant, so decreased RNA level in *aco2* nuclear mutants is because of post-

transcriptional process. Same as this case, in mammalian cell, ACO1 (IRP1) also binds to mRNA 3'UTR and increases its stability (Hentze et al., 2010). To find out another factors which have same effects in sub-telomeric loci, RNA level of many known heterochromatin protein mutants was tested. Among these mutants, *Δrrp6* mutant has same phenotype as *aco2ΔN* mutant (Fig. III-30. A-C). And their interaction was confirmed by co-IP experiments (Fig. III-31). Take it together Aco2 and Rrp6 are interacted near sub-telomeric locus and they may work together to prevent RNA degradation which is transcribed at sub-telomeric locus.

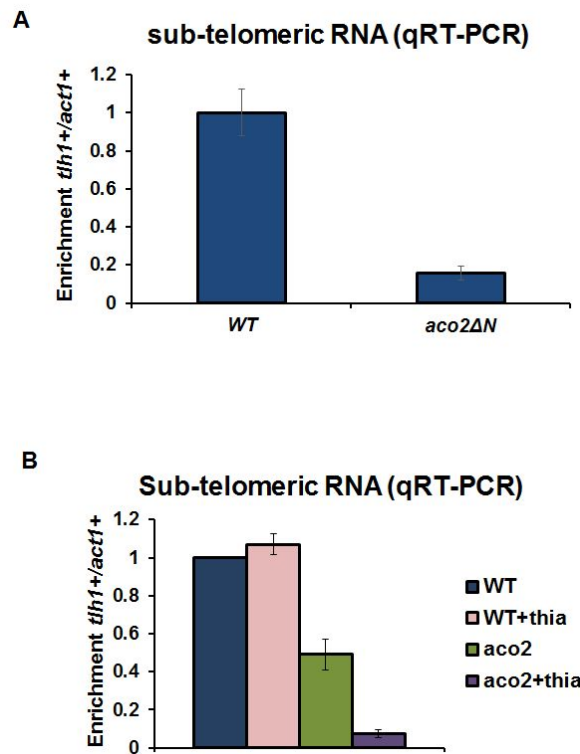


Fig. III-28. Effect of Aco2 nuclear mutant on RNA expression in the sub-telomeric region (*tlh1*)

A. Production of sub-telomeric *tlh1+* RNAs in *aco2ΔN* strain. RNA was prepared from the wild type and *aco2ΔN*. The *tlh1+* RNA was monitored by qRT-PCR along with *act1+* RNA as a control. Relative enrichment (*tlh1+*/*act1+*) value was plotted for each sample.

B. qRT PCR analysis of RNA level at subtelomeric-*tlh1+* relative to *act1+*. In *aco2ΔN nmt42* with thiamine, centromeric RNA level is decreased compare to *aco2ΔN nmt42* without thiamine.

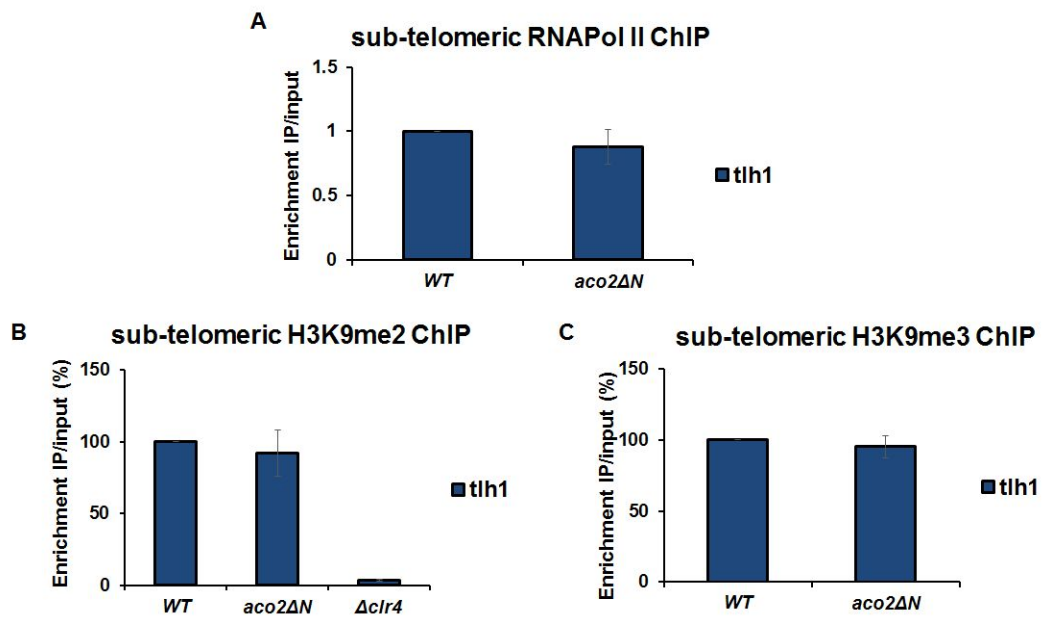


Fig. III--29. Chromatin immunoprecipitation (ChIP) in *aco2ΔN* mutant in the sub-telomeric region (*tlh1*)

Levels of RNA polymerase II (A), modified histone (H3K9me2; B, H3K9me3; C) in the sub-telomeric region were monitored by chromatin immunoprecipitation (ChIP) in *aco2ΔN* mutant.

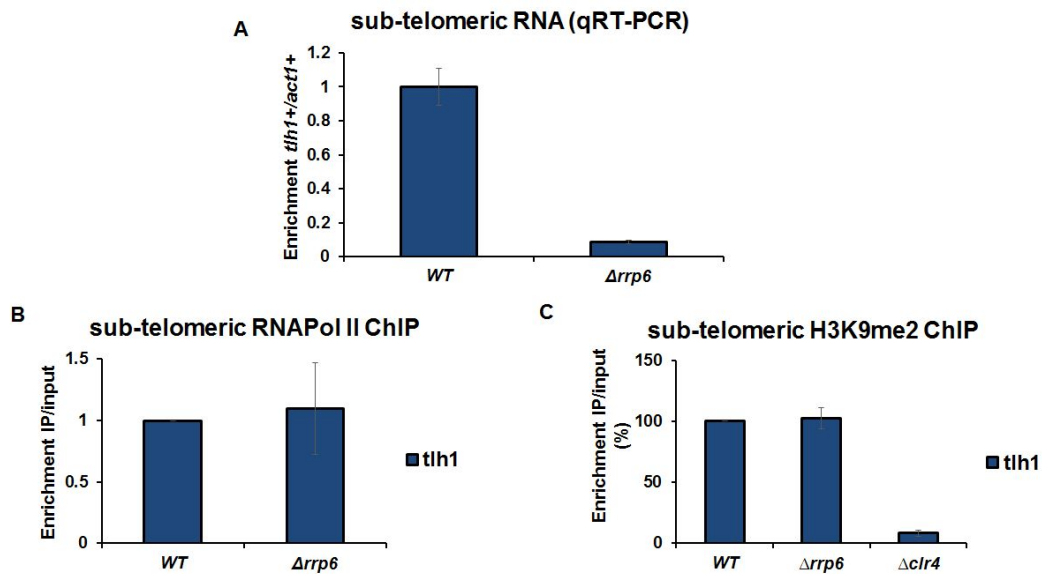


Fig. III-30. Effect of $\Delta rrp6$ mutant on the heterochromatin formation in the sub-telomeric region (*tlh1*)

A. Production of sub-telomeric *tlh1+* RNAs in $\Delta rrp6$ strain. RNA was prepared from the wild type and $\Delta rrp6$. The *tlh1+* RNA was monitored by qRT-PCR along with *act1+* RNA as a control. Relative enrichment (*tlh1+*/*act1+*) value was plotted for each sample.

Levels of RNA polymerase II (**A**), modified histone (H3K9me2; **B**) in the sub-telomeric region were monitored by chromatin immunoprecipitation (ChIP) in $\Delta rrp6$ mutant.

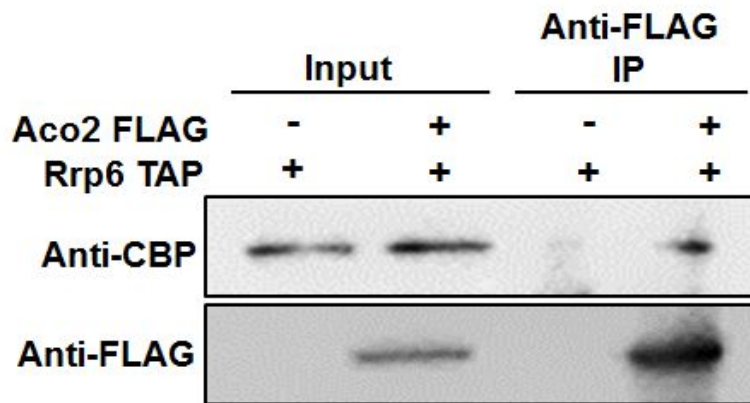


Fig. III-31. Interaction between Aco2 and Rrp6

Co-immunoprecipitation assay between Aco2-FLAG and Rrp6-TAP. Immunoprecipitation of Aco2 in cell extracts was done with anti-FLAG antibody, followed by immuno-blot analysis with anti-CBP antibody.

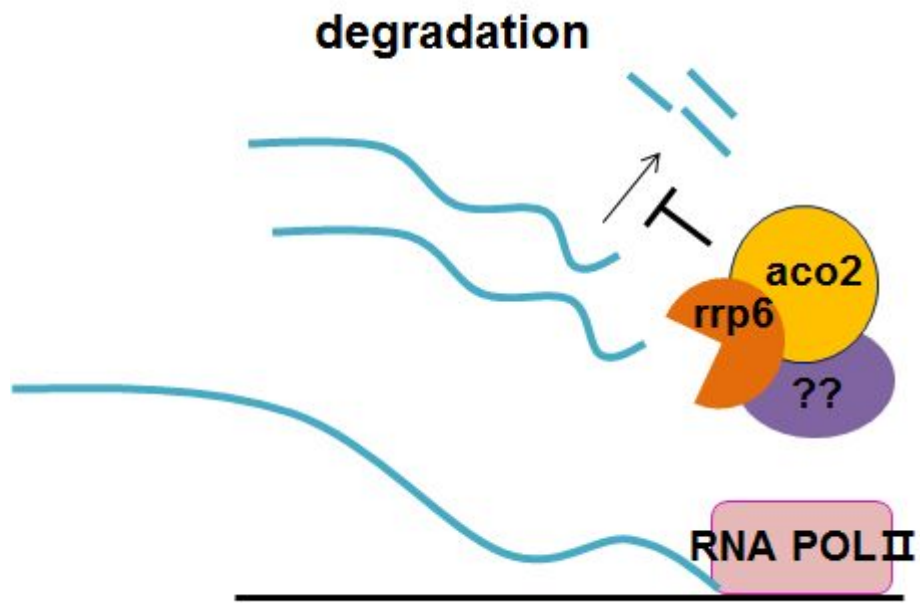


Fig. III-32. Model of Aco2 in sub-telomeric loci

Aco2 and Rrp6 may work together in sub-telomeric loci in post-transcriptional process.

III.3.4. Functions of Aco2 in mating type heterochromatin maintenance.

In addition to centromere and sub-telomeric regions, *mat* locus is one of the heterochromatin region (Grewal & Jia, 2007). There are three mating-type regions in fission yeast; *mat1*, *mat2* and *mat3* located in the middle of the right arm of chromosome II (Beach, 1983). Among them, *mat1* is transcriptionally active and determines the mating-type (P or M) of the cell. The *mat2* and *mat3* loci contain same genetic information as the *mat1-P* and *mat1-M*, respectively, and maintained transcriptionally silent state (Egel, Beach et al., 1984, Noma, Allis et al., 2001). *CenH* region between *mat2* and *mat3*, heterochromatin is assembled by RNAi dependent pathway (Grewal & Klar, 1997) but *mat3* locus, heterochromatin assembly occurs by RNAi independent pathway (Jia et al., 2004a, Kim, Choi et al., 2004, Petrie et al., 2005). To test *aco2ΔN* effects on *mat* locus, *h90 aco2ΔN* strain was stained with iodine vapor staining. In *h90* cells, cells can switch efficiently to the opposite mating type and colonies have homogenous distribution of *M* and *P* cells and thereby can readily mate and sporulate (Bresch, Muller et al., 1968). A starch-like compound produced by sporulating cells stained black by iodine vapor. So by iodine staining *h90* cell stained dark. But the cells which have problem in heterochromatin formation of *mat2P/mat3M*, have lower efficiency in sporulation and lightly stained (Jia, Yamada et al., 2004b). With iodine staining, *h90 aco2ΔN* cell was stained slight lightly compared to *h90* strain (Fig. III-33. A). To gain more insight of *aco2ΔN* effects on *mat* locus, transcribed RNA level at *mat::ura4+* locus was monitored by q RT-PCR. *Ura4+* RNA level was not changed in *aco2ΔN* mutant compared to wild-type *h90 mat::ura4+* cell (Fig. III-33. B). Take it together, *aco2* nuclear mutant has barely affects at *mat* locus. But though it is very subtle, iodine staining of *aco2ΔN* mutant was slightly lighter than *h90* cells, there is possibility that *Aco2* also some functions at *mat* locus.

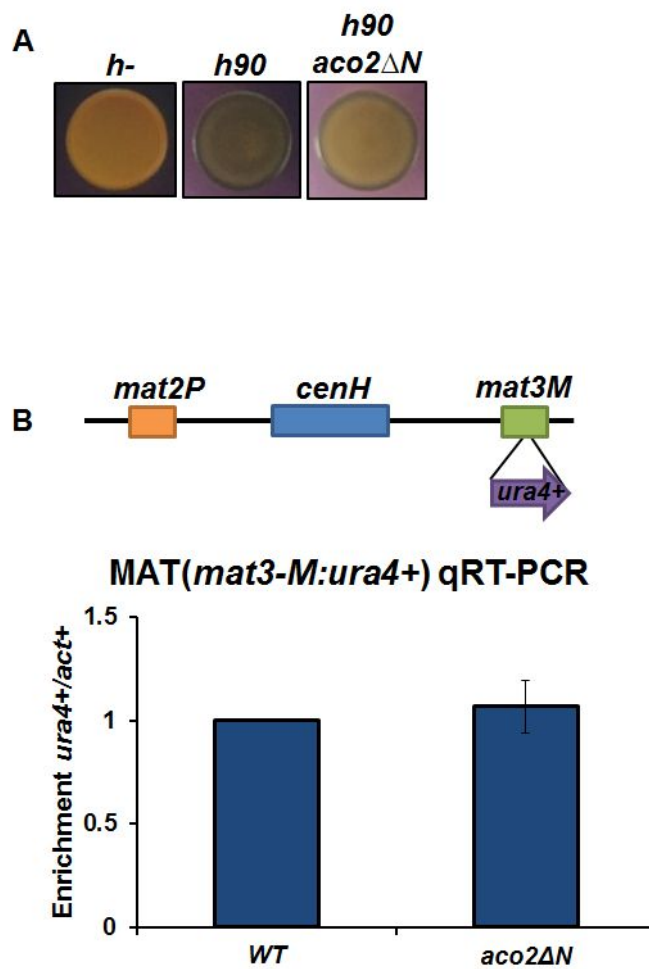


Fig. III-33. Effect of *aco2ΔN* mutant on the heterochromatin formation in mating type locus

A. Iodine staining. *H90 aco2ΔN* mutant was stained lightly than *h90* slightly.

B. Production of *mat3-M:ura4+* RNAs in *aco2ΔN* strain. The *ura4+* RNA was monitored by qRT-PCR along with *act1+* RNA as a control. Relative enrichment (*ura4+*/*act1+*) value was plotted for each sample.

III.4. Prospects for future studies

III.4.1. Roles of Aco2 in mitochondria

In the beginning of this work, it is demonstrated the production of both the sole aconitase domain protein and the aconitase-bL21 fusion protein from the wild type *aco2*⁺ gene in *S. pombe*. The ribosomal protein domain is essentially required for the cell viability since it contributes to mitochondrial translation. How the fused aconitase domain works in concert with the bL21 domain for optimal cellular function and what other function it may have in other cellular compartments other than mitochondria are interesting questions to solve in the future. This work suggests the possibility that aconitase could serve in mitochondrial translation in other organisms. Because though Aconitase and mitochondrial ribosomal protein is fused only in *Schizosaccharomyces* species as well (*S. japonicas*, *S. octosporus*) (Rhind, Chen et al., 2011), in *S. cerevisiae*, where the Aco2 protein contains only an aconitase domain, a genome-wide study has demonstrated its interaction with Mrp16 protein, suggesting a relationship between aconitase and mitochondrial ribosome function (Krogan, Cagney et al., 2006). So there would be a chance this mechanism could be applied in other organisms.

III.4.2. Roles of Aco2 in the nucleus

In this study, it discovered that Aco2 play roles in heterochromatin formation in the nucleus. Aco2 has role in maintenance of centromere, sub-telomere and mat locus. The growing list of proteins dual localized to mitochondria and the nucleus shows that many of these proteins have a role in gene expression or genome maintenance or telomere shortening. Aco2 is one of this case. It has been also hypothesized that, proteins are even shown to be relocated from one

compartment to another upon environmental or developmental cues, one rational of dual targeting is storage or sequestration of these proteins inside the organelles until specific conditions require their activity in the nucleus (Krause & Krupinska, 2009). So in future, it is worth to continue to figure out some environmental signals which activate Aco2's role in the nucleus. Actually, there is some clues that Aco2 NLS mutant has sensitivity in high glucose condition. Because Aconitase is a TCA cycle enzyme in mitochondria, glucose condition is one of the key which link Aco2 function in mitochondria and the nucleus.

REFERENCES

- Akhtar A, Zink D, Becker PB (2000) Chromodomains are protein-RNA interaction modules. *Nature* 407: 405-9
- Alen C, Sonenshein AL (1999a) *Bacillus subtilis* aconitase is an RNA-binding protein. *Proceedings of the National Academy of Sciences of the United States of America* 96: 10412-10417
- Alen C, Sonenshein AL (1999b) *Bacillus subtilis* aconitase is an RNA-binding protein. *Proceedings of the National Academy of Sciences of the United States of America* 96: 10412-7
- Allshire RC, Karpen GH (2008) Epigenetic regulation of centromeric chromatin: old dogs, new tricks? *Nature reviews Genetics* 9: 923-37
- Bartel DP (2004) MicroRNAs: genomics, biogenesis, mechanism, and function. *Cell* 116: 281-97
- Basi G, Schmid E, Maundrell K (1993) TATA box mutations in the *Schizosaccharomyces pombe* nmt1 promoter affect transcription efficiency but not the transcription start point or thiamine repressibility. *Gene* 123: 131-6
- Basilion JP, Rouault TA, Massinople CM, Klausner RD, Burgess WH (1994) The iron-responsive element-binding protein: localization of the RNA-binding site to the aconitase active-site cleft. *Proceedings of the National Academy of Sciences of the United States of America* 91: 574-8
- Beach DH (1983) Cell Type Switching by DNA Transposition in Fission Yeast. *Nature* 305: 682-688
- Beinert H, Kennedy MC, Stout CD (1996) Aconitase as iron-sulfur protein, enzyme, and iron-regulatory protein. *Chem Rev* 96: 2335-2373
- Ben-Menachem R, Tal M, Shadur T, Pines O (2011) A third of the yeast mitochondrial proteome is dual localized: a question of evolution. *Proteomics* 11: 4468-76
- Bernstein E, Caudy AA, Hammond SM, Hannon GJ (2001) Role for a bidentate ribonuclease in the initiation step of RNA interference. *Nature* 409: 363-6
- Bjerling P, Silverstein RA, Thon G, Caudy A, Grewal S, Ekwall K (2002) Functional divergence between histone deacetylases in fission yeast by distinct cellular localization and in vivo specificity. *Molecular and cellular biology* 22: 2170-2181
- Bresch C, Muller G, Egel R (1968) Genes involved in meiosis and sporulation of a yeast.

Molecular & general genetics : MGG 102: 301-6

- Buhler M, Moazed D (2007) Transcription and RNAi in heterochromatic gene silencing. *Nature structural & molecular biology* 14: 1041-8
- Buker SM, Iida T, Buhler M, Villen J, Gygi SP, Nakayama J, Moazed D (2007) Two different Argonaute complexes are required for siRNA generation and heterochromatin assembly in fission yeast. *Nature structural & molecular biology* 14: 200-7
- Bullerwell CE, Leigh J, Forget L, Lang BF (2003) A comparison of three fission yeast mitochondrial genomes. *Nucleic acids research* 31: 759-68
- Buren S, Ortega-Villasante C, Blanco-Rivero A, Martinez-Bernardini A, Shutova T, Shevela D, Messinger J, Bako L, Villarejo A, Samuelsson G (2011) Importance of post-translational modifications for functionality of a chloroplast-localized carbonic anhydrase (CAH1) in *Arabidopsis thaliana*. *PLoS one* 6: e21021
- Buscaino A, Lejeune E, Audergon P, Hamilton G, Pidoux A, Allshire RC (2013) Distinct roles for Sir2 and RNAi in centromeric heterochromatin nucleation, spreading and maintenance. *The EMBO journal* 32: 1250-64
- Carrie C, Kuhn K, Murcha MW, Duncan O, Small ID, O'Toole N, Whelan J (2009) Approaches to defining dual-targeted proteins in *Arabidopsis*. *The Plant journal : for cell and molecular biology* 57: 1128-39
- Caudy AA, Myers M, Hannon GJ, Hammond SM (2002) Fragile X-related protein and VIG associate with the RNA interference machinery. *Genes & development* 16: 2491-6
- Chen ES, Zhang K, Nicolas E, Cam HP, Zofall M, Grewal SI (2008) Cell cycle control of centromeric repeat transcription and heterochromatin assembly. *Nature* 451: 734-7
- Chen XJ, Butow RA (2005) The organization and inheritance of the mitochondrial genome. *Nature reviews Genetics* 6: 815-25
- Chen XJ, Wang X, Butow RA (2007) Yeast aconitase binds and provides metabolically coupled protection to mitochondrial DNA. *Proceedings of the National Academy of Sciences of the United States of America* 104: 13738-43
- Chen XJ, Wang X, Kaufman BA, Butow RA (2005) Aconitase couples metabolic regulation to mitochondrial DNA maintenance. *Science* 307: 714-7
- Costa B, Dettori D, Lorenzato A, Bardella C, Coltella N, Martino C, Cammarata C,

- Carmeliet P, Olivero M, Di Renzo MF (2010) Fumarase tumor suppressor gene and MET oncogene cooperate in upholding transformation and tumorigenesis. *FASEB journal : official publication of the Federation of American Societies for Experimental Biology* 24: 2680-8
- Creissen G, Reynolds H, Xue Y, Mullineaux P (1995) Simultaneous targeting of pea glutathione reductase and of a bacterial fusion protein to chloroplasts and mitochondria in transgenic tobacco. *The Plant journal : for cell and molecular biology* 8: 167-75
- Das M, Wiley DJ, Medina S, Vincent HA, Larrea M, Oriolo A, Verde F (2007) Regulation of cell diameter, For3p localization, and cell symmetry by fission yeast Rho-GAP Rga4p. *Molecular biology of the cell* 18: 2090-101
- Denton RM, Randle PJ, Bridges BJ, Cooper RH, Kerbey AL, Pask HT, Severson DL, Stansbie D, Whitehouse S (1975) Regulation of mammalian pyruvate dehydrogenase. *Molecular and cellular biochemistry* 9: 27-53
- Duchene AM, Giege P (2012) Dual localized mitochondrial and nuclear proteins as gene expression regulators in plants? *Frontiers in plant science* 3: 221
- Egel R, Beach DH, Klar AJ (1984) Genes required for initiation and resolution steps of mating-type switching in fission yeast. *Proceedings of the National Academy of Sciences of the United States of America* 81: 3481-5
- Eisenstein RS (2000) Iron regulatory proteins and the molecular control of mammalian iron metabolism. *Annual review of nutrition* 20: 627-62
- Fischer T, Cui B, Dhakshnamoorthy J, Zhou M, Rubin C, Zofall M, Veenstra TD, Grewal SI (2009) Diverse roles of HP1 proteins in heterochromatin assembly and functions in fission yeast. *Proceedings of the National Academy of Sciences of the United States of America* 106: 8998-9003
- Gaisne M, Bonnefoy N (2006) The COX18 gene, involved in mitochondrial biogenesis, is functionally conserved and tightly regulated in humans and fission yeast. *FEMS yeast research* 6: 869-82
- Galichet A, Hoyerova K, Kaminek M, Grisse W (2008) Farnesylation directs AtIPT3 subcellular localization and modulates cytokinin biosynthesis in Arabidopsis. *Plant physiology* 146: 1155-64
- Garrido N, Griparic L, Jokitalo E, Wartiovaara J, van der Blik AM, Spelbrink JN (2003) Composition and dynamics of human mitochondrial nucleoids. *Molecular biology of*

the cell 14: 1583-96

- Gilbert C, Kristjuhan A, Winkler GS, Svejstrup JQ (2004) Elongator interactions with nascent mRNA revealed by RNA immunoprecipitation. *Molecular cell* 14: 457-64
- Grewal SI, Jia S (2007) Heterochromatin revisited. *Nature reviews Genetics* 8: 35-46
- Grewal SI, Klar AJ (1997) A recombinationally repressed region between *mat2* and *mat3* loci shares homology to centromeric repeats and regulates directionality of mating-type switching in fission yeast. *Genetics* 146: 1221-38
- Gruer MJ, Artymiuk PJ, Guest JR (1997) The aconitase family: three structural variations on a common theme. *Trends in biochemical sciences* 22: 3-6
- Gruer MJ, Guest JR (1994) Two genetically-distinct and differentially-regulated aconitases (*AcnA* and *AcnB*) in *Escherichia coli*. *Microbiology* 140 (Pt 10): 2531-41
- Halic M, Moazed D (2010) Dicer-independent primal RNAs trigger RNAi and heterochromatin formation. *Cell* 140: 504-16
- Hall IM, Noma K, Grewal SI (2003) RNA interference machinery regulates chromosome dynamics during mitosis and meiosis in fission yeast. *Proceedings of the National Academy of Sciences of the United States of America* 100: 193-8
- Hall IM, Shankaranarayana GD, Noma K, Ayoub N, Cohen A, Grewal SI (2002) Establishment and maintenance of a heterochromatin domain. *Science* 297: 2232-7
- Hammond SM, Boettcher S, Caudy AA, Kobayashi R, Hannon GJ (2001) Argonaute2, a link between genetic and biochemical analyses of RNAi. *Science* 293: 1146-1150
- Hannon GJ (2002) RNA interference. *Nature* 418: 244-51
- Hansen KR, Ibarra PT, Thon G (2006) Evolutionary-conserved telomere-linked helicase genes of fission yeast are repressed by silencing factors, RNAi components and the telomere-binding protein Taz1. *Nucleic acids research* 34: 78-88
- Hayles J, Wood V, Jeffery L, Hoe KL, Kim DU, Park HO, Salas-Pino S, Heichinger C, Nurse P (2013) A genome-wide resource of cell cycle and cell shape genes of fission yeast. *Open biology* 3: 130053
- Hentze MW, Muckenthaler MU, Galy B, Camaschella C (2010) Two to tango: regulation of Mammalian iron metabolism. *Cell* 142: 24-38
- Hirling H, Henderson BR, Kuhn LC (1994) Mutational analysis of the [4Fe-4S]-cluster converting iron regulatory factor from its RNA-binding form to cytoplasmic aconitase. *The EMBO journal* 13: 453-61

- Hu CD, Chinenov Y, Kerppola TK (2002) Visualization of interactions among bZip and Rel family proteins in living cells using bimolecular fluorescence complementation. *Molecular cell* 9: 789-798
- Hurt E, Luo MJ, Rother S, Reed R, Strasser K (2004) Cotranscriptional recruitment of the serine-arginine-rich (SR)-like proteins Gbp2 and Hrb1 to nascent mRNA via the TREX complex. *Proceedings of the National Academy of Sciences of the United States of America* 101: 1858-62
- Hutvagner G, Zamore PD (2002) A microRNA in a multiple-turnover RNAi enzyme complex. *Science* 297: 2056-60
- Isaac S, Walfridsson J, Zohar T, Lazar D, Kahan T, Ekwall K, Cohen A (2007) Interaction of Epe1 with the heterochromatin assembly pathway in *Schizosaccharomyces pombe*. *Genetics* 175: 1549-60
- Ishida M, Shimojo H, Hayashi A, Kawaguchi R, Ohtani Y, Uegaki K, Nishimura Y, Nakayama J (2012) Intrinsic nucleic acid-binding activity of Chp1 chromodomain is required for heterochromatic gene silencing. *Molecular cell* 47: 228-41
- Jaffrey SR, Haile DJ, Klausner RD, Harford JB (1993) The interaction between the iron-responsive element binding protein and its cognate RNA is highly dependent upon both RNA sequence and structure. *Nucleic acids research* 21: 4627-31
- Jia S, Kobayashi R, Grewal SI (2005) Ubiquitin ligase component Cul4 associates with Clr4 histone methyltransferase to assemble heterochromatin. *Nature cell biology* 7: 1007-13
- Jia S, Noma K, Grewal SI (2004a) RNAi-independent heterochromatin nucleation by the stress-activated ATF/CREB family proteins. *Science* 304: 1971-6
- Jia S, Yamada T, Grewal SI (2004b) Heterochromatin regulates cell type-specific long-range chromatin interactions essential for directed recombination. *Cell* 119: 469-80
- Jung SJ, Seo Y, Lee KC, Lee D, Roe JH (2015) Essential function of Aco2, a fusion protein of aconitase and mitochondrial ribosomal protein bL21, in mitochondrial translation in fission yeast. *FEBS letters* 589: 822-8
- Kaufman BA, Newman SM, Hallberg RL, Slaughter CA, Perlman PS, Butow RA (2000) In organello formaldehyde crosslinking of proteins to mtDNA: identification of bifunctional proteins. *Proceedings of the National Academy of Sciences of the United States of America* 97: 7772-7

- Keller C, Adaixo R, Stunnenberg R, Woolcock KJ, Hiller S, Buhler M (2012) HP1(Swi6) mediates the recognition and destruction of heterochromatic RNA transcripts. *Molecular cell* 47: 215-27
- Kennedy MC, Mende-Mueller L, Blondin GA, Beinert H (1992) Purification and characterization of cytosolic aconitase from beef liver and its relationship to the iron-responsive element binding protein. *Proceedings of the National Academy of Sciences of the United States of America* 89: 11730-4
- Kim DU, Hayles J, Kim D, Wood V, Park HO, Won M, Yoo HS, Duhig T, Nam M, Palmer G, Han S, Jeffery L, Baek ST, Lee H, Shim YS, Lee M, Kim L, Heo KS, Noh EJ, Lee AR et al. (2010) Analysis of a genome-wide set of gene deletions in the fission yeast *Schizosaccharomyces pombe*. *Nature biotechnology* 28: 617-23
- Kim HS, Choi ES, Shin JA, Jang YK, Park SD (2004) Regulation of Swi6/HP1-dependent heterochromatin assembly by cooperation of components of the mitogen-activated protein kinase pathway and a histone deacetylase Clr6. *The Journal of biological chemistry* 279: 42850-9
- Kim JK, Gabel HW, Kamath RS, Tewari M, Pasquinelli A, Rual JF, Kennedy S, Dybbs M, Bertin N, Kaplan JM, Vidal M, Ruvkun G (2005) Functional genomic analysis of RNA interference in *C. elegans*. *Science* 308: 1164-7
- Klausner RD, Rouault TA (1993) A double life: cytosolic aconitase as a regulatory RNA binding protein. *Molecular biology of the cell* 4: 1-5
- Krause K, Krupinska K (2009) Nuclear regulators with a second home in organelles. *Trends in plant science* 14: 194-9
- Krawchuk MD, Wahls WP (1999) High-efficiency gene targeting in *Schizosaccharomyces pombe* using a modular, PCR-based approach with long tracts of flanking homology. *Yeast* 15: 1419-27
- Krogan NJ, Cagney G, Yu H, Zhong G, Guo X, Ignatchenko A, Li J, Pu S, Datta N, Tikuisis AP, Punna T, Peregrin-Alvarez JM, Shales M, Zhang X, Davey M, Robinson MD, Paccanaro A, Bray JE, Sheung A, Beattie B et al. (2006) Global landscape of protein complexes in the yeast *Saccharomyces cerevisiae*. *Nature* 440: 637-43
- Kuhl I, Dujancourt L, Gaisne M, Herbert CJ, Bonnefoy N (2011) A genome wide study in fission yeast reveals nine PPR proteins that regulate mitochondrial gene expression. *Nucleic acids research* 39: 8029-41
- Kulich D, Struhl K (2001) TFIIS enhances transcriptional elongation through an artificial

- arrest site in vivo. *Molecular and cellular biology* 21: 4162-8
- Lauble H, Kennedy MC, Beinert H, Stout CD (1992) Crystal structures of aconitase with isocitrate and nitroisocitrate bound. *Biochemistry* 31: 2735-48
- Legros F, Lombes A, Frachon P, Rojo M (2002) Mitochondrial fusion in human cells is efficient, requires the inner membrane potential, and is mediated by mitofusins. *Molecular biology of the cell* 13: 4343-4354
- Liu JD, Carmell MA, Rivas FV, Marsden CG, Thomson JM, Song JJ, Hammond SM, Joshua-Tor L, Hannon GJ (2004) Argonaute2 is the catalytic engine of mammalian RNAi. *Science* 305: 1437-1441
- Luger K, Mader AW, Richmond RK, Sargent DF, Richmond TJ (1997) Crystal structure of the nucleosome core particle at 2.8 Å resolution. *Nature* 389: 251-60
- Matsuyama A, Arai R, Yashiroda Y, Shirai A, Kamata A, Sekido S, Kobayashi Y, Hashimoto A, Hamamoto M, Hiraoka Y, Horinouchi S, Yoshida M (2006) ORFeome cloning and global analysis of protein localization in the fission yeast *Schizosaccharomyces pombe*. *Nature biotechnology* 24: 841-7
- McBride HM, Neuspiel M, Wasiak S (2006) Mitochondria: More than just a powerhouse. *Current Biology* 16: R551-R560
- Miyakawa I, Sando N, Kawano S, Nakamura S, Kuroiwa T (1987) Isolation of morphologically intact mitochondrial nucleoids from the yeast, *Saccharomyces cerevisiae*. *Journal of cell science* 88 (Pt 4): 431-9
- Moazed D (2009) Small RNAs in transcriptional gene silencing and genome defence. *Nature* 457: 413-20
- Moreno S, Klar A, Nurse P (1991) Molecular genetic analysis of fission yeast *Schizosaccharomyces pombe*. *Methods Enzymol* 194: 795-823
- Motamedi MR, Verdel A, Colmenares SU, Gerber SA, Gygi SP, Moazed D (2004) Two RNAi complexes, RITS and RDRC, physically interact and localize to noncoding centromeric RNAs. *Cell* 119: 789-802
- Mourelatos Z, Dostie J, Paushkin S, Sharma A, Charroux B, Abel L, Rappsilber J, Mann M, Dreyfuss G (2002) miRNPs: a novel class of ribonucleoproteins containing numerous microRNAs. *Genes & development* 16: 720-8
- Nakayama J, Rice JC, Strahl BD, Allis CD, Grewal SI (2001) Role of histone H3 lysine 9 methylation in epigenetic control of heterochromatin assembly. *Science* 292: 110-3

- Nanda SK, Leibowitz JL (2001) Mitochondrial aconitase binds to the 3' untranslated region of the mouse hepatitis virus genome. *Journal of virology* 75: 3352-62
- Nicolas E, Yamada T, Cam HP, FitzGerald PC, Kobayashi R, Grewal SIS (2007) Distinct roles of HDAC complexes in promoter silencing, antisense suppression and DNA damage protection. *Nature structural & molecular biology* 14: 372-380
- Noma K, Allis CD, Grewal SI (2001) Transitions in distinct histone H3 methylation patterns at the heterochromatin domain boundaries. *Science* 293: 1150-5
- Noma K, Sugiyama T, Cam H, Verdel A, Zofall M, Jia S, Moazed D, Grewal SI (2004) RITS acts in cis to promote RNA interference-mediated transcriptional and post-transcriptional silencing. *Nature genetics* 36: 1174-80
- Partridge JF, Borgstrom B, Allshire RC (2000) Distinct protein interaction domains and protein spreading in a complex centromere. *Genes & development* 14: 783-91
- Petrie VJ, Wuitschick JD, Givens CD, Kosinski AM, Partridge JF (2005) RNA interference (RNAi)-dependent and RNAi-independent association of the Chp1 chromodomain protein with distinct heterochromatic loci in fission yeast. *Molecular and cellular biology* 25: 2331-46
- Poschke H, Dees M, Chang M, Amberkar S, Kaderali L, Rothstein R, Luke B (2012) Rif2 promotes a telomere fold-back structure through Rpd3L recruitment in budding yeast. *PLoS genetics* 8: e1002960
- Rajpurohit R, Mansfield K, Ohyama K, Ewert D, Shapiro IM (1999) Chondrocyte death is linked to development of a mitochondrial membrane permeability transition in the growth plate. *Journal of cellular physiology* 179: 287-96
- Reyes-Turcu FE, Zhang K, Zofall M, Chen E, Grewal SI (2011) Defects in RNA quality control factors reveal RNAi-independent nucleation of heterochromatin. *Nature structural & molecular biology* 18: 1132-8
- Rhind N, Chen Z, Yassour M, Thompson DA, Haas BJ, Habib N, Wapinski I, Roy S, Lin MF, Heiman DI, Young SK, Furuya K, Guo Y, Pidoux A, Chen HM, Robbertse B, Goldberg JM, Aoki K, Bayne EH, Berlin AM et al. (2011) Comparative functional genomics of the fission yeasts. *Science* 332: 930-6
- Robbins AH, Stout CD (1985) Iron-sulfur cluster in aconitase. Crystallographic evidence for a three-iron center. *The Journal of biological chemistry* 260: 2328-33
- Robbins AH, Stout CD (1989) The structure of aconitase. *Proteins* 5: 289-312
- Schafer B (2003) Genetic conservation versus variability in mitochondria: the

- architecture of the mitochondrial genome in the petite-negative yeast *Schizosaccharomyces pombe*. *Current genetics* 43: 311-26
- Schafer B (2005) RNA maturation in mitochondria of *S. cerevisiae* and *S. pombe*. *Gene* 354: 80-5
- Schalch T, Job G, Shanker S, Partridge JF, Joshua-Tor L (2011) The Chp1-Tas3 core is a multifunctional platform critical for gene silencing by RITS. *Nature structural & molecular biology* 18: 1351-7
- Schmitt ME, Brown TA, Trumppower BL (1990) A rapid and simple method for preparation of RNA from *Saccharomyces cerevisiae*. *Nucleic acids research* 18: 3091-2
- Shadel GS (2005) Mitochondrial DNA, aconitase 'wraps' it up. *Trends in biochemical sciences* 30: 294-296
- Shimada A, Dohke K, Sadaie M, Shinmyozu K, Nakayama J, Urano T, Murakami Y (2009) Phosphorylation of Swi6/HP1 regulates transcriptional gene silencing at heterochromatin. *Genes & development* 23: 18-23
- Sipiczki (1989) Taxonomy and phylogenesis. In *molecular biology of the fission yeast*. Academic Press, London: 431-452
- Slane BG, Aykin-Burns N, Smith BJ, Kalen AL, Goswami PC, Domann FE, Spitz DR (2006) Mutation of succinate dehydrogenase subunit C results in increased O₂·, oxidative stress, and genomic instability. *Cancer research* 66: 7615-20
- Song JJ, Smith SK, Hannon GJ, Joshua-Tor L (2004) Crystal structure of Argonaute and its implications for RISC slicer activity. *Science* 305: 1434-7
- Srere PA (1990) Citric-Acid Cycle Redux. *Trends in biochemical sciences* 15: 411-412
- Sriram G, Martinez JA, McCabe ER, Liao JC, Dipple KM (2005) Single-gene disorders: what role could moonlighting enzymes play? *American journal of human genetics* 76: 911-24
- Strasser K, Masuda S, Mason P, Pfannstiel J, Oppizzi M, Rodriguez-Navarro S, Rondon AG, Aguilera A, Struhl K, Reed R, Hurt E (2002) TREX is a conserved complex coupling transcription with messenger RNA export. *Nature* 417: 304-8
- Sugiyama T, Cam HP, Sugiyama R, Noma K, Zofall M, Kobayashi R, Grewal SI (2007) SHREC, an effector complex for heterochromatic transcriptional silencing. *Cell* 128: 491-504
- Sung MK, Huh WK (2007) Bimolecular fluorescence complementation analysis system

- for in vivo detection of protein-protein interaction in *Saccharomyces cerevisiae*. *Yeast* 24: 767-75
- Takahashi K, Chen ES, Yanagida M (2000) Requirement of Mis6 centromere connector for localizing a CENP-A-like protein in fission yeast. *Science* 288: 2215-9
- Tang Y, Guest JR (1999) Direct evidence for mRNA binding and post-transcriptional regulation by *Escherichia coli* aconitases. *Microbiology* 145 (Pt 11): 3069-79
- Thakurta AG, Gopal G, Yoon JH, Kozak L, Dhar R (2005) Homolog of BRCA2-interacting Dss1p and Uap56p link Mlo3p and Rae1p for mRNA export in fission yeast. *The EMBO journal* 24: 2512-23
- Topfik J (2005) Regulation of mitochondrial translation in yeast. *Cellular & molecular biology letters* 10: 571-94
- Velot C, Srere PA (2000) Reversible transdominant inhibition of a metabolic pathway - In vivo evidence of interaction between two sequential, tricarboxylic acid cycle enzymes in yeast. *Journal of Biological Chemistry* 275: 12926-12933
- Verdel A, Jia S, Gerber S, Sugiyama T, Gygi S, Grewal SI, Moazed D (2004) RNAi-mediated targeting of heterochromatin by the RITS complex. *Science* 303: 672-6
- Volpe TA, Kidner C, Hall IM, Teng G, Grewal SI, Martienssen RA (2002) Regulation of heterochromatic silencing and histone H3 lysine-9 methylation by RNAi. *Science* 297: 1833-7
- Volz K (2008) The functional duality of iron regulatory protein 1. *Current opinion in structural biology* 18: 106-11
- Vuoristo KS, Mars AE, Sanders JP, Eggink G, Weusthuis RA (2016) Metabolic Engineering of TCA Cycle for Production of Chemicals. *Trends in biotechnology* 34: 191-7
- Wallander ML, Leibold EA, Eisenstein RS (2006) Molecular control of vertebrate iron homeostasis by iron regulatory proteins. *Biochimica et biophysica acta* 1763: 668-89
- Weir BA, Yaffe MP (2004) Mmd1p, a novel, conserved protein essential for normal mitochondrial morphology and distribution in the fission yeast *Schizosaccharomyces pombe*. *Molecular biology of the cell* 15: 1656-65
- Wiley DJ, Catanuto P, Fontanesi F, Rios C, Sanchez N, Barrientos A, Verde F (2008) Bot1p is required for mitochondrial translation, respiratory function, and normal cell morphology in the fission yeast *Schizosaccharomyces pombe*. *Eukaryotic cell*

7: 619-29

- Wood V, Gwilliam R, Rajandream MA, Lyne M, Lyne R, Stewart A, Sgouros J, Peat N, Hayles J, Baker S, Basham D, Bowman S, Brooks K, Brown D, Brown S, Chillingworth T, Churcher C, Collins M, Connor R, Cronin A et al. (2002) The genome sequence of *Schizosaccharomyces pombe*. *Nature* 415: 871-80
- Yamada T, Fischle W, Sugiyama T, Allis CD, Grewal SI (2005) The nucleation and maintenance of heterochromatin by a histone deacetylase in fission yeast. *Molecular cell* 20: 173-85
- Yogev O, Pines O (2011) Dual targeting of mitochondrial proteins: mechanism, regulation and function. *Biochimica et biophysica acta* 1808: 1012-20
- Zhang K, Mosch K, Fischle W, Grewal SI (2008) Roles of the Clr4 methyltransferase complex in nucleation, spreading and maintenance of heterochromatin. *Nature structural & molecular biology* 15: 381-8

국문초록

Aconitase는 크랩스 회로에서 시트르산을 아이소시트르산으로 바꾸는 효소이다. 이 과정은 박테리아로부터 진핵생물까지 보존되어 있다. Aconitase는 효소 활성화에 [철-황] 클러스터를 필요로 한다. Aconitase는 효소로서의 역할 뿐 아니라, 많은 종들에서 다양한 역할을 하는 것으로 알려져 있다. 그 중에는 RNA와 DNA에 결합하여 그들의 안정성을 조절하는 역할이 포함되어 있다.

분열성 효모는 두 가지 aconitase를 가지고 있다; *aco1⁺* (SPAC24C9.06c) 과 *aco2⁺* (SPBP4H10.15)가 그것이다. 그 중 *aco2⁺* 는 N-말단 쪽에 aconitase 도메인을 가지고 있고 C-말단 쪽에 마이토콘드리아 리보솜 도메인을 가진 융합 단백질이다. *Aco2⁺* 의 N-말단 앞쪽에는 이 단백질이 마이토콘드리아에 위치할 수 있게 도와주는 마이토콘드리아 위치 서열을 가지고 있고, C-말단 쪽에는 단백질을 핵으로 가게 하는 핵 위치 서열을 가지고 있다.

본 연구에서는 분열성 효모의 *aco2⁺*로부터 두 가지 타입의 RNA와 단백질이 만들어 지는 것을 확인하였다. 그 중 하나는 aconitase 도메인만을 가진 형태이고 또 다른 하나는 aconitase와 리보솜 도메인 모두를 가진 융합 단백질이다. 이 융합 단백질은 단백질 안에 코딩되어 있는 위치 서열에 의해 마이토콘드리아와 핵에 모두에 존재한다. 그 중 마이토콘드리아에 존재하는 Aco2 단백질의 경우는 마이토콘드리아 내에서 일어나는 단백질 합성을 조절하는데, 이 역할은 세포가 살아가는 데 있어서 필수적인 역할임을 확인하였다.

다음으로 핵에 위치하는 Aco2 단백질의 역할을 규명하였다. Aco2 단백질은 핵에서 헤테로크로마틴 형성에 필요한 것을 알게되었다. 핵에 있는 Aco2 단백질과 small RNA를 만드는 단백질들을 (Ago1, Dcr1) 함께 제거하였을 때 파괴된 센트로미어 기능이 다시 정상적으로 회복되었다. 또한 Aco2는 센트로미어 기능에 중요한 역할을 하는 단백질인 Chp1과 결합하고 Chp1에 의해 센트로

미어와 결합한다. Aco2는 센트로미어에서 전사되어 나오는 RNA와도 결합함을 알 수 있었는데 이 작용기작에도 역시 Chp1이 필요하다. 핵에서의 Aco2의 역할은 Aco2의 두 가지 도메인을 모두 필요로 하며 [철-황] 클러스터도 Aco2 기능에 필요함을 알게 되었다. 센트로미어 이외의 또 다른 헤테로크로마틴 부위인 메이팅 타입 로커스와 텔로미어에서의 Aco2 역할을 확인해 본 결과 Aco2 단백질이 없으면 이들 부근에서의 헤테로크로마틴 형성에도 문제가 생기는 것을 확인 할 수 있었다. 따라서 앞으로 이들 부근에서 Aco2가 어떻게 작용을 하는지 밝히는 연구가 계속되어야 할 것이다.

주요 단어

; 유전체학, 크로모솜, 철-황 단백질, 분열성 효모, 마이토콘드리아, 단백질 합성, 후성유전학, 헤테로크로마틴 형성

학 번

; 2009-20354